Titre: Title:	Software defined radar system
Auteur: Author:	Hui Zhang
Date:	2007
Type:	Mémoire ou thèse / Dissertation or Thesis
Référence: Citation:	Zhang, H. (2007). Software defined radar system [Thèse de doctorat, École Polytechnique de Montréal]. PolyPublie. https://publications.polymtl.ca/7993/

UNIVERSITÉ DE MONTRÉAL

SOFTWARE DEFINED RADAR SYSTEM

HUI ZHANG
DÉPARTEMENT DE GÉNIE ÉLECTRIQUE
ÉCOLE POLYTECHNIQUE DE MONTRÉAL

THÈSE PRÉSENTÉE EN VUE DE L'OBTENTION
DU DIPLÔME DE PHILOSOPHIAE DOCTOR (Ph.D.)
(GÉNIE ÉLECTRIQUE)
Aout 2007

Your file Votre référence
ISBN: 978-0-494-37140-4
Our file Notre référence
ISBN: 978-0-494-37140-4

UNIVERSITÉ DE MONTRÉAL

ÉCOLE POLYTECHNIQUE DE MONTRÉAL

Cette thèse intitulée:

SOFTWARE DEFINED RADAR SYSTEM

présenté par :Hui Zhang
en vue de l'obtention du diplôme de: Philosophiae Doctor
a été dûment accepté par le jury d'examen constitué de :

M. CEVDET AKYEL., Ph. D., président
M. WU KE, Ph. D., membre et directeur de recherche
M. JEAN-FRANCOIS FRIGON, Ph. D., membre
M. PAUL FORTIER, Ph. D., membre

DEDICATION

To my parents

AKNOWLEDGEMENTS

I would like to express my gratitude to my director, Professor Ke Wu, for his continuous support, invaluable guidance and encouragement throughout the work involved in this thesis, which gave me four extremely memorable and fruitful years of studying at École polytechnique de Montréal.

My gratitude is also due to my colleagues: Simone Winkler, Lin Li, Yanyang Zhao, Yang Ping, Li Duochuan, Xu Xinyu, Zhang Qingjun, Zhang Zhenyu and everyone in Poly-Grames for their generous help.

I would like to also thank to M. Jules Gauthier, M. Steve Dubé, and M. Roch Brassard for their patience during the elaboration of the prototypes and their technical assistance, to M. René Archambault and M. Jean-Sebastien Décarie for their software support.

Finally I would like to dedicate this thesis to my parents and to my sisters and brother. It is their love and support that have enabled me to complete this thesis successfully.

RESUME

Dans cette thèse, un nouveau type de système radar est proposé sous la forme d'un radar défini à l'aide d'un programme informatique. À l'aide d'une reconfigurabilité entièrement définie par un programme, un certain nombre de fonctionnalités différentes de systèmes radar conventionnels peuvent être obtenus et intégrés à l'intérieur d'un même dispositif dans le but de satisfaire les demandes et performances requises pour différentes applications.

Le système radar proposé peut être utilisés dans plusieurs domaines d'applications. Un des plus importants domaines d'application est relié à l'industrie automobile pour la mesure des distances et des vitesses en combinaison avec la communication haute performance inter-véhicule. D'autres champs d'application du radar présenté dans cette thèse sont reliés aux applications de sécurité, tels la sécurité dans les aéroports, les tâches de surveillance, ainsi qu'aux applications militaires.

Le système radar présenté dans ce travail offre la possibilité d'opérer selon trois différents régimes de modulation, soient la modulation en fréquence d'un régime harmonique (FMCW), le régime harmonique (CW) et le régime de spectre étendu (SS). De plus, différents algorithmes d'analyse de signaux pour chaque régime d'opération sont implémentés et testés, tels la méthode de corrélation PN super-résolution (SPM), la méthode Teager Kaiser (TK) et la méthode des ondelettes. La technique radar FMCW est utilisée pour trouver la distance approximative de la cible. Ensuite, un ensemble de

solutions possible mais précises est déterminée par une mesure CW. La distance de mesure obtenue par CW est résolue sur la base d'une solution FMCW approximative. De plus, un radar en régime SS est inclut dans le système pour mesurer la distance dans des environnements à haut degré d'interférence.

Le concept du système est modélisé dans un environnement MATLAB/Simulink dans le but de fournir un haut degré de performance et de prédiction pour le système radar proposé. De plus, ce modèle permet une évaluation détaillée de la performance et du principe de fonctionnement de chaque bloc de design et de chaque algorithme d'analyse de signal. Une étude extensive de la performance du système proposé est présentée pour fournir un bon aperçu théorique de la fonctionnalité radar et des différents objectifs de performance tels la résolution, l'exactitude et l'incertitude sur la distance.

Sur la base de ces simulations et de considérations théoriques, deux prototypes radars sont conçus, fabriqués et mesurés à 4 et 24 GHz respectivement. Ces prototypes incluent un récepteur-émetteur avec deux architectures différentes. La première architecture est un émetteur-récepteur hétérodyne basé sur un mélangeur conventionnel et la seconde structure est basée sur un détecteur à six ports à titre d'élément démodulateur. Également, le projet introduit une nouvelle approche de calibration à six ports en deux étapes qui prolonge la gamme d'opération six ports à des niveaux de puissance plus élevées. La performance des deux architectures est comparée et les résultats provenant des simulations, des mesures et de l'analyse théorique sont en accord.

ABSTRACT

In this thesis, a novel type of radar system in the form of a software defined radar is proposed. By means of an entirely software defined reconfigurability, a number of different functionalities of conventional radar systems can be realized and integrated within a single device in order to satisfy demands and performance requirements for multiple application scenarios.

The presented radar system can be used in a large variety of fields. One of its most important applications is related to the automotive industry for an accurate range and speed measurement in combination with a high-performance inter-vehicle communication capability. Other fields for the use of a software defined radar as presented in this work include safety applications, such as security screening at airports and surveillance tasks, but also airborne or military applications.

The radar system presented in this work provides three different modulation schemes: frequency modulated continuous wave (FMCW), continuous wave (CW), and spread spectrum (SS) operation. Moreover, different signal processing algorithms for each operation are implemented and tested, such as the superresolution PN correlation method (SPM), the Teager Kaiser (TK) method, and the wavelet method. The conventional FMCW radar technique is used to find the approximate range of the target. Then, an ambiguous but very accurate set of range solutions is determined by a CW measurement. The correct precision CW distance measurement is resolved on the basis

of the approximate FMCW solution. In addition, SS radar is included in the system to measure distance in high interference environments.

The entire system concept is modeled in a high-level MATLAB/Simulink environment in order to provide a good performance and functionality prediction for the proposed radar system. In addition, this model allows for a detailed assessment of performance and working principle of each single design block and each of the signal processing algorithms. An extensive performance study of the proposed system is presented in order to provide a good theoretical insight into the radar functionality and different achievable performance aims such as resolution, accuracy, and range ambiguity.

On the basis of these simulations and theoretical considerations, two software defined radar prototypes at frequencies of 4 GHz and 24 GHz, respectively, are designed, fabricated, and measured. These prototypes include a microwave front end with two different architectures. One is a heterodyne transceiver based on a conventional mixer, whereas the second proposed structure is based on a six-port detector as the demodulating element. Moreover, the project introduces a novel two-stage six-port calibration approach that extends the six-port conventional operation range to higher power levels. The performance of both architectures is compared and analyzed both in simulation and measurement and the results agree very well both in simulation, measurement, and theoretical analysis.

CONDENSÉ EN FRANÇAIS

1 Introduction

Avec l'avancement des technologies sans-fil radio-fréquence et des dispositifs informatiques et de communication intégrés, les réseaux de senseur sans-fil sont reconnus comme étant une des plus importantes révolutions technologique et commerciale de notre époque. La récente miniaturisation des dispositifs de télécommunication a engendré un intérêt mondial pour les applications et technologies des senseurs qui touchent essentiellement tout de notre quotidien tels les réseaux de communication, la sécurité domiciliaire, le suivi des inventaires, l'imagerie et le traitement médical, la cartographie géographique, le positionnement sans-fil, la détection minière par radar et l'automation industrielle.

À l'heure actuelle, nous retrouvons les senseurs avec connection par câble dans un très grand nombre d'activités industrielles de notre société. Plus récemment, certains véhicules de luxe ont été munis de senseurs de détection de glace ainsi que de senseurs d'assistance pour le stationnement de véhicule. Ce ne sont que quelques exemples parmi les différentes applications de radars commerciaux utilisés pour la sécurité et le positionnement. Les radars commerciaux actuels pour l'industrie automobile ont été conçus pour éviter les collisions lors de congestion sur les routes et ne peuvent pas être utilisés pour le positionnement local sans apporter des changements majeurs. De plus, la production actuelle de radars n'est pas optimale en terme de coûts et est donc principalement utilisable pour les véhicules haut de gamme.

La production de masse de radars à faible coût ayant des fonctionnalités ajustables est d'importance capitale pour des applications commerciales. Malgré le fait que les technologies radars ont été continuellement en développement depuis plus d'un demi siècle, la plupart des radars actuels ne peuvent être utilisés que pour applications spécifiques mentionnées ci haut. Leur architecture de base demeure pratiquement identique à celle des systèmes radars militaires initiaux. Les systèmes pour éviter les collisions et pour le contrôle adaptatif de la conduite (ACC) ont ouvert la voix à de nouvelles perspectives. D'ailleurs certains prototypes ACC sont en cours de fabrication pour la production de masse. Certains de ces systèmes sont basés sur la technique de modulation en fréquence en régime harmonique (FMCW), qui est accepté pour sa simplicité malgré plusieurs inconvénients tels que la difficulté à mesurer précisément la distance à courte portée. Un certain nombre de solutions alternatives sont basées sur la technique d'opération en régime harmonique (CW) qui permet la mesure précise des distances mais ne permet pas la détection de cibles multiples. Une troisième alternative est basée sur la technologie de spectre étendue (SS) qui est importante pour les milieux à haut degré d'interférence mais ne permet pas de mesurer précisément les distances à courte portée. Aucun de ces systèmes radars ne permet de mesurer simultanément les courtes et longues distances. De plus, ils ne satisfont pas les demandes multi-fonction et multi-système. En plus de ces contraintes, la précision restreinte et la distorsion des performances des détecteurs analogues limite l'amélioration des performances de tels systèmes radars. Par conséquent, nous observons une demande croissance pour la conception d'un système radar reconfigurable définit par logiciel. Un tel concept radar a

été proposé récemment mais ne fournit ni les performances voulues et n'utilise pas les techniques de design à jour.

Avec la recherche actuelle et le développement de radios définies par logiciels pour les communications sans-fil, il apparaît raisonnable de développer un concept radar définit par logiciel pour diverses applications impliquant différentes exigences. Les facteurs qui caractérisent ces différentes applications sont la gamme d'opération en fréquence avec une précision et résolution adaptative, la vitesse minimale et maximale de la cible, la résolution spatiale ainsi que les erreurs de détection. Il existe actuellement une demande importante pour le développement de telles plateformes de technologie radar pour les futurs réseaux sans-fil et pour des applications qui impliquent trois aspects critiques de recherche et développement : la technologie de réception-transmission, l'architecture du système et le traitement du signal.

Pour obtenir un gain important des architectures de réception configurables par logiciel et utilisables dans différents contextes, il est important de fournir des techniques de génération de signaux flexibles pour l'horloge ou les oscillateurs de référence par rapport à la fréquence et l'amplitude du signal. Les technologies des synthétiseurs qui permettent de générer un signal analogue de haute fréquence directement d'un tableau de données, fournissent une grande flexibilité par rapport à une commutation rapide de la fréquence qui maintient une continuité de la phase. L'état de l'art dans le développement de ces synthétiseurs digitaux directs (DDS) permet d'obtenir des fréquences de sortie jusqu'à 2 GHz. Puisque la sortie des DDS est traitée de manière digitale, sa fonctionnalité est aisément configurable ce qui la rend encore plus flexible.

Les techniques DDS offrent des capacités uniques en contraste avec les autres méthodes de synthèses. Par exemple, il est possible d'obtenir un contrôle sur la résolution en fréquence de l'ordre du mHz et une résolution sur la phase de l'ordre du mHz et même du nHz pour une fréquence intermédiaire allant jusqu'à 1 GHz. De plus, les DDS n'imposent aucune contrainte d'ajustement du temps pour des changements de fréquences autres que ce qui est nécessaire pour le contrôle digital. Puisque le signal généré est digital, il peut être varié avec une précision exceptionnelle. Ceci permet un contrôle précis et une modulation de la fréquence et de la phase. Le tableau de données est utilisé pour stocker des échantillonnages de sinusoïdes. Un accumulateur digital est utilisé pour générer une phase appropriée qui est cartographiée par le tableau de données à la forme voulue de l'onde de sortie. Les DDS sont spécialement avantageux par rapport aux oscillateurs analogues multiples si des modulations de distribution spectrale arbitraire sont utilisées. Les systèmes radars qui nécessitent une grande précision et stabilité en fréquence et une commutation rapide de la fréquence tout en maintenant la phase peuvent bénéficier de l'utilisation duale des DDS dans le module de transmission.

La technique de conversion à six ports est une approche alternative intéressante vers l'implémentation d'émetteur-récepteurs configurable par logiciel aux fréquences millimétriques. L'avantage crucial par rapport à l'architecture d'échantillonnage est sa simplicité de construction qui nécessite seulement l'oscillateur de référence à titre de composent RF actif, ce qui rend cette technologie particulièrement intéressante pour les futurs récepteurs-transmetteurs RF large bande et à faible coût qui opèrent aux fréquences millimétriques. À l'aide d'un réflectromètre à six ports, il est possible de

mesurer les coefficients de réflexion complexes d'un dispositif sous test (DUT). De plus, à l'aide de deux dispositifs à six ports – un de chaque côté du DUT – il est possible de déterminer l'ensemble des paramètres *S*. Depuis le milieu des années 1990, le principe du dispositif à six ports a été étudié pour un récepteur à conversion directe. D'autres applications possibles sont les radars anti-collision, pour la mesure précise de courtes distances et pour déterminer la direction. Le principe de fonctionnement du dispositif à six ports est basé sur la mesure de quatre puissances de sortie indépendantes qui correspondent au rapport de deux ondes électromagnétiques superposées ayant différentes phases.

Le principal avantage de la technologie à six ports est la possibilité d'effectuer une calibration et configuration par logiciel. De plus, la technologie à six ports devient très intéressante lorsque des très hautes fréquences (de longueur d'onde millimétrique) sont utilisées. De plus, le même système peut, de manière générale, être utilisé pour différents standards simplement en chargeant les algorithmes utiles pour la bande de fréquences. Ceci permet un récepteur-transmetteur RF à six ports de très grande largeur de bande, ce qui représente une technologie prometteuse pour les futures plateformes SDR puisque différentes bandes de fréquences et différents standards peuvent être couverts. La technique à six ports est très bien adaptée pour mesurer avec exactitude la différence de phase entre deux ondes.

En considérant tous ces aspects, la cible est adressée vers le développement d'un radar défini par logiciel à des fréquences de plusieurs GHz allant jusqu'aux ondes millimétriques. Les systèmes radars définis par logiciel peuvent réduire le besoin des

ADC et par conséquent mener à des radars multi-standards pour des ondes millimétriques. La technologie à six ports représente un avantage inhérent de cette architecture. La combinaison de réseaux d'entrées programmables par champs (FPGA) qui contiennent le logiciel en combinaison avec les DDS pour effectuer la modulation et les changements de fréquences introduit une configurabilité dans la section de transmission de systèmes radars micro-ondes. Puisque les modulations FMCW, CW et SS sont relativement similaires en ce qui concerne les besoins matériels, ils peuvent être combinés en un seul module de réception-transmission. Chaque mode d'opération est défini par une technique de modulation et démodulation distincte. Il est connu des utilisateurs de radars que des compromis sont toujours nécessaires puisqu'il n'y a pas d'unique mode d'opération qui fournit l'exactitude de la distance et de la vitesse dans toutes les situations possibles. Les conditions d'opération incluent la vitesse de la cible et la mesure de courtes ou longues distances. C'est pourquoi nous dirigeons nos efforts vers le design d'une architecture radar définie par logiciel dans laquelle les paramètres de modulation peuvent être ajustés et/ou changés à l'intérieur d'une courte période de temps (de l'ordre des millisecondes).

Ce projet inclut le développement d'un radar défini par logiciel pour une technologie de récepteur-transmetteur à des fréquences millimétriques, ayant une architecture flexible à faible coût, et une technique de traitement de signal rapide et versatile. Pour obtenir un tel système radar, des projets de mesures adaptatives sont conçus et simulés sur plusieurs gammes de fréquences avec certaines précisions fixées. Plus précisément,

le système radar est capable de mesurer avec exactitude les courtes distances (inférieures à 5 m) et les longues distances (supérieures à 5 m).

Ce projet de doctorat est résumé comme suit : ***(i) Développement de deux radars à architecture de réception-détection.*** Le but de cette étape de design est vouée au développement et l'application d'une nouvelle technologie pour ondes millimétriques par le design et la fabrication de deux unités de réception-transmission pour un radar fonctionnant à 24 GHz. La première structure est basée sur un transmetteur-récepteur avec un mélangeur et le second design implique un dispositif à six ports. Ainsi, nous développons une nouvelle architecture multi-applications pour la réception-détection. ***(ii) Architecture de système avec des techniques définit par logiciel pour un format multi-signal***; Cet aspect de la recherche traite avec plusieurs étapes de modulation ou modes d'opération pouvant être adaptés à plusieurs applications, et ce tout en étudiant les techniques de génération de signaux à faible coût. Dans ce travail, les techniques FMCW, CW et SS et un scénario hybride combinant ces trois différents types de modulation sont étudiées pour un environnement définit par logiciel. ***(iii) Analyse de signaux à bande de fréquence adaptative avec paramètre d'extraction pour une réponse multi-fonctions.*** L'acquisition de données est sujette aux techniques d'estimation de la fréquence et de la phase qui sont différentes pour les modulations FMCW, CW et SS. Des techniques d'analyse de signaux spécialisées seront étudiées pour les différentes applications.

2 Méthodologie

Ce projet de recherche implique des méthodes de recherche expérimentales et théoriques. Ce qui suit décrira en détail la méthodologie et les activités pour compléter le projet de recherche.

2.1 Design et implémentation de deux architectures de réception-transmission

Une des architectures réception-transmission est basée sur un récepteur hétérodyne tandis que l'autre architecture est basée sur une technologie à six ports. Le récepteur hétérodyne et le circuit à six ports sont utilisés à titre de détecteur de phase en modulation CW à double fréquence, comme mélangeur en mode d'opération FMCW et comme démodulateur de phase en mode SS. Puisque les deux architectures sont couramment utilisées dans les systèmes radars et de communication, les avantages et désavantages de la technologie à six ports comparés aux architectures conventionnelles hétérodynes (mélangeur) dépendent fortement de la forme du signal et des applications.

2.2 Design et implémentation d'une modulation du synthétiseur

L'unité de modulation du synthétiseur permet une modulation adaptative, ce qui représente une intéressante propriété pour le design du SDR. Dans ce travail, trois modes d'opération sont implémentés : FMCW, CW, SS et un mode hybride FMCW/CW/SS.

Dans l'unité de modulation du synthétiseur, le DDS sera utilisé pour générer le signal modulé. En plus des trois techniques de modulation décrites ci haut, le mode d'opération hybride permet une excellente exactitude sur une plus grande plage de conditions d'opération. Le point central de cette architecture radar définie par logiciel

réside dans le contrôleur interfacé avec un ordinateur (PC), ce qui permet au manufacturier de configurer le radar pour une application spécifique et d'enregistrer et analyser les données

2.3 Analyse des données et traitement des signaux

Suite à l'acquisition des données, les techniques d'estimation de la fréquence et de la phase sont appliquées. Pour un signal de retour FMCW, des techniques d'estimation de la fréquence telles la transformation de Fourier rapide (FFT) sont nécessaires pour obtenir des informations sur la vitesse et la distance. De plus, des algorithmes alternatifs de traitement de signaux tels MUSIC sont étudiés. Dans le cas de signaux de retour CW, la vitesse et la distance sont calculées à partir de l'estimation de la phase. Dans ce travail, deux méthodes sont utilisées pour obtenir l'information sur la phase. La première est basée sur un discriminateur de phase à six ports. La deuxième technique implique le conditionnement et traitement de signaux analogues, ce qui requiert un démodulateur à quadrature ou un démodulateur I&Q. Les deux techniques seront étudiées et constituent la base pour les mesures de distances et vitesses pour le radar. Finalement, pour le radar SS, trois algorithmes d'estimation seront appliqués : la méthode super résolution (SPM), la méthode Teager Kaiser (TK) et la méthode des ondelettes.

3 Conclusion

Dans ce travail, un radar défini par logiciel, flexible et reconfigurable, a été développé pour un usage à 4 et 24 GHz. La reconfigurabilité du radar s'appuie sur les points suivants : le radar utilise un mode CW à double fréquence en utilisant un

détecteur de phase, un mode FMCW avec un mélangeur et un mode SS avec un démodulateur de phase. Pour chacun de ces modes d'opération, un DDS génère les signaux requis ce qui entraîne une versatilité et flexibilité en combinaison avec une très grande vitesse de commutation du système de radar proposé.

De plus, un certain nombre d'algorithmes de traitement de signaux tels que la FFT, MUSIC, TK et la méthode des ondelettes ont été utilisés pour les différentes techniques de modulation dans le but d'augmenter la résolution.

Des architectures à six ports et à partir d'un mélangeur ont été étudiées en détail. Les points forts du récepteur à six ports résident en la possibilité de combiner trois fonctions en un seul dispositif et ses faibles puissances requises pour le LO. Un inconvénient est la fréquence de sortie limitée. En contrepartie, les mélangeurs traditionnels offrent deux circuits de fonction au même moment tout en étant moins restreint sur la fréquence de sortie. Cependant, de plus grandes puissances de sortie sont nécessaires pour les LO et seuls les mélangeurs IQ sont capables de détecter précisément la phase.

De plus, la résolution sur le positionnement et la distance maximale atteinte pour les différents types de radars ont été discutés. Le radar FMCW est adapté pour les mesures de longues distances et sa résolution dépend de la vitesse de balayage du DDS. Une plus grande largeur de bande donne une vitesse de balayage plus rapide et donc une meilleure mesure de la distance. Au contraire, le radar CW à double fréquence est précis pour les mesures de courtes distances. Sa résolution dépend de l'exactitude de la phase qui est déterminée par le processus de calibration du dispositif à six ports. Le radar SS offre

une mesure anti-interférence pour les longues distances et sa résolution dépend du code PN.

En combinant tous ces aspects, les mesures FMCW/CW/SS ont montré une meilleure précision que ce qui a été obtenu avec le système FMCW et est donc pleinement adapté pour des applications de grande précision. De plus, les systèmes de mesures SS offrent de bonnes possibilités pour éliminer les interférences. En terme de miniaturisation, le récepteur hétérodyne démontre d'excellentes performances, mais le dispositif à six ports possède également de bonnes propriétés et est applicable à titre de démodulateur pour les systèmes de télécommuncations. La viabilité économique de ce type de dispositif semble prometteuse. La plupart des prototypes de systèmes ont été fabriqués avec des matériaux commerciaux à faible coût. Un DDS permet d'ajuster la modulation et les variations en fréquence ce qui permet d'inclure une configurabilité par logiciel dans le transmetteur. Également, un DSP fournit l'argorithme digital correspondant pour un signal particulier du récepteur. Le coût le plus élevé pour la fabrication du dispositif serait associé à l'obtention d'un récepteur-transmetteur compact et synthétisé.

Le système à six ports définit par logiciel représente une alternative à faible coût pour des systèmes FMCW/CW. La précision sur la mesure de la distance est supérieure à 5 cm. Le système à six ports effectue une détection cohérente sans le besoin de mélangeurs balancés et de déphaseurs précis. Une étape importante du travail associé avec le dispositif à six ports est liée à la procédure de calibration. De plus, il est possible d'effectuer des mesures de l'ordre du décimètre sans difficulté supplémentaire.

L'adaptabilité du dispositif à six ports pour la modulation complexe et sa compétitivité au niveau des propriétés dynamiques a été démontrée.

Les contributions majeures peuvent être résumées comme suit :

- Développement d'un radar définit par logiciel
- Design d'un radar définit par logiciel base sur un dispositif à six ports et un mélangeur IQ
- Mesures d'un système composite FMCW/CW/SS ayant une précision de 5 cm
- Design d'un SDR CW à trois tonalités
- Design d'un radar à 24 GHz à codage de type PN
- Comparaison des performances de la distance du dispositif FMCW/CW/SS en utilisant CMLB
- Comparaison de deux architectures pour SDR

L'objectif primaire du travail est de designer un radar définit par logiciel base sur des récepteurs-émetteurs obtenus à partir d'un mélangeur et d'un dispositif à six ports. Une approche à senseurs multiples a été adoptée, ce qui permet de fusionner les différentes fonctionnalités des senseurs et donc prendre avantage de leur complémentarité. Avec le développement d'une technologie DDS et d'un traitement de signaux digitaux (DSP), il a été possible de designer un radar multifonction, multimode et de haute performance à un coût raisonnable. Le récepteur radar digital échantillonne directement les signaux IF des canaux de réception avant la détection. Dans le cas de l'architecture à six ports, la détermination sur la phase est basée sur le processus de calibration. Les mesures des fréquences sont basées sur les fonctions du mélangeur. Le traitement subséquent et le

processus de détection sont accomplis dans le domaine digital. Avec cette méthode, une meilleure précision sur la détection peut être obtenue. Ces avantages incluent une meilleure précision, une interface flexible vers le contrôle du radar ainsi qu'un contrôle sur le mode d'opération, la forme des signaux et sur les fréquences LO des récepteurs. Également, un traitement de signal complexe peut être effectué, ce qui élimine un grand nombre de problèmes présents dans les méthodes analogues tels une variation et sensibilité en température, et résulte en une meilleure stabilité du système.

TABLE OF CONTENTS

LIST OF FIGURES

LIST OF TABLES

LIST OF ABBREVATIONS

ADC	Analog-to-digital converter
ADS	Advanced design system
AWGN	Additive white Gaussian noise
BER	Bit error rate
BPSK	Binary phase shift keying
CW	Continuous wave
DSP	Digital signal processing
DUT	Device under test
FCC	Federal communications commission
FFT	Fast Fourier Transform
FMCW	Frequency modulation continuous wave
FPGA	Field programmable gate array
GPS	Global positioning system
IF	Intermediate frequency
IP	Intellectual property
LO	Local oscillator
MMIC	Monolithic microwave integrated circuit
MUSIC	Multiple Signal Classification

NF	Noise figure
PLL	Phase locked loop
PN	Pseudo random
PSD	Power spectral density
PSM	Phase spectrum modulation
QPSM	Quaternary phase spectrum modulation
RF	Radio frequency
SDR	Software defined radar
SIW	Substrate Integrated Wavequie
SS	Spread spectrum
SPM	Super Resolution Method
TK	Teager-Kaiser
UWB	Ultra wideband
WPAN	Wireless personal area network

CHAPTER 1

INTRODUCTION

With the unprecedented advancement of radio-frequency (RF) wireless techniques and daily progress of integrated computing and communicating devices, wireless sensor networks have already been recognized as one of the most important technological and commercial revolutions in our new century [1]. The recent downsizing of telecommunication industries has in fact fuelled up a worldwide interest in sensor technologies and applications that basically touch on everything in our everyday lives including communication networks, homeland security and safety, inventory and asset tracking, medical treatment and imaging, geographic mapping and wireless positioning, ground penetrating radar for detection of landmines, and industrial automation.

Today, wired sensors are still found in a very large number of industrial activities of our modern society. More recently, some luxury commercial vehicles have been equipped with ice detection radar sensors and parking aid radar sensors [2], which are becoming more and more popular. This represents only one of numerous examples for commercial radar applications with a huge market share of safety, security, and positioning devices. Commercial automotive radars available so far have been designed to a large extent for collision avoidance in dense highway traffic and cannot be used for other applications such as local positioning and perimeter security without major modifications. In other words, they are designed as single oriented. In addition, current

radar manufacturing is still not cost-effective and therefore such radar systems are not readily applicable to popular and low-end vehicles.

Low-cost and mass-producible radar with highly flexible functionalities is of paramount importance for widespread commercial applications and great market penetration. Even though the radar technology has been continuously in development for more than half a century, most radars being deployed today can only be used for specific applications as mentioned above, and their basic architectures with respect to the early version of military systems remain largely unchanged. Collision avoidance and adaptive cruise control (ACC) systems [3] have opened up great perspectives, with some ACC prototypes being on the way to mass production. Some of these systems are based on the frequency modulation continuous wave (FMCW) [4] technique, which is well accepted for its simplicity, even if it has a few drawbacks such as difficulties in obtaining accurate distance measurements at short ranges. A number of other solutions are based on the continuous wave (CW) [5] technique, which provides highly accurate range measurements but cannot be used for multi-target detection. A third alternative in the development of such systems is based on spread spectrum (SS) technology [6], which is beneficial for high interference environments but cannot provide high accuracy measurements at short range. None of these radar systems is capable of giving short and long range measurements at the same time. Moreover, they do not satisfy multi-function and multi-system requirements. In addition to these constraints, the restricted precision and distortion performance of analog detectors greatly limit the performance improvement of such radar systems [8]. Therefore, an increased demand for developing

a universally re-configurable so-called software-defined radar system is observed, which represents a very challenging topic. Such a software-defined radar concept has been proposed recently [7]-[8] but provides neither performance investigation nor up-to-date design techniques.

With the ongoing research and development of software-defined radio (SDR) for wireless communication, it appears reasonable to consider a software-defined radar concept for various applications involving different performance requirements. Factors that characterize such different applications include the operating range with adaptive resolution and accuracy, the minimum and maximum target velocity, the desired spatial resolution, and clutter discrepancies. Currently, an urgent need for developing such a universal radar technology platform for future wireless sensor networks and applications is observed, which involves three critical aspects of research and development: front-end technology, system architecture, and signal processing.

In order to gain full benefit from software-configurable receiver architectures with respect to their use in different application scenarios, it is necessary to provide flexible signal generation techniques for the clock or reference oscillators with respect to frequency and amplitude of the signal. Synthesizer technologies, which generate the analog high frequency signal directly from a digitally stored look-up table, provide the highest flexibility with respect to a fast frequency switching maintaining phase continuity. The state of the art development for these so-called direct digital synthesizers (DDSs) provides output frequencies of up to 2 GHz. Since the DDS output is digitally processed, its functionality is easily software configurable, making it more flexible.

DDS techniques offer unique capabilities in contrast to other synthesis methods, such as a frequency resolution control in the order of mHz step size and a phase-resolution in the range of mHz or even nHz [9] for an intermediate frequency (IF) of up to 1 GHz. Additionally, DDS imposes no settling time constraint for frequency changes other than what is required for digital control. Since the signal being generated is in the digital domain, it can be varied with exceptional accuracy. This allows precise control of frequency or phase and can readily accommodate frequency and phase modulation. The look-up table is used to store samples of a sinusoid. A digital accumulator is used to generate a suitable phase argument that is mapped by the look-up table to the desired output waveform. The DDS is especially advantageous with respect to the use of multiple analog oscillators if modulation schemes with arbitrary spectral distributions are used. Radar systems, which require both high frequency accuracy and stability and a fast-frequency switching maintaining phase continuity can benefit from the dual use of DDS in the transmitter section.

The six-port direct conversion technique is another promising approach towards the implementation of software configurable transceivers at millimeter-wave carrier frequencies. The crucial advantage over the sampling architecture is its simple construction requiring only the reference oscillator as an active RF component, making this technology particularly attractive for future low-cost and broadband RF front-ends operating at millimeter-wave frequencies. By means of a six-port reflectometer, it is possible to measure the complex reflection coefficients of a device under test (DUT). Furthermore, by the use of two six-ports — one on each side of the unknown DUT — it

is possible to determine the complete set of *S*-parameters. Starting in the mid 1990s, the six-port principle has been investigated for use as a direct conversion receiver [10]. Other applications include anti-collision radars [11], very accurate short-range distance measurements [12], and direction finding systems. The functional principle of six-port devices is based on the measurement of four independent output powers corresponding to the complex ratio between two superposed electromagnetic waves under different phase angles.

The main advantage of six-port technology is its possibility for software configuration and calibration. Furthermore, the six-port technology becomes very attractive when extremely high carrier frequencies at millimeter wavelengths are used. Additionally, the same hardware can, in general, be used for different standards simply by loading suitable baseband processing algorithms. This suggests extremely broadband six-port RF front-ends as a promising technology of choice for future SDR platforms, as different bands and standards can be covered. The six-port technique is very well suitable for accurately measuring the phase difference of two waves.

Considering all these aspects, the main focus needs to be addressed to the development of software-defined radar up to several GHz and a subsequent up-conversion into millimeter-wave frequencies. Software defined radar systems can reduce the requirements on the ADCs and therefore lead to multi-standard millimeter-wave radars. Six-port technology represents the inherent advantage of this architecture. The combination of field-programmable gate arrays (FPGAs) containing the system software in combination with a DDS to realize modulation schemes and frequency shifts

introduce software configurability also in the transmitter section of micro-wave and millimeter-wave radar systems. Since FMCW, CW, and SS modulations are quite similar regarding the radar hardware requirements, they can be combined into a single front-end module. Each mode of operation is defined by a distinctive modulation and demodulation technique. It is well known to radar users that compromises are always required because there is no unique mode of operation that can provide consistent accuracy of range and velocity estimates in every possible condition. Operation conditions include target velocity and short- or long-range measurements. This is why we direct our efforts on designing a software-defined radar architecture, in which the modulation parameters can be adjusted and/or changed within a short period of time (milliseconds).

This project includes the development of software defined radar-oriented millimeter-wave transceiver technology, cost-effective and flexible system architecture, and versatile and high-speed signal processing technique. To realize such a radar system, adaptive measurement schemes are designed and simulated over various ranges with pre-designated accuracy. More precisely, the radar system is able to accurately measure short-range distances (< 5 m) as well as long–range distances (> 5 m).

This doctoral research project is summarized as follows: ***(i) Development of two radar transceiver front-end architectures***. The purpose of this design step is the development and application of a newly proposed millimeter-wave technology in the design and realization of two front-end building blocks for the proposed 24 GHz radar. The first structure is based on a mixer front-end, whereas the second design involves a

six-port device. In this way, we develop a novel multi-application transceiver architecture. ***(ii) System architecture with software-defined techniques for multi-signal format.*** This research aspect deals with multiple modulation schemes or modes of operation that can be adapted to various application scenarios while cost-effective signal generation techniques should be studied. In our work, FMCW, CW, and SS techniques, as well as a hybrid scheme combining these three modulations will be investigated for the software-defined framework. ***(iii) Adaptive baseband signal processing with parameter extraction for multi-function response.*** The data acquisition is subject to frequency and phase estimation techniques that will be different for the three basic FMCW, CW, and SS modulations. Sophisticated signal processing techniques will be studied for different applications.

1.1 Methodology

This research project involves both theoretical and experimental research methods. The following will describe details of our methodologies and activities for completing the project.

1.1.1 Design and implementation of two front-end architectures

One of our front-end architectures is based on a heterodyne receiver, whereas the other is based on a six-port technology. The heterodyne receiver and six-port circuits are used as a phase detector in dual frequency CW modulation operation, as a mixer in

FMCW operation mode, and as phase demodulator in SS mode. Since both architectures are widely used in radar and communication systems, the advantages and disadvantages of six-port technology compared to conventional heterodyne architectures (mixer) strongly depend on the signal waveforms and applications.

1.1.2 Design and implementation of the modulation synthesizer module

The modulation synthesizer module shown in Figure 1.1 allows for adaptive modulation schemes (modes of operation), which presents interesting and new features to SDR design. In this work, three modes of operation are implemented: FMCW, CW, SS, and hybrid FMCW/CW/SS mode.

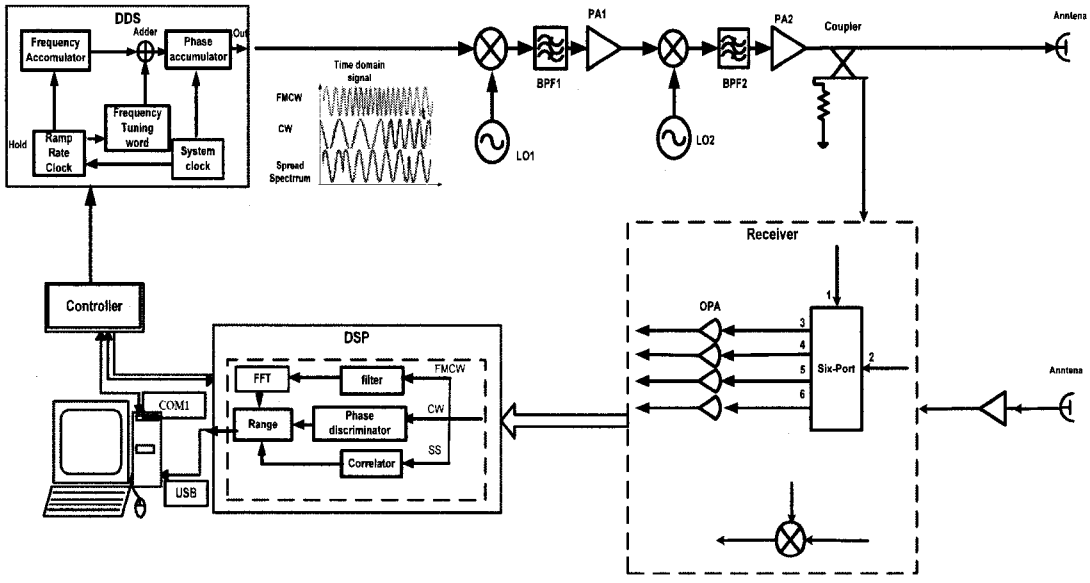

Figure 1.1: Block diagram of the proposed software defined module

Figure 1.1 illustrates the modulation synthesizer module, which will be used to generate the modulated signal. In addition to the above-described three modulation techniques, the hybrid operation mode provides excellent accuracy in a broader range of operating conditions. The center point of this software-defined radar architecture resides in the controller being interfaced with a personal computer (PC), which allows the manufacturer to configure the radar for a given application and to store and analyze data.

1.1.3 Data analysis and signal processing

Following data acquisition, frequency and phase estimation techniques have to be applied in order to retain information from the measurement. For an FMCW return signal, frequency estimation techniques such as Fast Fourier Transform (FFT) are required to obtain both range and velocity information. Furthermore, alternative signal processing algorithms are investigated such as MUSIC [13]. In the case of CW return signals, range and velocity are calculated from the phase estimate. In this work, there are two methods to obtain phase information. The first is the six-port phase discriminator. The second technique of interest involves analog hardware signal conditioning and processing, which requires a quadrature demodulator or I&Q demodulator. Both techniques will be studied and they constitute the basis for range and velocity measurements with the proposed software-defined radar. Finally, for the SS radar, three estimation algorithms will be applied including the super resolution method (SPM) [14], the Teager Kaiser (TK) operator method [15], and the wavelets method [16].

The primary objective of this work is to design a software defined radar based on mixer and six-port transceiver architectures. A multiple-sensor approach is adopted, merging the functionality of these different sensors in a way that takes advantage of their complementarities. With the development of DDS technology and general-purpose digital signal processors (DSP), it has become possible to design a multifunction, multimode, high-performance radar at a reasonable cost. The digital radar receiver of the software defined radar proposed in this work directly samples the IF signal of the receiving channels prior to detection. In the case of the six-port architecture, the phase discriminator is based on the calibration. Frequency measurement is based on the mixer function. The entire subsequent processing and detection process is accomplished in the digital domain. With this method, improved detection accuracy can be achieved. These advantages include greatly improved processing accuracy of the system, a flexible interface with the radar control center, as well as a convenient control of the operation mode, signal wave-form, and LO frequencies of the receivers. Moreover, complex signal processing can be accomplished, which eliminates a high number of problems that are present in analog methods such as temperature sensitivity and drifts in component values, resulting in a highly superior stability of the entire system.

This thesis is organized as follows. In chapter 2, the development of a synthetic software defined radar is outlined. The perspective and motivation for the proposed software defined architecture are presented. Chapter 3 presents a multiple signal classified (MUSIC) algorithm that is used for the signal processing of this operation mode and also the multiple frequencies algorithm for CW mode and the SS processing

methods including SPM, TK operator algorithm, and wavelet algorithm. Chapter 4 introduces the implementation of the software defined radar based on mixer and demonstrates a considerable improvement in terms of range resolution. The waveforms are generated by a DDS in order to implement adaptive functionality. Chapter 5 describes the design of the synthetic software defined radar based on six-port technology. Furthermore, six-port and mixer architecture are compared. Chapter 6 presents the performance analysis of the proposed software defined radar prototype and finally, chapter 7 presents conclusions and future work.

CHAPTER 2

SYNTHETIC SOFTWARE DEFINED RADAR: CONCEPT AND SIMULATION

At present, the range radar is widely used in a large variety of fields [17]. One of its most important applications is related to the automotive industry, where a good real-time measurement accuracy of speed and range is necessary [18]–[20]. Most range radars developed in this field are based on the FMCW scheme. However, the FMCW-based range resolution mainly depends on the bandwidth of the baseband signal transmitted. A very broadband and linear frequency sweeping signal is needed in this case to achieve a reasonably good range resolution for practical applications. This leads to some difficulty in realizing a high-quality signal source at low cost. On the other hand, CW radar has been well known in terms of its simplicity and range accuracy [21]. However, the CW radar has its own problem of phase ambiguity, which directly causes range ambiguity. In order to solve this problem, in general, multiple signals with different frequencies are used. Another problem of the CW radar is that it cannot be implemented for multi-target measurements. Therefore, the combination of FMCW and CW radars into one system platform promises a very attractive solution for practical applications. Also FMCW radars are unable to exchange and communicate front-panel and vehicle information (e.g. direction information and braking information) with each other among adjacent vehicles. To further enhance traffic safety, there have been intensive studies on inter-vehicle communication among individual running vehicles. As SS communication systems are

known to provide a number of attractive advantages such as interference immunity and multiple access capability, many research results in connection with inter-vehicle SS communication systems have been reported. There have been a few case studies on PN code assignment methods for code division multiple accesses (CDMA) communications.

Generally, radar and communication systems require different hardware configurations. The concept of a unified solution that does not require reengineering for every new or specified application has been proposed but it has still been limited to a group of radio functionalities [7]. Software defined radio [22], which realizes classical receiver functions, can be reconfigurable for different scenarios. According to this concept, the solution for reconfiguration is to shift system functionality from hardware to software. A digital receiver based on this principle has also been presented recently [23]. In order to gain full benefits from software configurable measurement architectures [24] with respect to the use of transceivers in different application scenarios, it will be necessary to provide flexible signal generation techniques for the clock or reference oscillators with respect to phase and amplitude of the signal [25]. A DDS, which generates an analog high frequency signal directly from a digitally stored look-up table, provides the highest flexibility with respect to fast waveform switching [22]. DDSs may now reach an operation frequency of up to S band [26]. This leaves many challenging issues for software configurable measurement systems. Changing operating frequency is a solution to avoid interference. Optimizing the parameters (waveform and frequency modulation (FM) sweep rates, etc.) [7], [27], [28] is another way to enhance the measurement performances in different environments. A software configurable system

offers a programmable and dynamically re-configurable method of reusing hardware to implement the physical layer processing. In this work, we propose a software defined radar and communication system that combines FMCW, CW and SS radar. Such three functions are switched in different time schedule or slot.

The term "software defined" refers to an entirely software-controlled operation of a radar, by a full control of the transmitted and the received signal. This means that highly sophisticated correlating codes can be implemented, even on a pulse by pulse basis. Such a transmitter can't only be implemented in radar applications, but can be used for communications as well. Furthermore, digital beam forming is on the way to become an important tool in communications for space division multiple access (SDMA) or multiple input multiple output (MIMO) architectures for the improvement of service of quality (SoQ) and network capacities. Transmitters of such type have been discussed for a long time, and with the new system concept they become more easily realizable. It has to be mentioned that each of these transmitters is not necessarily advantageous for each operation. The goals of the novel proposed system are:

- low cost
- high reliability
- high resolution
- high coverage.

In addition, Low cost is achieved by a lower hardware complexity. Many functions are integrated into the software and offer high modularity. Reliability can be increased because 70% of wired connections can be omitted. Weight is reduced because of the

smaller RF hardware and higher DC power efficiency. The resolution is increased by the combination of different radar types. Wide coverage is achieved by a considerably higher RF transmitter and receiver efficiency.

In this chapter, we will present and discuss the general radar equation in section 2.1. The signal models of FMCW, CW and Spread Spectrum radar will be presented in section 2.2. The six-port technology will be introduced in section 2.3. The comparison between the conventional radar and software defined radar will be shown in section 2.4. In the last three sections, we will give the overview of software defined radar as well as related simulation aspects.

2.1 Radar Equation

The radar equation relates the range of the transmitter, receiver, antenna, target, and the environment. It is useful not only for determining the maximum range for particular radar in connection with a target, but also for observing the factors affecting radar performance. It is an important tool to aid in radar system design.

Radar radiates an electromagnetic signal and detects the echo returned from targets. The echo signal provides information about the target. The range is found from the time delay it takes for the signal to travel to the target and back. The angle of the target is found with a directive antenna to sense the angle of arrival of the echo signal. If the target is moving, radar can track the location of the target [4]. The Doppler shift in frequency of the received signal is caused by a moving target. With sufficiently high

resolution, radar can detect the target's size and shape. Radar resolution is obtained in range or angle. Range resolution requires large bandwidth. Angle resolution requires large antennas.

The radar equation gives the relations between the range of radar, the transmitter, receiver, antenna, target, and the environment. The simple form of the radar equation expresses the maximum radar range $R_{\max}$ for the radar parameters and the target's radar cross section when the radar sensitivity is limited by receiver noise. It is as follows [4]:

$$R_{\max} = \left[\frac{P_t G A_e \sigma}{(4\pi)^2 S_{\min}} \right]^{1/4} \tag{2.1}$$

where

$P_t =$ Transmitted power, W

$G =$ Antenna gain

$A_e =$ Antenna effective aperture, m^2

$\sigma =$ Radar cross section of the target, m^2

$S_{\min} =$ Minimum detectable signal, W

Except for the target's radar cross section (RCS), the parameters in radar equation are controlled by the radar designer. We need to consider the transmitted power, antenna gain power and directivity, and receiver sensitivity.

The range to a target is related by the delay τ_R which the transmitted radar signal travels to the target and back. Electromagnetic energy in free space travels with the speed of light. So the time for the signal to travel to a target located at a range R and

return back to the radar is $2R/c$ where c is the velocity of light. The range to a target is $R = \frac{c\tau_R}{2}$.

The transmitter for the software defined radar produces three desired waveforms (FMCW, CW, SS), which provides a tunable bandwidth for each mode and a stable power. The same horn antenna is used for both transmitting and receiving in this system. Now the key issue for software defined radar design is to find the minimum detectable signal S_{min}. In next section, the signal models of three types of radar are discussed.

2.2 Signal Models of Three Types of Radar

2.2.1 FMCW radar

The basic principle of the frequency modulation continuous wave (FMCW) radar is well known as for the frequency of the transmitted signal changes with time in a prescribed manner. By comparing the frequency of the (time-delayed) received signal with the frequency of a sample of the non-delayed transmitted signal, a measure of transit time can be obtained from the beat frequency [29].

For simplicity, we consider a signal reflected from a static target. The range data can easily be obtained in this case. In our work, a software-defined radar platform has been proposed and developed on the basis of an FMCW scheme. We have presented a software-defined radar concept [8], [9], [30] with a bi-static radar prototype developed

for the 24 GHz industrial, scientific, and medical (ISM) band. The radar signal is generated with a DDS, then up-converted and multiplied to transmit a signal of 24.125 GHz. Although the proposed architecture allows for more than one type of modulation signals, only the FMCW scheme has been implemented, tested, and discussed within this work in order to highlight the proposed super-resolution technique. A homodyne receiver is used to down-convert radar echoes to base-band frequencies using the transmitter signal as a reference. This base-band signal is then digitized for signal processing.

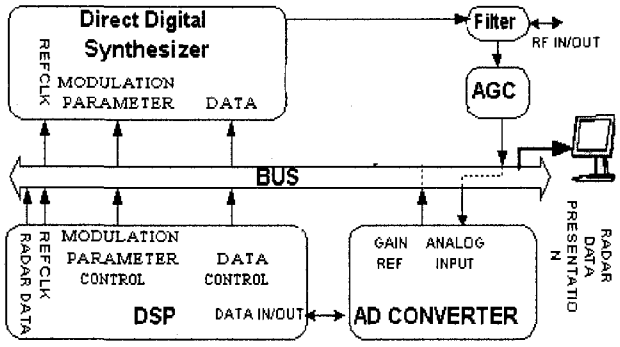

Fig. 2.1. Software-defined radar architecture

Fig 2.1 shows the basic architecture of our proposed software defined radar. The first part includes the Echo Signal Acquisition module and the Intelligent Radar Signal Generator, which can generate a number of signal formats under various modulation techniques. The second part represents the so-called IF module and up-converts the radar signals. Finally, the RF front-end operating at a frequency of 24 GHz includes RF

circuitry as well as transmitter and receiver antennas. The FMCW system block diagram is shown in Fig 2.2.

Since a DDS (AD9854) is used as modulator, the transmitted signal can be expressed as:

$$s_t(t) = A\cos(w_c t + \phi_i(t)) \tag{2.2}$$

where $\phi_i(t)$ is the phase (i = 1, 2, ···, N) and w_c the frequency of the transmitted signal. The frequency w_c shows a linear change with a discrete step in DDS. After being reflected at the target, the received signal is given by:

$$s_r(t) = B\cos(w_c t + \phi_i(t - T_D)) + n(t) \tag{2.3}$$

where T_D represents the time delay of the signal and $n(t)$ describes additive white noise.

In this work, we will apply spectral analysis to the extracted data from the IF branch after the mixer as seen in Fig. 2.2. The dominant frequency component of this signal needs to be determined by means of signal processing. As it is well known from FMCW radar theory, the triangular modulation of the transmitted signal $s_t(t)$ combined with the frequency response of our millimeter-wave front-end yields an amplitude modulation of the beat signal.

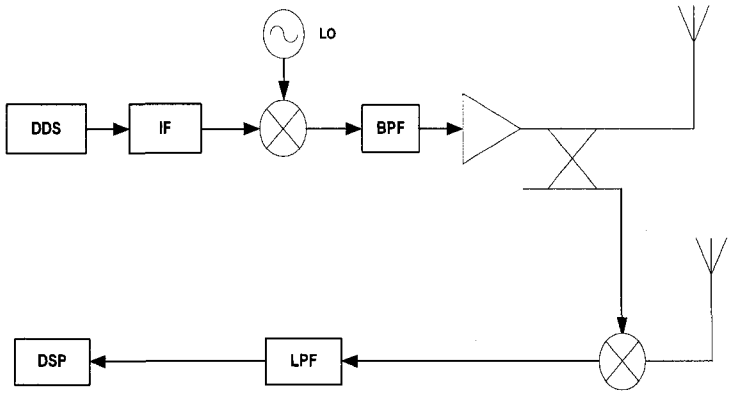

Fig. 2.2. System Block Diagram of an FMCW radar

In the FMCW measurement, the output signal of the ADC is processed in a DSP in order to precisely extract the beat frequency. A modified Hanning window $G(vT_s)$ reduces the side lobes to a tolerable level. The spectrum is calculated by

$$P_{if}(\omega_n) = \sum_{v=0}^{N-1} G(vT_s) P_{if}(vT_s) e^{-j\omega_n vT_s} \tag{2.4}$$

where ω_n is the discrete frequency. $G(vT_s)$ is hanning window in frequency domain. T_s is the sampling interval. v is the sample point.

$$\omega_n = n\frac{2\pi}{NT_s},\ n = 0 \cdots N-1$$

N is the number of samples taken in one sweep, and T_s is the period of adjacent samples. Subsequently, the maximum spectral peak at frequency ω_m, which represents the target distance, is evaluated in the spectral domain.

2.2.2 CW radar

The FMCW technique has been well accepted for its simplicity, even if it has a few drawbacks such as the difficulty of obtaining accurate distance measurements for short ranges. To give a general idea of the most important requirements for automotive radar systems, the maximum range for common commercial automotive radars is about 160 m with a range resolution of 1 m. The near range refers to distances below approximately 40 m.

To meet certain system requirements, specific waveform design techniques must be considered. The main advantage of CW radar systems in comparison with classical pulsed radars lies in its low measurement time and low computation complexity for long range and small resolution system requirements. The frequency shift keying (FSK) CW waveform [10], which uses at least two different discrete transmit frequencies (see Fig. 2.3) for an unambiguous range measurement, has been proposed.

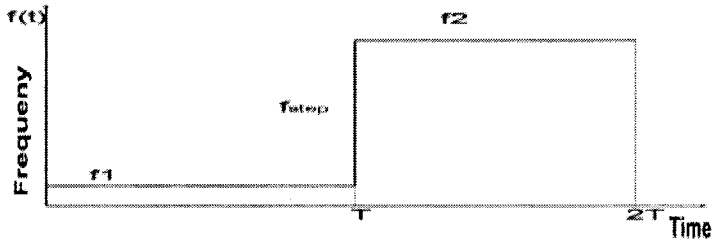

Fig 2.3 CW waveform principles: FSK modulation.

It has been well known that radars operating with a single CW signal cannot measure time delay without ambiguity. Therefore, they cannot measure target range. Because

distances measured with millimeter wave radars are much larger than the transmitted signal's wavelength, the measurement may be ambiguous according to the following equations:

$$\begin{aligned} \omega \cdot \tau_d &= \phi + 2\pi n \\ \tau_d &= \frac{2d}{c} \quad \omega = \frac{2\pi \cdot c}{\lambda} \\ \frac{4\pi \cdot d}{\lambda} &= \varphi + 2\pi n \end{aligned} \tag{2.5}$$

where n is an unknown integer ω is the transmitted frequency, c is the velocity of light and d is the measured distance.

To avoid this ambiguity problem, a minimum of two discrete transmitted frequencies is required. The resulting modulation is similar to a 2FSK modulation [5] used in communications. With two frequencies involved, the ranging measurement is achieved by measuring the relative phase difference between the two received signals as follows: As shown in Fig. 2.3, each frequency is transmitted within a coherent processing interval of length T. Using a receiver with a phase discriminator, the relative phase between the received echo signal and the reference signal is measured. This process is repeated sequentially for both frequencies f_1 and f_2. The frequency difference $\Delta f = f_2 - f_1$ is selected dependent on the desired unambiguous range.

It is assumed that the difference Δf is very small compared to f_1 or f_2, i.e. $\Delta f/f_i \cong 10^{-6}$. Because f_1 and f_2 are very close to each other, their Doppler shift will be approximately the same.

$$f_{Doppler} \approx \frac{2vf_1}{c} \approx \frac{2vf_2}{c} \tag{2.6}$$

The time-discrete received signal is Fourier-transformed in each coherent time interval T, and targets are detected by an amplitude threshold according to the constant false alarm rate (CFAR) technique [4]. Due to the small frequency difference between the transmitted signals for both frequencies, a single target is detected at a given Doppler frequency for adjacent time intervals T, but different phases are observed. A complex spectral analysis provides phase information and it is the basis for target range estimation:

$$\Delta\phi = \omega_1\tau_d - \omega_2\tau_d = |\omega_1 - \omega_2|\tau_d \tag{2.7}$$

$\Delta\phi$ is the phase difference, ω_1 is the first frequency and ω_2 is the second frequency. The transmitted and received signals can be expressed by the following equations:

$$s_t(t) = A\cos[\omega_n t + \phi_{o,n}] \tag{2.8}$$

$$s_r(t) = B\cos[(\omega_n \pm \omega_D) * (t - \tau_d) + \phi_{o,n}] + n(t) \tag{2.9}$$

ω_n is the transmitted frequency with $n = 0, 1, 2$ where the product $\omega\ \tau_d$ represents the phase contribution due to the propagation delay and ω_D the Doppler shift due to target movement. The echo signal is correlated with its own reference signal during target illumination in order to measure the phase associated to the propagating delay. This is repeated for each frequency. In the case of a moving target, the Doppler shift needs to be evaluated by means of an FFT. The mixer is used as a phase discriminator and the IF output provides a relative phase to voltage relation as follows:

$$V_{out} = a_1 a_2 \sin(\varphi_1 - \varphi_2) \tag{2.10}$$

where the product a_1a_2 represents the product of reference and echo signal amplitudes at the mixer LO and RF ports, respectively.

2.2.3 SS radar

SS signals are a general class of ranging waveforms, which utilize a code sequence as a means for achieving high range resolution and good self-clutter performance [6]. The SS technology has been widely used in wireless communication systems [31]. The transmitted BPSK signal can be written as:

$$\begin{aligned} s(t) &= cos(\omega_c t + \phi(t)) \\ s(t) &= m(t).cos(\omega_c t) \end{aligned} \tag{2.11}$$

with $\mathrm{m}(t)\begin{cases} 0 & 1 \\ \pi & -1 \end{cases}$

Then, the received BPSK signal is:

$$s(t-\Delta t) = m(t-\Delta t)cos(\omega_c + (t-\Delta t)) \tag{2.12}$$

The range of a target is calculated from the traveling time of the reflected wave. This range R is calculated in an SS system by

$$R = cnT_c / 2 \tag{2.13}$$

where c is the velocity of light, T_c is the chip duration and nT_c is the signal traveling

time. By measuring T_c, the distance can be calculated. The ideal code uses a Dirac impulse as an autocorrelation function. This allows the code to have the maximal correlation with a non-delayed version of itself and not to interfere with itself if a portion of the code appears in the signal at a different delay. The most important codes in use are the maximal length sequences using an autocorrelation code that shows nearly impulse characteristics. Its value is $2n - 1$ at an offset of $t = 0$ and -1 at all other offsets. The typical acquisition method used when precise information is not available is to scan through all possible code positions until the correct delay is found. In general, the detection of the chip delay is simple due to the strong correlation at the correct delay. In this proposed system, an SS technique is adopted for range measurement. The traveling time T_c is evaluated by correlating the received pseudorandom (PN) code with a reference PN code, which is shifted by the transmitted PN code. A PN code with a sequence of 1, 2 ... is used. The autocorrelation function for the PN code is given by:

$$R_{aa}(\tau) = \frac{1}{2N}\int_{-N}^{N} c(t)c(t-\tau)dt$$

$$= \begin{cases} 1 - \dfrac{|\tau|}{T_c} & |\tau| < T_c \\ 0 & |\tau| \geq T_c \end{cases} \qquad (2.14)$$

where $c(t)$ is the PN code and N denotes the length of PN code. T_c is the chip duration and τ is the time delay. In our case, we use a code length N of 32. Subsequently, the range information can be deduced from the autocorrelation characteristics of the PN code.

2.3 Six-Port Technology for Software Define Radar

The software defined radar where the following key components are used: at first, it is necessary to incorporate a flexible signal generation technique in connection with the frequency and the amplitude of the signal. Therefore, the DDS is an excellent candidate for realizing a flexible signal source. For the purpose of the signal processing, the received signal can be processed in a DSP with different algorithms corresponding to different radar modes. In terms of front-end hardware, the FMCW radar mode requires a down-converting element, such as a mixer, in the receiver to generate the beat frequency between the transmitted and received signals, while the CW radar mode needs a precision phase detector to extract the phase difference between the transmitted and received signals containing the required distance information. Usually, a phase detector can also work as a mixer. In this work, we deploy the six-port technique that can be used to replace the mixer.

The six-port is a passive device that can perform accurate phase measurements. It determines the phase difference between the received signal and the reference signal by measuring the power level at its four output ports. Six-ports can be fabricated in monolithic microwave integrated circuit (MMIC) technology [32], which is very attractive for low-cost and compact size applications [33]. The six-port-based radar sensor has been introduced as an alternative approach for the realization of CW systems [34]. Furthermore, the six-port direct conversion technique is very promising for the design of a software-reconfigurable receiver at millimeter-wave frequencies. The main

advantage of the six-port technique compared to the sampling architecture is its simple construction only requiring the reference oscillator as an active microwave component in the structure, making this technology particularly attractive for future low-cost microwave and millimeter-wave front-ends. Therefore, it is feasible to use the six-port technique to realize the receiver part of a software-reconfigurable range radar with a unique hardware configuration.

2.3.1 Six-port concept

A typical example of a six-port circuit is shown in Fig. 2.4. A six-port presents a linear and passive topology. The complex relationship between the incident signals at two of its ports can be determined from relatively simple power readings at the remaining four ports [35], [36]. The signal at port 1 is usually used as the reference source, and the signal at port 2 is received as the unknown signal. The signals at the power detectors can be written as a linear combination of the incident signal a_2 and the reflected signal b_2 as follows [37]:

$$b_i = A_i \cdot a_2 + B_i \cdot b_2, \qquad i = 3...6 . \tag{2.15}$$

With $\Gamma = (a_2/b_2)$, the readings by the power detectors are

$$P_i = |b_i|^2 = |A_i|^2 \cdot |b_2|^2 \left| \Gamma + \frac{B_i}{A_i} \right|^2, \qquad i = 3...6 . \tag{2.16}$$

Once the relations between the input and output ports are known, the vector relation (amplitude and phase) between the two signals a_1 and a_2 can be determined by measuring the scalar power levels at the other four output ports. The relation between the input and output ports can be found very accurately with a calibration procedure.

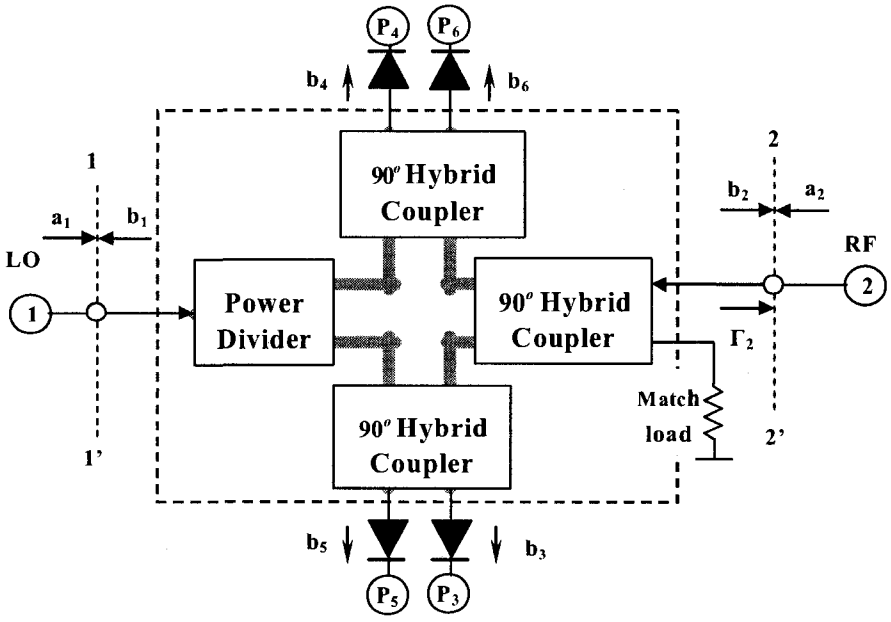

(a)

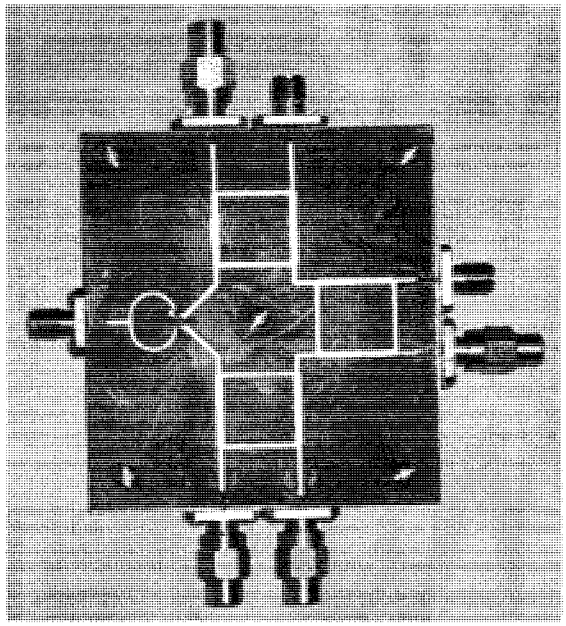

(b)

Fig. 2.4 (a) Block diagram of a typical six-port circuit that involves hybrid couplers and power dividers; (b) Photograph of the fabricated 4 GHz six-port in microstrip technology.

With respect to the CW radar, the distance of a target can be calculated by comparing the phase difference between the transmitted and received signals [38]. If the distance is much larger than the wavelength, the distance measurement becomes ambiguous, which can be expressed as equation 2.5. To avoid this ambiguity problem, a second signal with a different frequency f_2 can be used to yield a two-tone CW system capable of performing distance measurements, and the range can be obtained by measuring the phase shift between these two frequencies f_1 and f_2

The CW radar can primarily not be used for distance measurements unless we

introduce two- or three-frequency modulation schemes. In the latter case, the range can be obtained easily from a measurement of the phase shift between the output signals at the two frequencies, which is easily implementable with the six-port demodulator.

2.4 Conventional Radars versus Software Defined Radar

Why do we need to design a software defined radar? This question was briefly mentioned in the introduction of this thesis but we will present a number of quantitative cases to show the importance of the proposed software-defined radar technique. Let's compare four different radar types with the software defined radar. As an example, we consider the design of a radar with a range resolution requirement of 0.05 m. For the FMCW radar, the range resolution [4] is:

$$R_{resolution} = \frac{c}{2f} \tag{2.17}$$

The required FMCW bandwidth is 3 GHz. On the other hand, for the CW radar, assuming a phase discrimination of 1°, the range [4] is:

$$R = \frac{c \cdot \Delta\varphi}{4\pi \cdot \Delta f} \tag{2.18}$$

Thus, the required bandwidth to achieve a range resolution of 0.05 m is 8.3 MHz. The direct sequence spread spectrum (DSSS) radar range resolution [39] is:

$$R = c \bullet Tc/2 \tag{2.19}$$

where c is the speed of light and T_c is the chip duration. Thus, the required spread bandwidth and chip duration is 3 GHz and 0.33 ns, respectively. The range resolution of the frequency hopping spread spectrum (FHSS) radar [40] is given by:

$$R = c \cdot \tau / 2 \tag{2.20}$$

where τ is the hop shift. Thus, the required shift between hop frequencies is calculated to be 0.33 ns.

From theses considerations, we determine a required bandwidth of up to 3 GHz for the FMCW and DSSS radars, which are difficult to implement in hardware. Moreover, it is hard to control the required shift of 0.33 ns in the FHSS radar. In the software defined radar these requirements are simple and easy to implement as a combination of different radars can be used. In Table 2.1, a comparison of bandwidth, noise resistance ability, multitarget recognizant, and maximum range for five types of radars are shown for a range resolution of 0.05 m.

The comprehensive performance of the software defined radar is better than any single type of radar, even without having to offer a large bandwidth. Its key feature is the merging of the functionality of different radar sensors taking advantage of their complementarities.

Table 2.1 Performance comparison of five types of radars

	Bandwidth/hopping shift (MHz)	Noise resistance ability	Multitarget reorganization	Maximum Range (m)
FMCW radar	3000	intermediate	yes	150
CW radar	8.3	low	no	18
DSSS radar	3000	high	yes	60
FHSS radar	3000	high	yes	60
Software defined radar	300	high	yes	150

2.5 Software Defined Radar Algorithm

The software defined radar is fully controlled by a single DSP board including transmitter and receiver. The proposed system has only a single microwave front-end, but the type of radar used for a specific operation is selected by the software. A system block diagram is shown in Fig. 2.5.

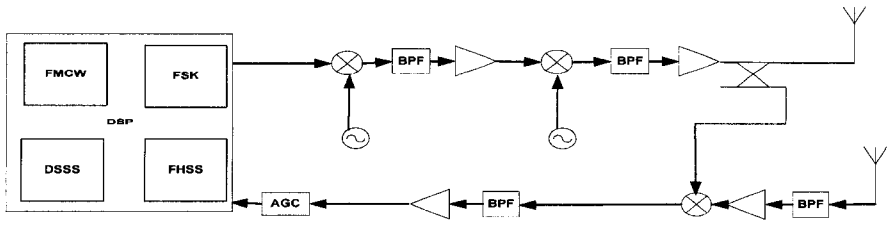

Fig 2.5 Block diagram of the proposed software defined radar

The digital output of each receiver channel is directly fed to the DSP. The signal processing modes for the received signals are adapted to the transmit modes by the DSP software and their operation can be modified with changes in target velocity and range, as well as the required specifications in resolution and processing accuracy.

The flow diagram for the software defined radar algorithm is shown in Fig 2.6. At startup, the FMCW mode is used in order to obtain a rough estimate for target range and velocity. The received signal, which contains target velocity information, is fed to the corresponding circuit. If the target is moving away ($v < 0$), the radar continues operating in FMCW mode. On the other hand, if the target is approaching ($v > 0$), the algorithm switches to another mode depending on the range. For distances larger than 18 m, it changes to DSSS or FHSS mode. If the range is smaller than 18 m, the CW mode is activated.

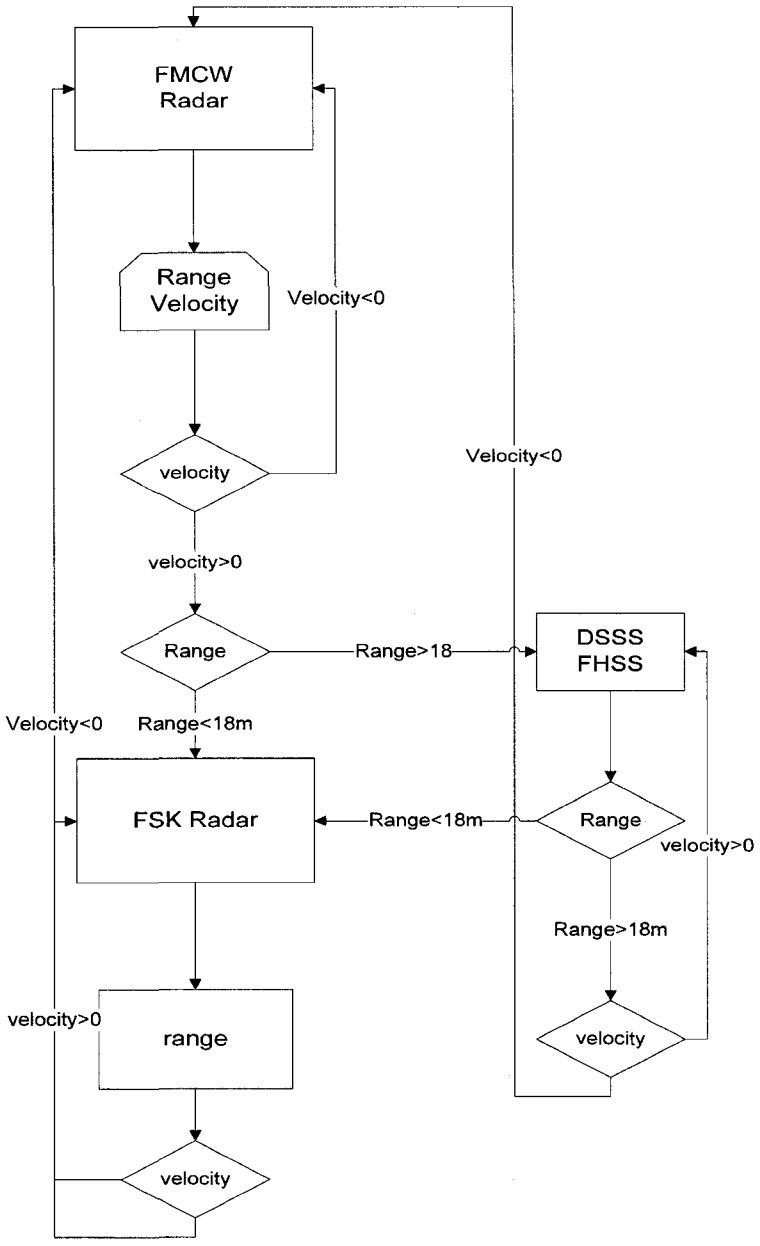

Fig 2.6 Flow diagram for the software defined radar algorithm.

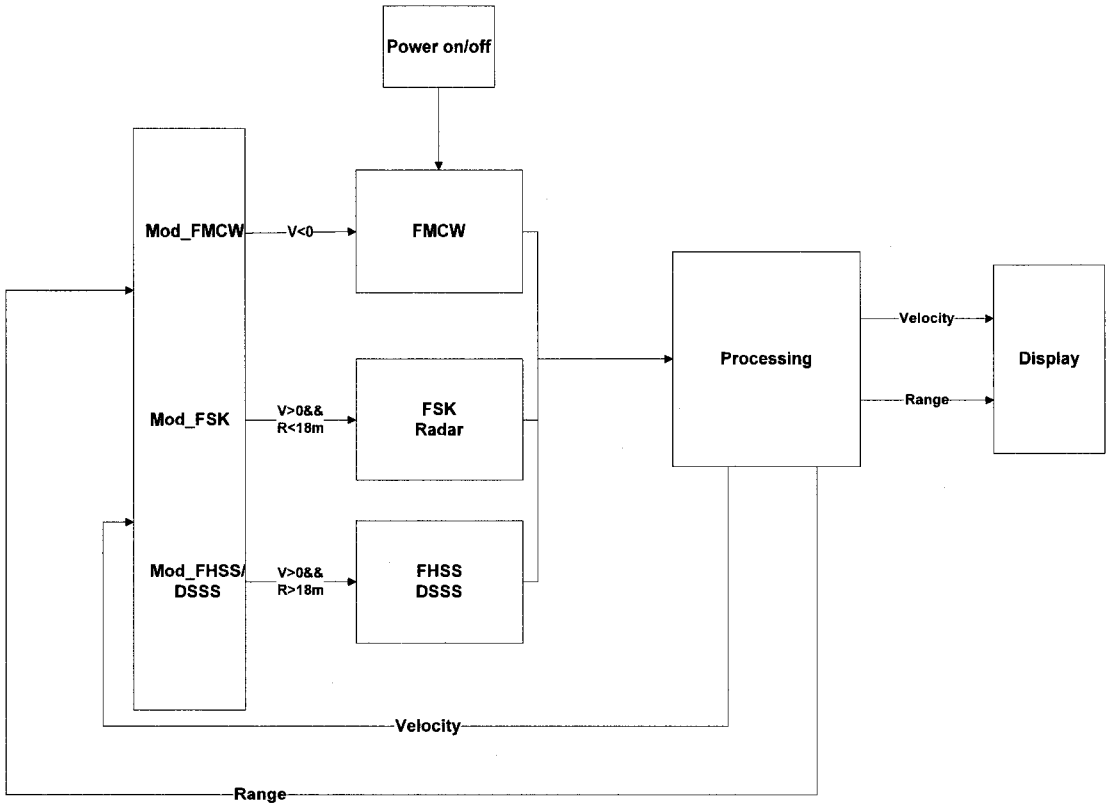

Fig 2.7 Block diagram of controller system

To verify the functionality of this novel concept, several different simulations were made. The design process includes high level MATLAB simulations of the entire radar system. After verification of the system behavior, we use high-level code to simulate the algorithm of each individual module. The following section briefly introduces the five radar types and focuses on the system architecture implementation in MATLAB/ Simulink. MATLAB is also used to build the model for the controlling part of the software defined radar as shown in Fig 2.7.

2.6 Functional Simulation of Synthetic Software Defined Radar

2.6.1 Simulation of the software defined radar based on mixer

In this section, a functional simulation of the entire synthetic software defined radar in a MATLAB/Simulink environment is presented. This simulation offers a good insight into the system operation and is able to predict performance, thus reducing cost-intensive fabrication failures. The simulation has three parts: software defined radar algorithm, RF transceiver and controlling algorithm. These three parts are related to and affected each other. Finally, an overview of software defined radar is presented in this section.

The goal of this section is to simulate the synthetic software defined radar, starting with a simple model and then increasing the complexity of the model by incorporating the control system. The inclusion of noise effects makes the output of the simulation more realistic. The simulations are performed in MATLAB. The synthetic software defined radar simulation is shown in Fig 2.8.

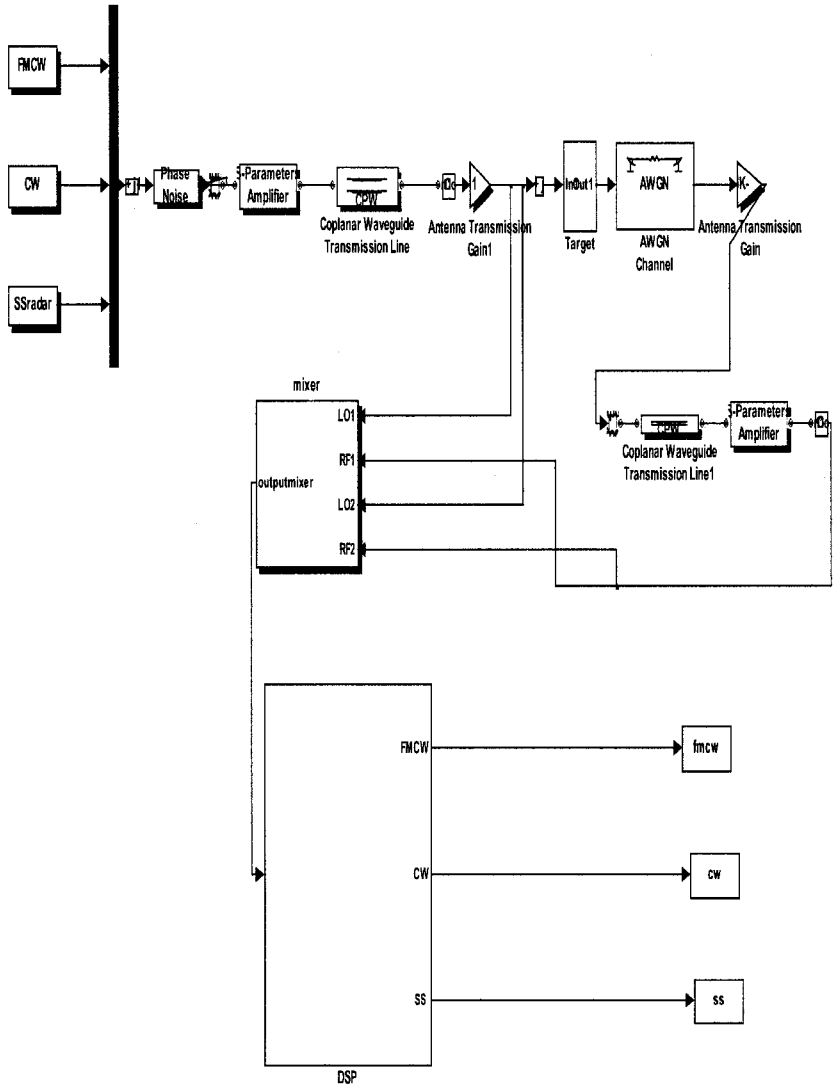

Fig 2.8 Software defined radar based on mixer simulation in MATLAB

2.6.2 Simulation of software defined radar based on six-port technique

Before building a six-port software radar, a MATLAB/Simulink model as shown in Fig. 2.9 is developed in order to perform a good performance prediction of the system. The simulation results will be compared with measurements in the next section.

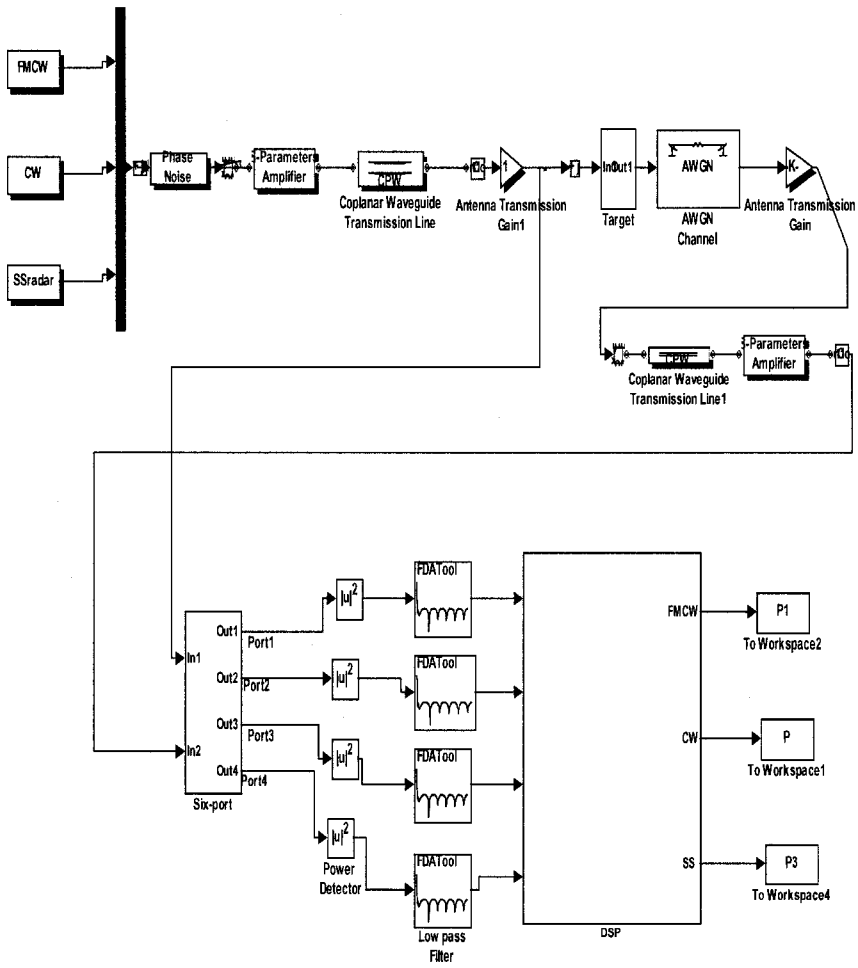

Fig. 2.9. Software defined radar based on six-port simulation in MATLAB.

There are three signal blocks at the transmitter. The phase noise is injected after the amplifier of RF block in Simulink. The time delay and attenuator are built to simulate the target. The AWGN channel follows after the target. Then the coupled signal and the received signal are fed into the six-port. After the signal output, the square blocks and low pass filter are inserted as the power detector. The simulation results will be shown in the following section.

2.6.3 FMCW mode

The software defined radar uses a digital transceiver. Each mode is represented as a different block in the DSP. The FMCW radar bandwidth is 20 MHz and the carrier frequency is 45 MHz [41]. The MATLAB level system model is shown in Fig 2.10. Fig 2.11 shows the simulation results.

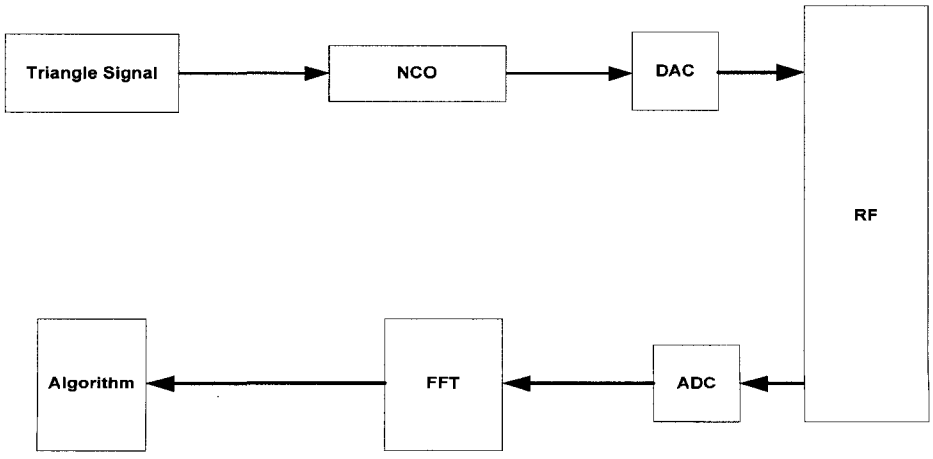

Fig 2.10 Block diagram of the FMCW radar

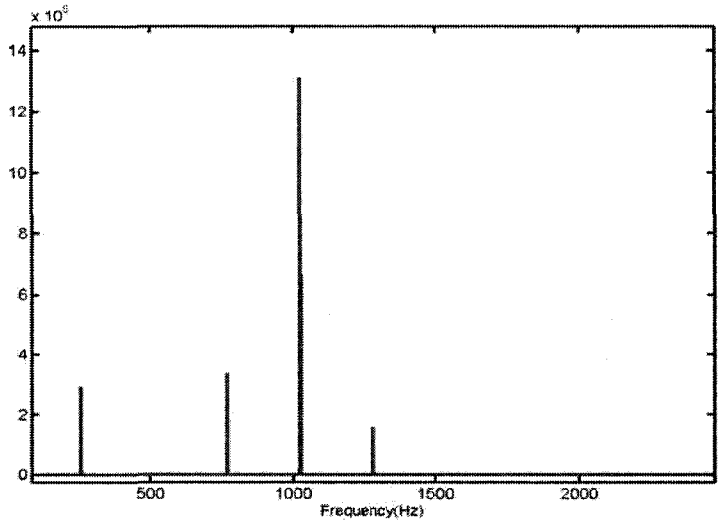

Fig 2.11 Simulation results of the FMCW radar

From Fig 2.11 the beat frequency is the maximum one in the spectrum from which the range can be calculated. Also, we can use the MUSIC algorithm in chapter 3 to generate more accurate results.

2.6.4 CW mode

The conventional CW mode makes use of a modulation of two frequencies, but in the present work, the three-frequency modulation as described in chapter 5, which follows up the same principle, is adopted. The carrier frequency used in this simulation setup is 45 MHz with a frequency step $\Delta f = 14\,\text{MHz}$. The system model is show in Fig 2.12. Fig 2.13 shows the MATLAB simulation results. From these results, the target distance can be determined with the help of (4.2).

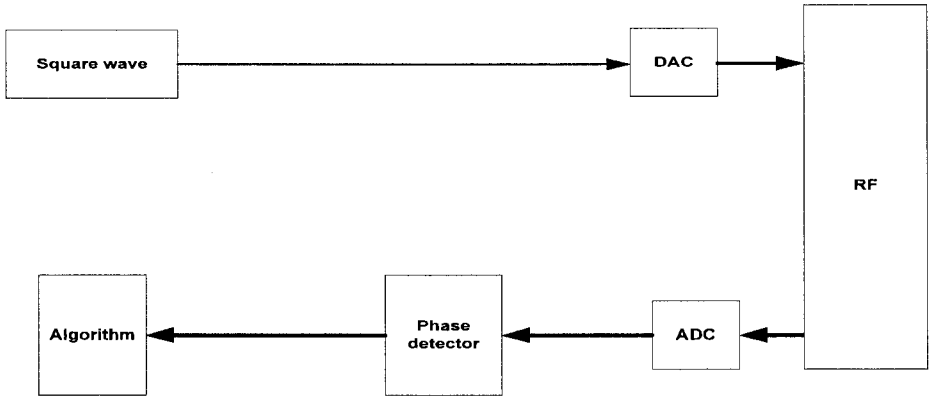

Fig 2.12 Block diagram of the CW radar

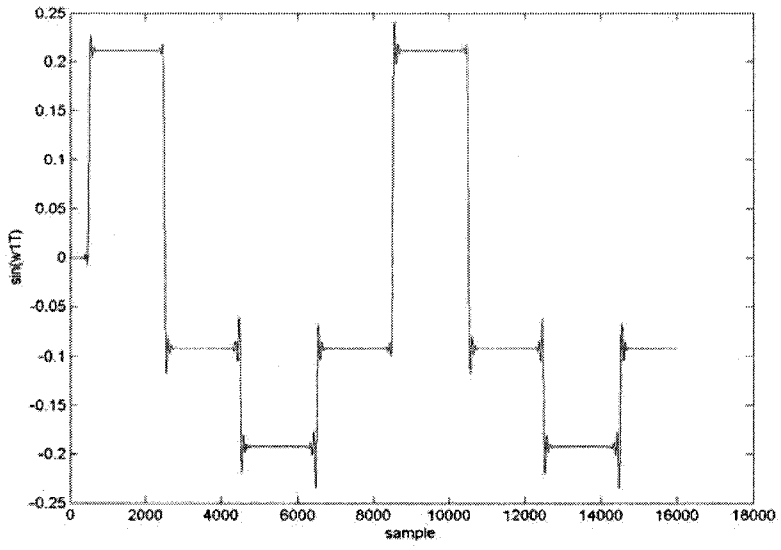

Fig 2.13 Simulation results of the CW radar

There are three frequency differences, so two phase differences are plotted in Fig 2.13. All the comparisons will be shown in chapter 5.

2.6.5 DSSS Mode

The DSSS radar [27], [42] is similar to the SS radar. The code generator, modulator, correlator, DAC, and ADC are included in the FPGA board, which allows for an easy implementation. Therefore, the range can be determined from a measurement of the chip duration T_c. The MATLAB level system model for the DSSS radar module is shown in Fig 2.14. Fig. 2.15 shows the simulation results.

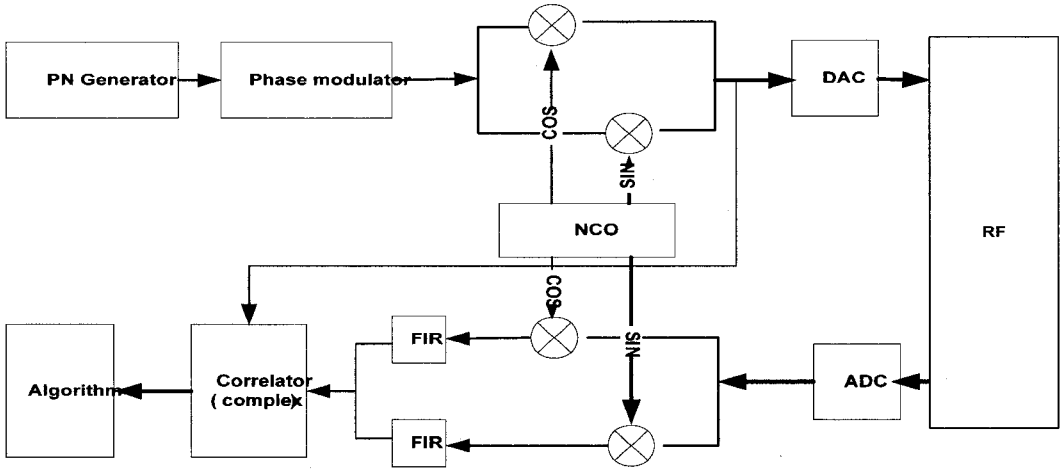

Fig 2.14 Block diagram of the DSSS radar

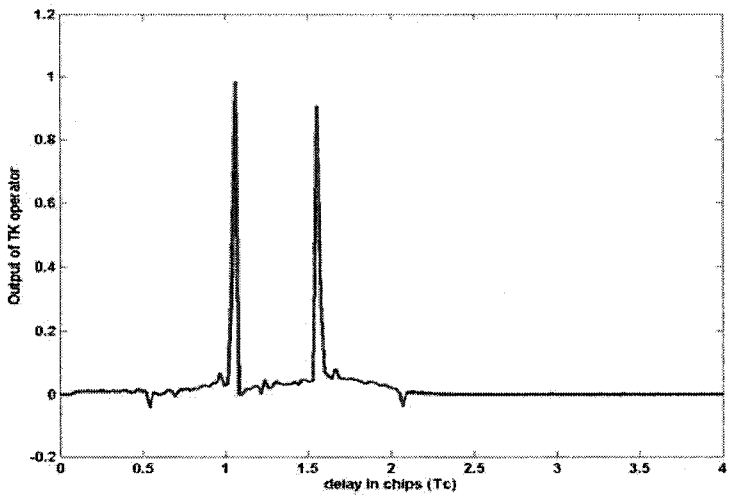

Fig 2.15 Simulation results of the DSSS radar

In Fig 2.14, the two targets are simulated in MATLAB. One target is at the 5.6 meter, another one is at 8.6 meter. So we can see the two peak with half chip delay in Fig 2.15.

2.6.6 FHSS Mode

The working principle of the FHSS radar [40] is based on the application of the SS frequency hopping technique. It shows a very high resistance against any kind of interferences, including those originating from other similar systems. The range resolution of FHSS radar is independent of the bandwidth, but varies with the hop rate. Its MATLAB level system model is shown in Fig 2.16. The mathematical relation for range measurement is similar to that for the DSSS radar but is not dependent on the chip duration. Fig 2.17 shows the simulation results.

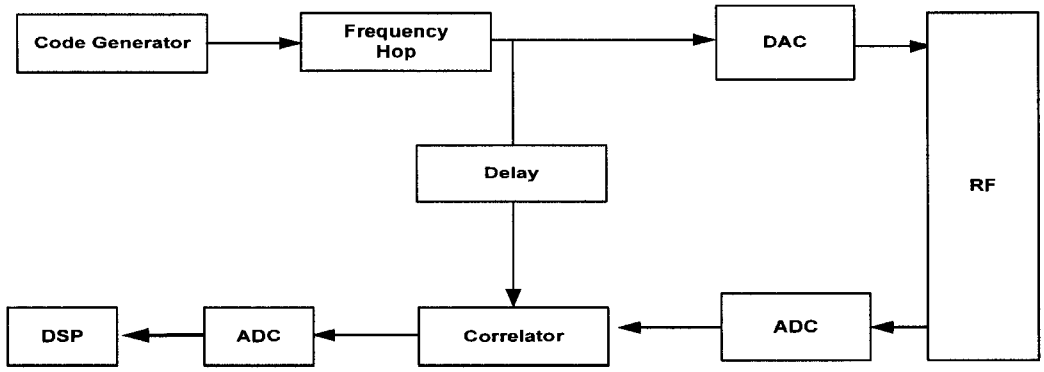

Fig 2.16 Block diagram of the FHSS radar

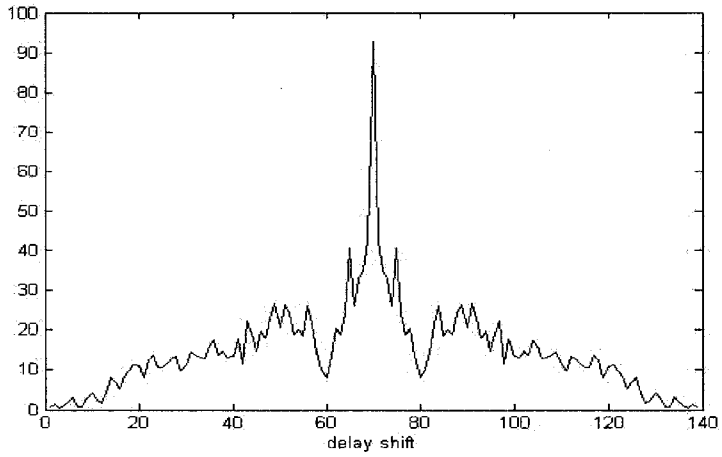

Fig 2.17 Simulation results of the FHSS radar

The target is simulated at 105 meter, so the peak is at a delay of 70 chips. There is a difference related to the modulation scheme such as BPSK modulation in DSSS, and FSK modulation in FHSS.

2.7 Summary

In the present work, four types of radars are proposed and discussed for their use and implementation in software defined radar system. The common part for the entire system is the RF front-end. Table 2.2 shows the parameters of each of these radars. Each type has its own characteristic functions and features. Based on different range resolution requirements, a certain type of radar can be selected. Moreover, DSSS and FHSS radars can work in high interference environments. Thus, in the far region they give better range measurement performance than FMCW and CW radar. The range resolution of the CW radar is independent of the frequency and bandwidth and depends only on the phase detector resolution. Among all the presented radar types, the CW radar yields the smallest range resolution. Therefore, the CW radar is used to measure near or short-range distances. In addition, if the proper frequency interval is selected, ambiguous range measurement in the CW radar can be avoided. The range resolution of the FMCW radar is not as good as for the CW radar but better than for DSSS and FHSS radars. The FMCW radar shows more capacity to withstand the distortion originating from interferences than CW radar. It is not as good as the DSSS/FHSS radar. Consequently, the FMCW radar is used as the prediction radar in the synthetic software defined radar.

Table 2.2 Parameters of software defined radar

	center frequency (MHz)	bandwidth (MHz)	range resolution (m)
CW	45	8.3	0.05
FMCW	45	30	5
DSSS	45	20	5.6
FHSS	45	6	3

We can learn a great deal from communications, where similar concepts for software-defined radio are realized. For future applications, the processing needs for communications are comparable to remote sensing or even higher. The calibration is also done digitally: the reference is digitized, the system is calibrated, and the data are stored before operation and used for calibration in the processing.

By using these novel digital techniques, the software defined radar provides persuasive advantages that are difficult or impossible to achieve with an analog system. These advantages include a greatly improved processing accuracy, a flexible interface with radar control center, a convenient control of the work form, signal wave forms and LO frequencies of the receivers to obtain a much higher stability, complex signal processing, and the use of more complex waveforms for radar systems with anti-jam

features. With the digital radar receiver, it is possible to generate and process most types of complex waveforms, arbitrary time bandwidth, and arbitrary processing control. It affords more flexibility and higher performance and offers better time and environment stability than traditional analog techniques.

Because the entire functionality of this new type of software defined radar sensors can be included in the software, their operating modes may be multifunctional, selective, active, passive, and corrective. In addition to the typical radar function, they may operate as radiometers, for communication applications, or even as electronic warfare transmitters. Several components and subsystems of these envisioned software defined radar sensors are already under development. Market cost and power consumption are still high for DSP, but, like for most digital hardware, they are expected to decrease in a near-distant future. Appropriate antennas with excellent features, such as wide bandwidth, dual polarization, and low loss are under development. We also consider that the system requires a trade off between resolution, bandwidth, antenna size, and power balance.

CHAPTER 3

SIGNAL PROCESSING METHODS OF SYNTHETIC SOFTWARE DEFINED RADAR

The software defined radar techniques have been introduced in the previous chapter. In this chapter, several algorithms will be described and discussed. With respect to FMCW, CW and SS radar schemes, there are different signal processing methods. Generally, FFT and MUSIC (Multiple Signal Classification) algorithms are used for FMCW type of radar for frequency estimations. Multiple frequency methods for CW radar have also been presented. On the other hand, it is found that SS radar provides good interference immunity but it is not easy to achieve a good range resolution. In this section, SPM, TK operator and wavelet algorithms will be studied in order to improve the range resolution in SS radar.

3.1 FFT and Music algorithms for FMCW radar mode

FMCW radar signal processing is usually made on the basis of a simple fast Fourier transform (FFT) algorithm. This allows mathematically removing unwanted signal responses that appear as ripples. However, the response resolution of the FFT scheme essentially depends on the frequency bandwidth of measured data. In general, it is difficult to distinguish the desired direct response from the unwanted signals in some

range measurements, in particular, when the target is too near or too far from the radar with reference to the operating wavelength. Even though the peaks are resolved distinctly, we may not be able to eliminate the unwanted signals when skirts of the response become overlapped. Therefore, a high-resolution frequency estimation technique has been desired in practice. In addition, signal or environmental noise including white noise can be greatly reduced or eliminated with the desired technique.

In this chapter, we begin with the investigation of an algorithm based on the MUSIC framework [14], which allows for effective frequency estimates at locations of the highest peaks. Super-resolution techniques are applied in the processing of the time-domain data that are measured with our software-defined radar showing their high-resolution capability in the handling of experimental results.

Super-resolution techniques for time-frequency estimation are proposed in this work and applied in time-domain data acquisitions with a software-defined radar system. With reference to a number of existing super-resolution techniques, the MUSIC algorithm is studied in detail. Frequency estimates are made in terms of locations of the highest peaks. This technique eliminates unexpected or unwanted signals that appear as ripples in the frequency domain. Experimental results suggest that the frequency bandwidth required by the MUSIC algorithm in resolving distinct time-domain responses and eliminating unexpected signals is much narrower than what is required by the FFT scheme. Therefore, it can be concluded that the MUSIC algorithm is applicable to time-domain measurements with software-defined radars and has a much higher resolution capability than the conventional FFT technique.

It is known that the FFT is an efficient algorithm for computing the DFT of a data sequence. It is extremely useful for power spectrum estimation, as it breaks down a signal into constituent sinusoids of different frequencies. We assume that there are N frequency components in the sampled data. The received signal $s_r(t)$ can be written as

$$s_r(t) = Ks_t(t) + n(t) \tag{2.3}$$

where $s_t(t)$ is the frequency modulated (FM) transmitted signal and K is the amplitude of the received signal, and $n(t)$ is additive white noise. It detects frequencies in a signal by performing an eigen-decomposition on the covariance matrix of a data vector obtained from the samples of the received signal. The key to MUSIC is its data model

$$\mathbf{s_r} = \mathbf{A}\,\mathbf{s_t} + \mathbf{n}$$

where $\mathbf{n}$ is a vector of M noise samples, $\mathbf{s_t}$ is a vector of N signal amplitudes, and $\mathbf{A}$ is the M x N Vandermonde matrix of samples of the signal frequencies. Then, the $M \times M$ covariance matrix [15] of $\mathbf{s_r}$ can be written as

$$\begin{aligned} \overline{R} &= E\left[s_r(t) s_r(t)^* \right] \\ &= ASA^* + W \end{aligned} \tag{3.1}$$

where $\mathbf{S}$ and $\mathbf{W}$ are the covariance matrices of the source and noise, respectively. White noise is usually assumed spatially and temporally uncorrelated with the desired signal. Assuming that the mean of the noise vector is zero, and its variance equals σ^2, the noise matrix can be written as

$$\begin{aligned} W &= \lambda_{\min} S_o \\ &= \sigma^2 I \end{aligned} \tag{3.2}$$

where S_0 is the covariance matrix and $\lambda_{\min}$ represents the smallest solution satisfying $|S-\lambda S_0|=0$. I denotes the identity matrix. The received IF signal is shown in Fig,3.1.

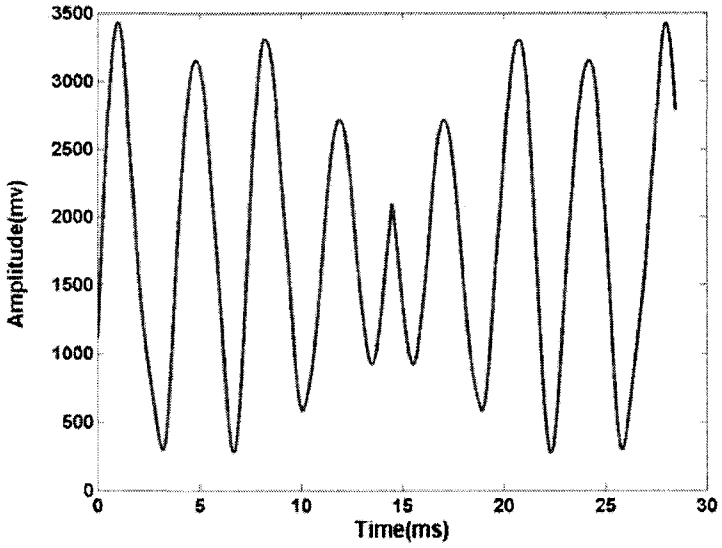

Fig. 3.1. Time-domain IF signal

From the eigen-decomposition of **R**, we use the eigenvectors associated with N maximum eigenvalues to define the signal subspace (the column space of **A**), and use the other eigenvectors to define the noise subspace.

The rank of ASA^* is D and can be determined directly from the eigenvalues of R in the matrix S_o. Because the minimum eigenvalue of $R-\sigma^2 I = APA^*$ is zero, $\lambda_{\min}$ must occur N times. Therefore, the number of signal estimators is

$$D = M - N \tag{3.3}$$

It is obvious that if $D<M$ and **S** is positive definite, the matrix $R-\sigma I$ has rank D, and therefore a null space of dimension $M-D$. Furthermore, it follows that all columns of **A** are orthogonal to this null space.

The $M-D$ eigenvectors corresponding to the minimal eigenvalues are orthogonal to the D signature vectors. We define E_N to be the $M\times(M-D)$ matrix whose columns are the $M-D$ noise eigenvectors. Taking advantage of the orthogonality of the signal and noise subspaces, the pseudo-spectrum [43] can be estimated by

$$P_{music}(f)=\frac{a(f)^H a(f)}{a(f)^H E_N E_N^H a(f)} \tag{3.4}$$

where $a(f)$ is the received profile corresponding to the columns of **A**. Then, we can estimate the position of each frequency point by searching for the peak position of (3.4). We will show the experimental result in chapter 4.

3.2 Multiple frequencies algorithm for CW radar mode

This section proposes and describes a new waveform modulation scheme based on CW signals, which leads to more accurate range measurements and larger measurement range. This new waveform is based on the FSK radar that uses two CW signals with different frequencies [44]. In this work, we propose the use of three frequencies. Unambiguous ranging with high resolution and accuracy can be obtained in this case. In the following, we will describe our novel three-frequency radar technique in section 2.2 after a brief introduction to the FSK waveform design technique.

Using the relation between propagation delay τ and range R and rearranging accordingly provides a linear relation between the target distance and phase difference as follows:

$$R = \frac{c \cdot \Delta\varphi}{4\pi \cdot \Delta f} \tag{3.5}$$

Δf is the frequency difference from the central frequencies.

Equation (3.5) clearly indicates that a maximum range interval must be defined to avoid ambiguous range measurement due to the periodicity of the phase difference exceeding 2π. This maximum unambiguous range can be controlled by a proper selection of Δf. For example, to obtain an unambiguous range of 10 m, a frequency difference of 15 MHz is required We can define a parameter σ_R proportional to the range resolution but independent of the phase measurement hardware and technique, such as,

$$\sigma_R = \frac{2\pi}{R_{\max}} \tag{3.6}$$

Depending on the achieved phase measurement resolution for the given radar, range resolution can be evaluated from (3.6). To optimize the resolution for short distances without introducing ambiguity for long ranges, three frequencies can be used, which will be presented in the following section.

To achieve an unambiguous maximum range measurement of 100 m, a frequency difference equal to 1.5 MHz is necessary. The use of a DDS is an additional advantage of this modulation technique, since the desired waveform can be easily realized. The disadvantage is related to the restrictions imposed by the maximum range and range

resolution of FSK CW. Therefore, we propose to use a three-frequency waveform as shown in Fig. 3.2.

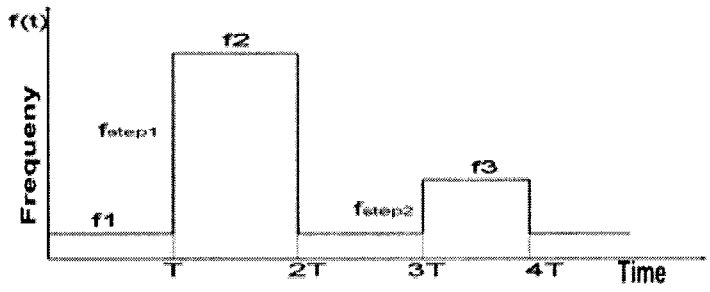

Fig.3.2 Three frequency waveform CW modulation

In this waveform, Δf_1 is optimized for close range and Δf_2 for far range. With an appropriate timing, we can calculate two ranging values from two phase differences defined as follows:

$$\Delta\varphi_1 = \varphi_2 - \varphi_1 \tag{3.7}$$

$$\Delta\varphi_2 = \varphi_3 - \varphi_1 \tag{3.8}$$

where φ_1, φ_2, φ_3 relate to the frequencies f_1, f_2, f_3 as shown in Fig. 3.2.

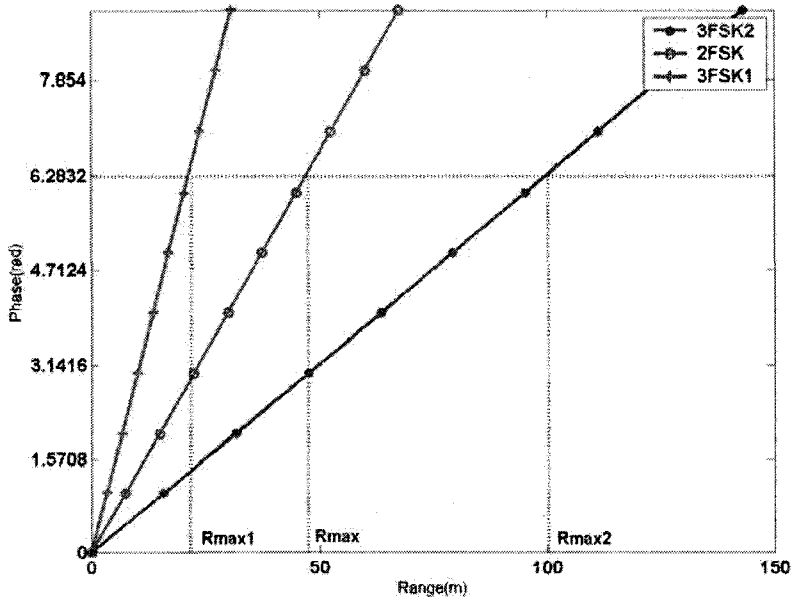

Fig. 3.3 Phase versus range plot for three-frequency and two-frequency modulation

This signal configuration results in two distinctive unambiguous range limits and range resolutions over the respective range intervals:

$$R_{\max,i} = \frac{c}{2\Delta f_i} \tag{3.9}$$

Δf_i is the frequency difference from the multi-carrier frequency.

A configuration example for this type of signal modulation is to set $\Delta f_1 = 7$ MHz and $\Delta f_2 = 1.5$ MHz, which yields $R_{max,1} = 21$ m, $\sigma_{R,1} = 18$ deg/m, $R_{max,2} = 100$ m, and $\sigma_{R,2} = 3.6$ deg/m. This shows that for a given phase measurement technique, the ranging resolution can be improved by using a larger frequency separation at the expense of a shorter unambiguous range. In order to select the right range value among the set $\{R_{mes,1},$

$R_{mes,2}\}$, rules must be established based on the range ambiguity limits $\{R_{max,1}, R_{max,2}\}$.

Table 3.1 shows these conditions that need to be verified for three different test cases.

Case	Range(m)	$R_{max,1}$	$R_{max,2}$	$R_{mes,1}$	$R_{mes,2}$	Valid(Y/N)
1	$R_{mes,1}$	$<$	$<$	-	$\cong$	Y**
	$R_{mes,2}$	$<$	$<$	$\cong$	-	Y
2	$R_{mes,1}$	$>$	$<$	-	$\neq$	N
	$R_{mes,2}$	$>$	$<$	$\neq$	-	Y
3	$R_{mes,1}$	$>$	$>$	-	$\neq$*	N
	$R_{mes,2}$	$>$	$>$	$\neq$*	-	N

Table 3.1: Conditions for an unambiguous range measurement using the three frequency scheme

*More than the effective radar range resolution.

** More accurate results than $R_{mes,2}$

From multiple frequency algorithm, we can choose different maximum unambiguous range and minimum detectable range. We will show experiment results in chapter 5 about the above-mentioned theoretical and modeling discussions.

3.3 Time delay Estimation Algorithms for SS Radar Mode

The traditional method that has been employed to measure the delay profile is the PN correlation method. The drawback of the conventional PN correlation method is that the delay time resolution is limited to the chip interval of the PN sequence. For example, today's traffic conditions in our towns and cities and on the motorways are characterized by high vehicle densities with stop-and-go traffic movement. Generally, the transmitted signal arrives at the receiver via multiple propagation paths with different delays which are caused by multiple targets. If the delay is smaller than the chip interval, introducing overlapped multipath components, this may cause significant errors to the line-of-sight (LOS) [14] time of arrival estimation. Now we will propose and use the SPM, TK operator and wavelet method to solve successive paths even if they are spaced at less than one chip distance.

3.3.1 The SPM Algorithms

3.3.1.1 Signal and channel model

In the conventional PN correlation method, a pseudorandom code sequence is used as the baseband modulation signal to modulate the transmitted carrier. At the receiver, the received signal is correlated with the transmitted PN code sequence. Then, the output of

the correlator yields an estimate of the delay profile of the transmission channel between the transmitter and receiver due to the fact that the autocorrelation function of the PN sequence can be approximately given by the delta function. If the correlation is taken over a time interval T, the complex valued delay profile measured by this method is given by:

$$z(\tau) = \frac{1}{T}\int_0^T x(t-\tau)v(t)dt \tag{3.9}$$

The delay profile can be expressed as:

$$z(\tau) = \sum_{i=1}^{M} h_i e^{-jwT_i} r(\tau - T_i) + n(t) \tag{3.10}$$

$r(\tau)$ is the autocorrelation function of the transmitted PN sequence signal given by:

$$r(\tau) = \frac{1}{T}\int_0^T x(t-\tau)x(t)dt \tag{3.11}$$

and $n(t)$ is the additive noise term given by:

$$n(t) = \frac{1}{T}\int_0^T x(t-\tau)v(t)dt \tag{3.12}$$

In measuring the delay profiles, a maximal-length sequence m-sequence is commonly used as a PN sequence. The autocorrelation function with an infinitely narrow width is a triangular shape with a spread of $\pm T_c$ around the correlation peak where T_c is the chip interval of the sequence. Due to the triangular autocorrelation function, the conventional PN correlation method cannot resolve the delay times of multipath components arriving within an interval smaller than the chip interval T_c. This means that the range resolution is $cT_c/2$. If we can obtain a smaller T_c, we can get a better range resolution.

The simplest method of improving the time delay resolution of the PN correlation method is to increase the chip rate of the PN sequence. However, this generally leads to hardware complexity in the transmitters and receivers. The higher the chip rate of the PN sequence, the more difficult and the more complex it becomes to implement the digital circuit. In the following section, we propose other methods.

3.3.1.2 The SPM algorithm

The super resolution method (SPM) [45]-[47] algorithm will be presented in the following, which is in fact an extended MUSIC algorithm in the time domain. The MUSIC algorithm has been described in Section 3.1. From equation (2.2), the data vector z is expressed as

$$h(t) = \sum_{i=1}^{K} h_i \delta(t - \tau) \tag{3.13}$$

$$z = \sum_{i=1}^{K} h_i e^{-jwT_i} r(T_i) + n(t) \tag{3.14}$$

In (3.14), $r(\tau)$ is the mode vector defined as $r(\tau) = (r(\tau_1 - \tau), r(\tau_2 - \tau), \cdots, r(\tau_K - \tau))^t$, and $n = (n(\tau_1), n(\tau_2), \cdots, n(\tau_K))^t$, where τ denotes transpose. The correlation matrix R of this data vector z is expressed as

$$R = E\left[zz^{\dagger}\right]$$

$$= \sum_{i,j} h_i h_j^* e^{jw(T_j - T_i)} r(T_i) r(T_j)^t + E\left[nn^{\dagger}\right] \tag{3.15}$$

where † and * denote Hermitian and complex conjugates, respectively. The noise correlation matrix $E\left[nn^{\dagger}\right]$ can be expressed as

$$E\left[nn^{\dagger}\right]=\sigma_n^2 R_0 \tag{3.16}$$

where R_0 is a symmetric matrix whose klth element is $r(\tau_k-\tau_l)$. With a finite correlation time T_c, $v(\tau)$ is white noise, and R_0 is not the identity matrix because the sampling interval is a small fraction of T_c:

$$\overline{R}=\Gamma G\Gamma^H+V \tag{3.17}$$

In order for the SPM [15] algorithm based on the eigendecomposition to be applicable, the degeneracy of the signal subspace should be removed by decorrelating the coherence of the multipath component signals. The coherence among different paths can be suppressed by averaging the correlation matrix over a range of carrier frequencies:

$$\overline{R}=\frac{1}{K}\sum_{k=1}^{K} z(w_k)z(w_k)^{\dagger} \tag{3.18}$$

The rank of the average signal correlation matrix $(R-\sigma_n^2 R_0)$ becomes M. Then the number of paths and the time delay can be estimated by an eigenvalue analysis as in the MUSIC method. Since R_0 is not the identity matrix, the eigenvalue problem to be solved is given by a general eigenvalue equation as:

$$\overline{R}e_i=\lambda_i R_0 e_i \tag{3.19}$$

$i=1,2,\cdots,K$. The number of discrete paths can be estimated by comparing the magnitude of the K generalized eigenvalues, if the signal-to-noise ratio is sufficiently

high, the M largest generalized eigenvalues are much larger than σ_n^2, while the remaining $K-M$ eigenvalues are comparable to σ_n^2. The eigenvectors corresponding to the $K-M$ smallest eigenvalues span the noise subspace, which is orthogonal to the signal subspace spanned by those corresponding to the M largest eigenvalues. Once the number of paths has been estimated, a superresolution delay profile $S(\tau)$ can be estimated by

$$S(\tau) = \frac{r(\tau)^t R_0^{-1} r(\tau)}{\sum_{i=1}^{K-M} \left| r(\tau)^t e_i \right|^2} \tag{3.20}$$

where $r(\tau)$ is the mode vector for delay time τ. If the signal-to-noise ratio is sufficiently high, $S(\tau)$ has M sharp peaks which correspond to the delay time of the M discrete paths. Then the delay times can be determined from the peak positions of $S(\tau)$.

3.3.1.3 K Snapshots Smoothing for SPM

In order to improve the path decorrelation, we propose the K snapshots over a center sampling frequency w_o. The decorrelation can be accomplished by averaging the delay profile $z(w_k)$ at K snapshots $w_k (k = 1, 2, \cdots, K)$ as:

$$\begin{aligned} \overline{R} &= \frac{1}{K} \sum_{k=1}^{K} z(w_k) z(w_k)^{\dagger} \\ &= \frac{1}{K} \sum_{k=1}^{K} R_k \end{aligned} \tag{3.21}$$

where R_k is the covariance matrix estimation with the sampling frequency w_k, and $\overline{R}$ is the K snapshots smoothed estimated covariance matrix.

$$\begin{aligned} R_k &= \sum_{ij} E(h_i h_j^*) e^{j(w_o(k\tau_j - k\tau_i)+\theta(\tau_j)+\theta(\tau_i))} r(k\tau_i) r(k\tau_j)^H \\ &= \sum_{ij} E(h_i h_j^*) e^{j(w_o k(\tau_j - \tau_i)+\theta(\tau_j)+\theta(\tau_i))} r(k\tau_i) r(k\tau_j)^H \end{aligned} \tag{3.22}$$

Let us now analyze the performance of the decorrelation technique. We start by rewriting the data vector, the dependence on the kth [29] snapshot.

$$z_k = \Gamma \begin{bmatrix} h_1 \exp\left[-j(w_o\tau_1 + \theta_k(\tau_1))\right] \\ h_2 \exp\left[-j(w_o\tau_2 + \theta_k(\tau_2))\right] \\ \vdots \\ h_N \exp\left[-j(w_o\tau_N + \theta_k(\tau_N))\right] \end{bmatrix} \tag{3.23}$$

$$k = 1, 2 \cdots, K$$

$\theta(\tau)$ is the phase for the received signal at every snapshot.

It can also be written as

$$\overline{R} = \sum_{k=1}^{K} \Gamma G_k \Gamma^H + V \tag{3.24}$$

$$\overline{R} = \Gamma \overline{G} \Gamma^H + V \tag{3.25}$$

where

$$\overline{G} = \frac{1}{K} \sum_{k=1}^{K} \Phi_k G \Phi_k^H \tag{3.26}$$

Here, $\overline{G}$ is the K snapshots smoothed path gain covariance matrix. Since this matrix should approach a diagonal form, let us look at the individual terms of $\overline{G}$ to see if its

diagonal terms go to zero and if its diagonal terms are equal to the diagonal terms of G. The i, j th element of the smoothed path gain covariance matrix can be expressed as:

$$\overline{G}_{ij} = G_{ij} \frac{1}{K} \sum_{k=1}^{K} (\Phi_k)_i (\Phi_k)_j^* \tag{3.27}$$

It is clear that when $i = j$, $\overline{G}_{i,i} = G_{i,i}$. On the other hand, when $i \neq j$

$$\overline{G}_{ij} = G_{ij} P^{(K)}(i, j) \tag{3.28}$$

$$P^{(K)} = \frac{1}{K} \sum_{k=1}^{K} \exp(-j\Delta\theta_{k-1}(\tau_i - \tau_j)) \tag{3.29}$$

If $K \to \infty$, $P^k \to 0$.

We will refer to P^k as the decorrelation factor for SPM. The magnitude of the decorrelation [47] factor quantifies the ability of the SPM algorithm to decorrelate the i th and j th paths when the signal is obtained by K snapshots. If P^k is equal to zero, then SPM completely decorrelates the i th and j th paths. If it is $P^k = 1$, then the method does not decorrelate the path at all. Note that the decorrelation factor presented in equation (3.29) differs from the decorrelation factor P^k since the former was obtained by integration of a number of carrier frequencies. This makes the process computationally expensive and difficult to implement in a radar system. The latter was easily obtained. This improves the resolution of the delay profile measured by conventional PN correlation method without any changes in hardware.

We would now like to make an important observation by employing the following expression for the decorrelation factor. For any profile, K is larger and the result is

better. So the coherence is decorrelated according to the K increase. From Equation (3.29), we find that the K snapshots smoothing can fail if K is large enough. If we want to decorrelate the signal completely, a large number of snapshots are needed. But the number of snapshots is limited by the implementation. So a better performance can be obtained with the TK energy operator algorithm.

3.3.2 TK Operator Algorithm

3.3.2.1 TK Operator

Teager Kaiser (TK) is an energy operator. Before we start on the TK operator in detail later, it makes sense to briefly describe the Teager Energy Operator here. In 1983, "A Phenomenological Model for Vowel Production in the Vocal Tract" by Herbert M. Teager and Shushan M. Teager [15], was published. J. F. Kaiser presented the algorithm to compute the energy of the generator of a sound in 1990. During the twelve years of research, many applications have been developed using Teager's Energy Operator. It was found that this nonlinear operator exhibits several attractive features such as simplicity, efficiency and ability to track instantaneously-varying spatial modulation patterns. It has been widely used in various speech processing and image processing applications and it has also been applied to CDMA [48]-[50].

3.3.2.2 Using the TK operator in Spread Spectrum Radar

A TK-based algorithm for estimating the multipath delays in a CDMA system was first introduced in [48]. The idea is the following: if we apply the TK operator of equation (3.21) to the squared envelope of the correlation function, the peaks at the output of TK operator correspond to the multipath delays. To show this idea, consider first the autocorrelation function (ACF) of a rectangular pulse shape of duration N_s:

$$\Psi[x_{ideal}(n)] = \begin{cases} \frac{2}{N_s} - \frac{1}{N_s^2} & n = 0 \\ \frac{1}{N_s^2} & 0 < n < |N_s| \\ 0 & otherwise \end{cases} \tag{3.30}$$

The TK energy of this function is equation (3.30) and it exhibits a peak at delay point, as shown in Fig.3.4. In the previous section, the autocorrelation function of the received signal is equation (3.30), it can also be written as:

$$R = \sum_{i=1}^{L} \alpha_n R(\tau - \tau_l) + V \tag{3.31}$$

$R(\bullet)$ is the pulse shape autocorrelation function. If we assume rectangular pulse shapes, the pulse shape autocorrelation function $R(\bullet)$ can be written as:

$$R(\tau) = \begin{cases} 1 - \frac{\tau}{T_c} & |\tau| \le T_c \\ 0 & otherwise \end{cases} \tag{3.32}$$

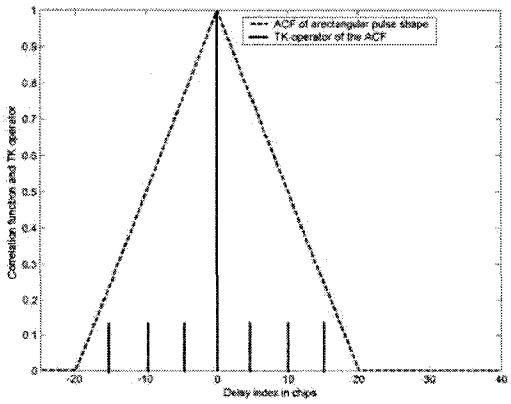

Fig. 3.4 Normalized TK energy of a triangular pulse

We notice for rectangular pulse shape triangular pulses weighted by the complex channel within white noise, we can use the correlation function with the nonlinear TK [49] operator. The discrete-time Teager operator of a complex valued signal is given by :

$$\begin{aligned}\Psi_C[y_n(\tau)] = &\frac{1}{T_c}\sum_{i=1}^{L}\sum_{j=1}^{L}\mathrm{Re}\{\alpha_i\alpha_j^*\}R(\tau-\tau_i)\\ &\times\delta(\tau-\tau_i)+\frac{1}{T_c^2}\sum_{i=1}^{L}\sum_{j=1}^{L}\alpha_i\alpha_j^*\\ &\times\mathrm{sign}((\tau-\tau_i)(\tau-\tau_j))\Pi(\tau-\tau_i,T_c)\\ &\times\Pi(\tau-\tau_j,T_c)+\bar{n}_{TK}(\tau)\end{aligned} \tag{3.33}$$

where $\Pi(\tau,T_c)$ stands for a rectangular function with unit amplitude and duration $2T_c$ centered at $\tau=0$:

$$\Pi(t,T_c)\triangleq\begin{cases}1 & |t|\le T_c\\ 0 & otherwise\end{cases} \tag{3.34}$$

and where $\delta(\tau)$ stands for the Dirac function, and $\bar{n}_{TK}(\bullet)$ is additive white Gaussian noise at the output of the TK operator.

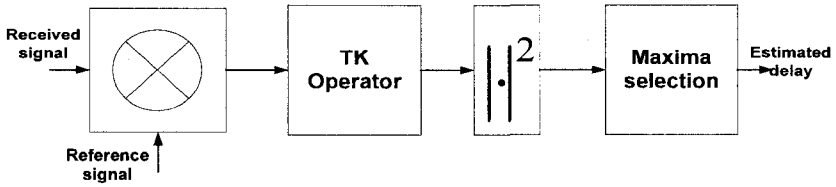

Fig. 3.5 TK algorithm for multipath delay estimation

Equation (3.30) shows that the TK operator applied to the output of the correlator provides clear time-aligned peak locations of the desired closely-spaced paths in the presence of the noise. The block diagram of the proposed TK-based approach is illustrated in Fig. 3.5. Here, the discrete TK operator is applied at the output of the correlator. Discrete-time implementation as given is more suitable for digital receivers. The L maxima outputs of the TK operator are the estimated multipath delays. In the simulation part, we will show that TK algorithm outperforms SPM algorithm.

3.3.2.3 Signal Processing and Result

In our spread spectrum radar, BPSK modulation is considered in the simulation. The chip rate of the proposed radar is 25 MHz. This means T_c is 40 nsec. There are two targets supposed in the range direction. The number of samples per chip and in the simulations is $N_{sampling} = 20$. The correlation function is computed in two code intervals. The code is a PN code whose length is 512. The signal to noise ratio is defined by $SNR = 10\log_{10}(P_r/P_i)$, where P_r is the power of the desired received signal and P_i is

the power of the white noise. The probability of detection is defined as the probability that both paths are estimated correctly with ± 5 sample errors.

In order to examine the delay-time resolution of two paths with small delay difference, computer simulations were carried out for multipath transmission channel model which consisted of two paths with equal relative arrival phases. Fig. 3.6 shows the result of SPM algorithm with N ($N_{sampling} = 20$) snapshots. When the delay-time difference is $0.2T_c$, two paths are found to be resolved by the SPM with peaks.

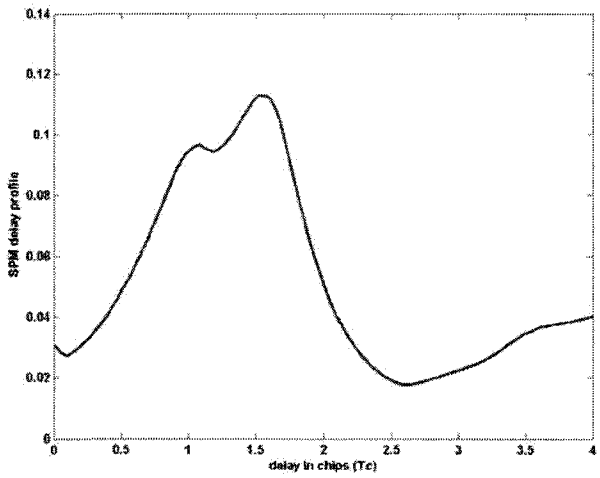

Fig. 3.6 Delay profile of SPM algorithm with two paths

Fig. 3.7 shows the output of the Teager-Kaiser energy applied to the delay profile using the approach described in the previous section. The system parameter is the same as for the SPM algorithm.

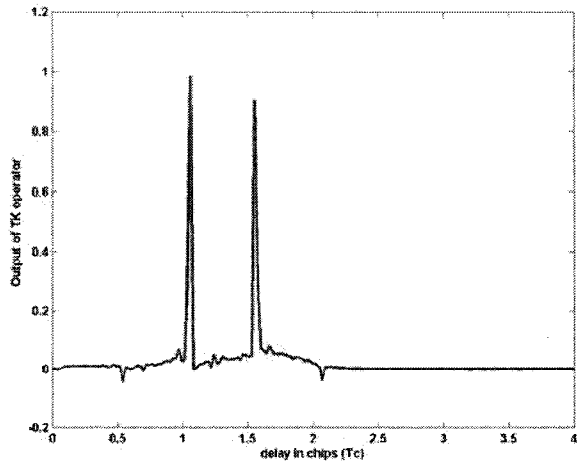

Fig. 3.7 Delay profile of TK algorithm with two paths

Fig. 3.8 shows the results of estimation for three targets of (a) $0.4T_c$, (b) $0.6T_c$, (c) $0.8T_c$. The solid line is used for the TK algorithm while the dotted curve for the SPM algorithm. It is found that three peaks appear in the estimated superresolution delay profile at correct positions corresponding to the actual delay times of the three paths. Fig. 3.9 shows the probability of detection of the two algorithms. Both algorithms show a significant deterioration in the presence of a strong interference. The performance of the TK algorithm is close to the optimum at low levels of noise. TK algorithm is better than SPM algorithm. Furthermore, SPM algorithm has a much higher complexity of implementation than TK algorithm.

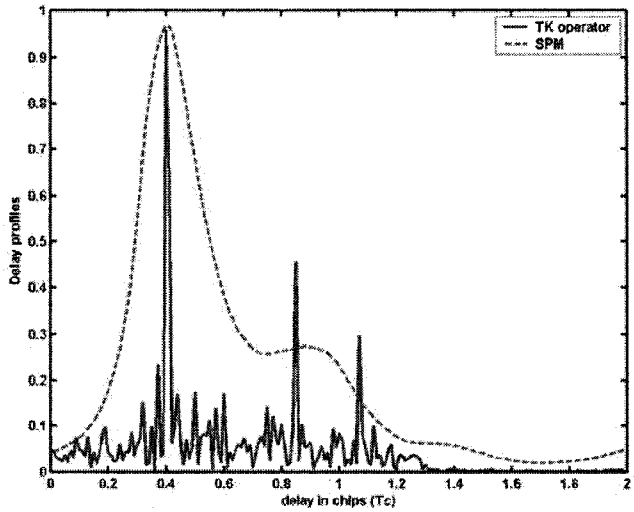

Fig. 3.8 Delay profiles by the SPM (dotted curve) and the TK (solid curve) for three-path.

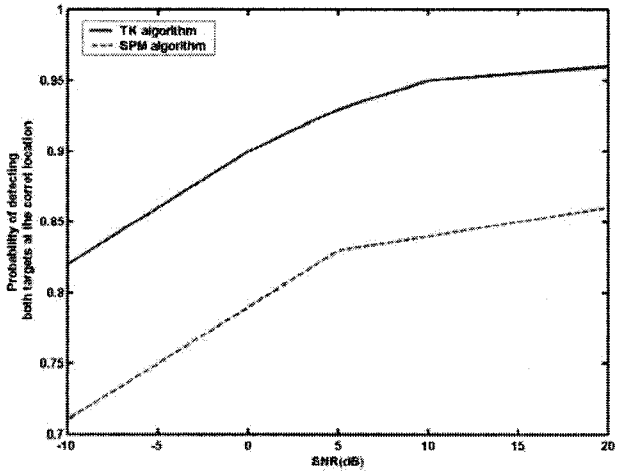

Fig. 3.9 Probability of detection with the SPM algorithm and TK algorithm

3.3.2.4 Conclusion

In this section, we have presented two super-resolution algorithms to deal with the closely-spaced multipath problem in spread spectrum (SS) radar systems. One algorithm is an extension of the well-known MUSIC algorithm, and the second is based on a simple and efficient operator, called the Teager-Kaiser operator. By processing the delay profile, it has been confirmed that the TK algorithm is able to yield more accurate results. The TK algorithm shows more capacity to withstand the distortion from white noise and the TK algorithm gives a better performance in the multi-target case. The SPM algorithm is too complex for practical purposes.

The results indicate that the TK algorithm is a very efficient method to deal with closely-spaced paths. The main advantage of the TK algorithm comes from its simplicity of implementation. The TK algorithm provides a better approach to the problem of measuring the target range.

3.3.3 The Wavelet Algorithms

The radar which uses spread spectrum modulation makes it possible to conduct accurate measurements of distance to detect the simultaneous presence of several targets, and to eliminate the interference. In spread spectrum modulation, the target range is found by correlating the received pseudorandom (PN) code, which is made from a digital signal, and the reference (or fixed) code that provides a basis for comparison. The

PN correlation method is used to measure the delay profile. This time delay naturally varies with the distance from the different targets.

In this section, we propose a wavelet method in the context of a software defined spread spectrum radar system with closely spaced targets. A time delay estimation profile is proposed using a discrete wavelet transform (DWT). If the time delay of two targets is smaller than one chip, this method will be very useful in improving the range resolution. This algorithm is based on the Haar wavelets for the delay profile and it is used for the ideal rectangular pulse shapes. The proposed scheme is then applied to a problem of target detection from simulation data. The accurate estimation of time delay is very important to obtain good classification results when range profiles are used as feature vectors for radar target recognition. The wavelet approach is then discussed in this chapter in order to overcome the limitations of the autocorrelation method and to estimate the range profile peak locations with superior accuracy.

The aim is to compare the performance of the autocorrelation and the wavelet method for spread spectrum radar to determine which algorithm gives better results. The wavelet method is not affected by the length of the PN code, since it is applied on the correlation function, after the effects of the code has been removed. The main features of the two approaches are highlighted through computer simulations on noisy data.

3.3.3.1 The Wavelet algorithm

The purpose of this section is to show the wavelet analysis can detect the exact

instant in the presence of signal change. The signal model is the same as in section 2.4.1. These wavelets have no explicit expression except for $db1$, which is the Haar wavelet [51]-[53]. However, the square modulus of the transfer function of haar is explicit and fairly simple.

$$P(y) = \sum_{k=0}^{N-1} C_k^{N-1+k} y^k \tag{3.35}$$

where C_k^{N-1+k} denotes the binomial coefficients. Then

$$|m_0(w)|^2 = \left(\cos^2(\frac{w}{2})\right)^N P\left(\sin^2(\frac{w}{2})\right) \tag{3.36}$$

where $m_0(w) = \frac{1}{\sqrt{2}} \sum_{k=0}^{2N-1} h_k e^{-ikw}$

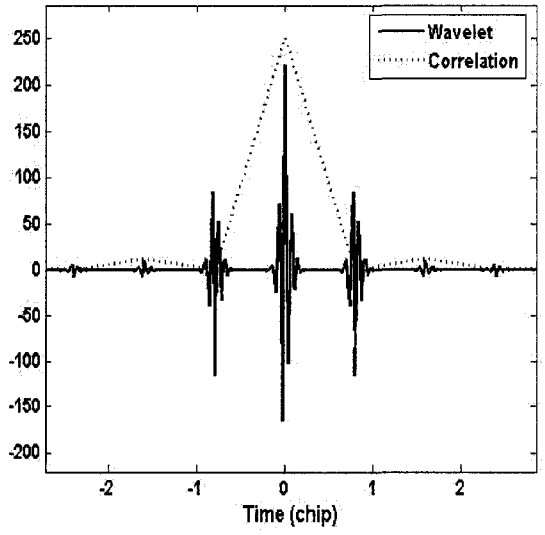

Fig. 3.10 Wavelet output of a triangular pulse

The first-level and second-level details (D1 and D2) show the discontinuity most clearly, because the rupture contains the high-frequency part. In this case, we are only

interested in identifying the discontinuity, $db1$ could be a more useful wavelet to use for the analysis than $db5$. The discontinuity is localized very precisely: only a small domain around time = $0.1\,T_c$ contains many details.

The deterministic part of the signal may undergo abrupt changes such as a jump, or a sharp change in the first or second derivative. In our case, the autocorrelation of PN code is triangular shape which is discontinuous at the peak. The wavelets method finds the peak position accurately. It is shown in Fig. 3. 10.

In the simulation, two targets are presented. It could be used as an input signal of a 2-path channel. T_c is chip duration and the signal duration is set to $0.2T_c$. Channel delays are arbitrarily selected to be $0.5T_c$, $0.7T_c$. Note that between the two paths the delay separation is less than one chip. Particular attention is paid to the performance of the algorithm at different SNRs. 200 samples are taken from the main lobe of the output of the matched filter.

Fig. 3.11 shows a significant resolution improvement in the case of the wavelet algorithm, while the autocorrelation technique is blind for the scattering centers too closely spaced and is confused by the noise in the case of small amplitude peaks. As expected, the error of all these methods decreases as the SNR increases. When the SNR is less than 15 dB, the threshold of wavelet coefficients essentially removes a considerable amount of corrupting noise, but at the same time suppresses the source signal. Therefore, there is a great potential in exploiting the denoising method for many applications if we can classify the input signal and optimize the threshold accordingly.

The simulations performed on the range profiles have shown that the wavelet

method is statistically slightly superior in resolution and robustness. This conclusion is supported by Fig. 3.12, which illustrates the resolution improvement for a range profile, corresponding to our software defined spread spectrum radar. The simulation results are depicted in Fig. 3.12. The asterisks show the outcome of the wavelet method without denoising. It is close to the autocorrelation values (dash-dotted lines) at high SNR, but performance is remarkably better at low SNR. The reason is that in our simulation, denoising is made. With the denoising approach the estimation error is significantly reduced.

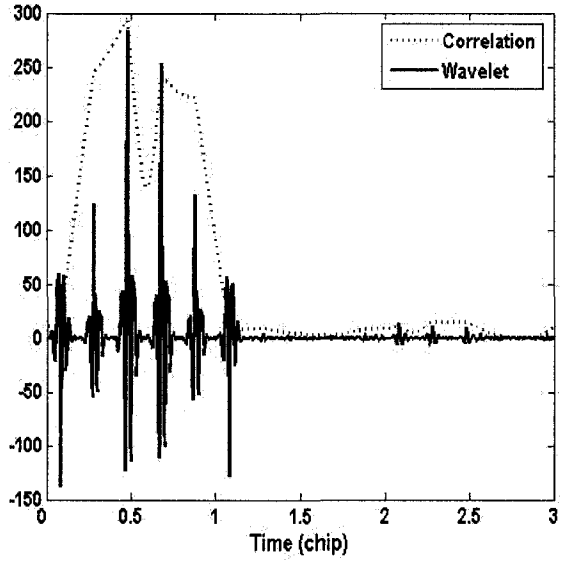

Fig. 3.11 Delay profiles by the autocorrelation (dotted curve) and the wavelet (solid curve) for two-path.

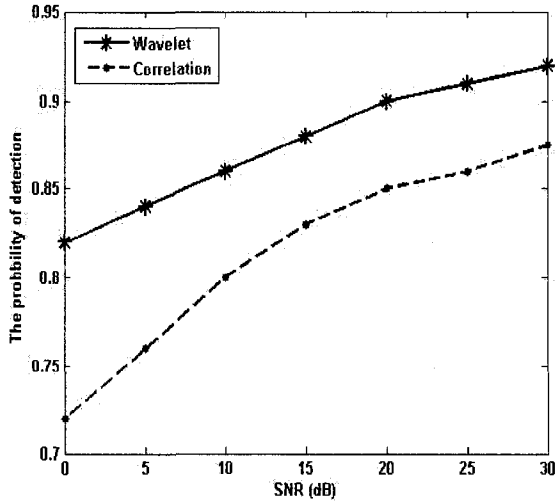

Fig. 3.12 Probability of detection of the autocorrelation and wavelet method.

3.3.3.2 Conclusion

A method for time delay estimation that makes use of wavelets and denoising is proposed. It has been shown to be globally convergent with a high probability and also computationally efficient. Simulation results show its superiority over conventional methods, including the commonly used direct cross correlation method.

A wavelet packet decomposition based technique and denoising algorithm have been used to overcome the limitations of the autocorrelation technique and to estimate the radar target positions along the line of sight. We have found that statistically the wavelet method shows the most ability to provide stable, accurate and robust estimates for the range profile peak positions. The high resolution estimated range profile peak positions accurately describe the distribution of the radar target along the line of sight. It could be

a good candidate for feature vectors for the automatic radar target classification schemes. This method has considered the time delay estimation problem under a noisy environment. The source signal is assumed to be deterministic rather than a stationary Gaussian process.

CHAPTER 4

MIXER-BASED SYNTHETIC SOFTWARE DEFINED RADAR

Different conventional analog radar configurations [54] are used to realize different radar functions. However, in software-configurable radar, we can generate and manipulate different waveforms [55] in the base-band and use different algorithms to process the received signals because both DDS and the DSP are programmable. Therefore, various types of radar having different modulation schemes including FMCW, CW and SS radars can be realized within a unified platform in connection with a single hardware interface. In this chapter, the mixer-based software-configurable radar is designed and realized especially outlining two functions: FMCW and SS.

4.1 Design of 4GHz software defined measurement system

In this work, we built the 4GHz prototype. We have validated the proposed scheme with a set of cables which have also been used in past work. In fact, the use of those cables allows us to look at the accuracy issue without free-space propagation problems which would contribute to the accuracy of the measurements. In this case, it is easy for us to implement and measure. Later, we also design and implement the 24 GHz system. The objective of this effort was to design a low-cost automotive collision warning radar that could be operated under Part 15 of the U.S. Federal Communications Commission

regulations regarding intentional radiators including proximity sensors. Similar regulations are valid for Europe (ETSI EN 300440-1 and –2) and for most other countries in the world.

4.1.1Architecture of the 4 GHz software defined measurement system

Two distinct waveforms are generated by the DDS, namely FMCW waveform and SS signal. The FMCW waveform is a triangular frequency sweeping (chirp) signal at a repetition frequency of 12.5 kHz in our design with a chirp bandwidth of 75 MHz. The SS signal is a BPSK modulated signal with a modulation bandwidth of up to 40 MHz. The SS signal can also be used for digital communications, which may allow the complete integration of radar and communication functionalities within the same block. The sweep data consisting of the chirp bandwidth and the sweep time are programmable in the DDS and so is the chip rate (the number of bits per second in the spreading signals) of the SS signals. The received signal can be processed in the DSP with different well-established processing algorithms.

The block diagram of the proposed system is shown in Fig. 4.1. It consists of the transmitting part that includes a DDS, a microwave up-converter chain, and the receiving part that include a mixer, an analog-to-digital-converter (ADC), a DSP, and a PC working as a controlling and monitoring device. In this work, the up-converter chain translates the base-band signal to a microwave signal with a center frequency of 4 GHz. The received signal passes through a low noise amplifier and is then alternately mixed

with the transmitted signal and the local carrier with a switch. Subsequently, this signal is directly digitized by the ADC and the data acquired is processed by the DSP platform. In our system, lossy transmission lines (delay lines) are used to simulate the transmitting and receiving channels instead of a real propagating channel in the wireless radar system in order to facilitate simulation and system characterization.

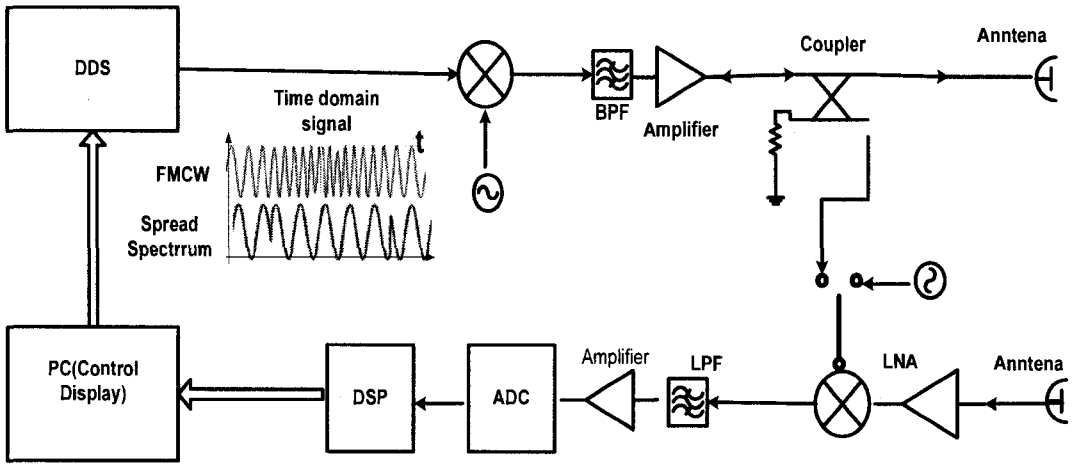

Fig. 4.1. System block diagram of the proposed 4 GHz heterodyne radar receiver.

4.1.2 Measurements of the 4 GHz software defined measurement radar

In order to test the performance of the S-band composite software configurable range radar, cables of different lengths are measured to estimate the accuracy of the software configurable range radar in distance measurements. The cable lengths vary from 0.5 m to 16 m. In addition, as a reference their lengths are determined by a commercial network analyzer. The test bench setup for this experiment is shown in Fig. 4.2.

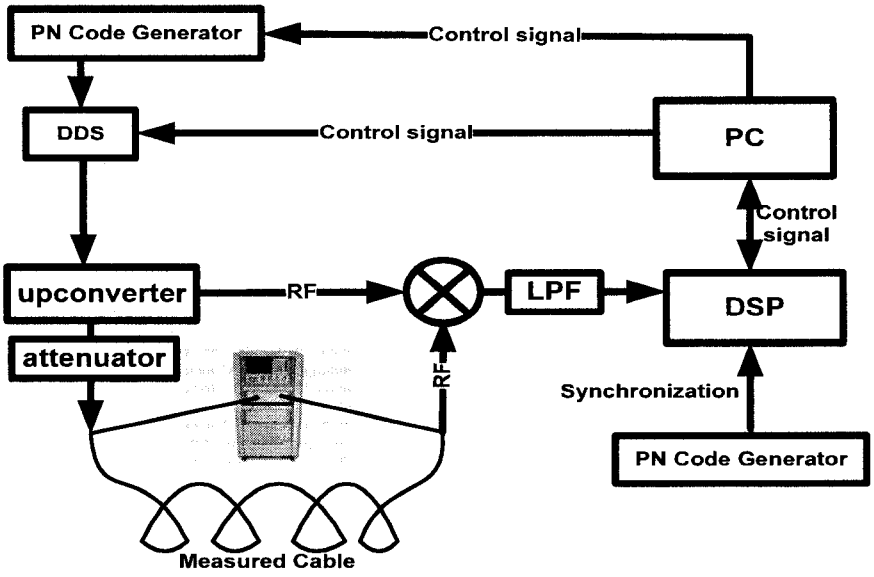

Fig. 4.2 Measurement setup for the 4 GHz radar system evaluation using cables.

FMCW signal measurement

As a first step, the FMCW radar is used to determine the cable lengths. The frequency sweeping range of the transmitted FMCW signal is from 3.965 GHz to 4.040 GHz with a sweep period of 80 ms. The time-domain output signal from the mixer for a measurement of a line length of 8 m, denoting the beat signal between the transmitted and the received (delayed) signals, is shown in Fig. 4.3.

Subsequently, this time domain data is processed in the DSP with the help of an FFT. Fig. 4.4 shows the spectral components of the output time domain signal from the mixer. From the frequency at which the peak value is observed, we can calculate the length of

the line under measurement yielding a maximum range error of the FMCW measurement of 0.5 m in the experiment. As we already mentioned in chapter 2, the range error is mainly determined by the sweeping bandwidth of the FMCW signal [24] and can be reduced by increasing the bandwidth.

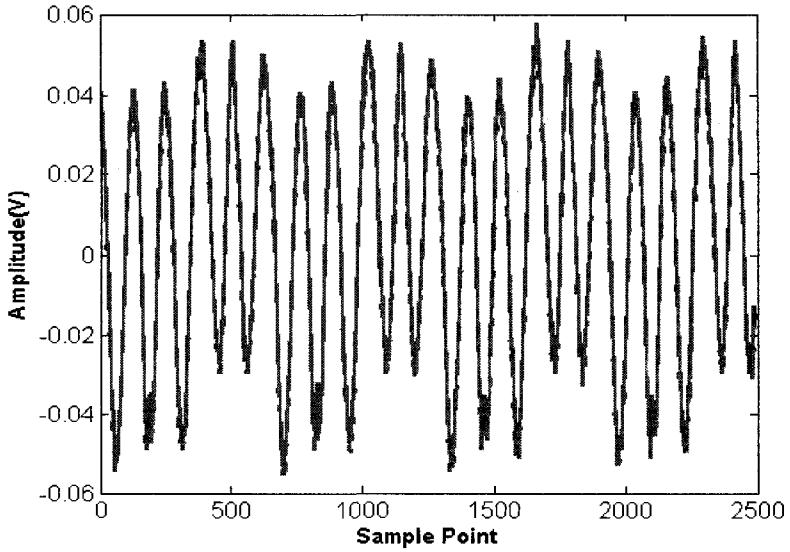

Fig.4.3. The received signal of the heterodyne radar receiver for the FMCW radar and a line length of 8 m.

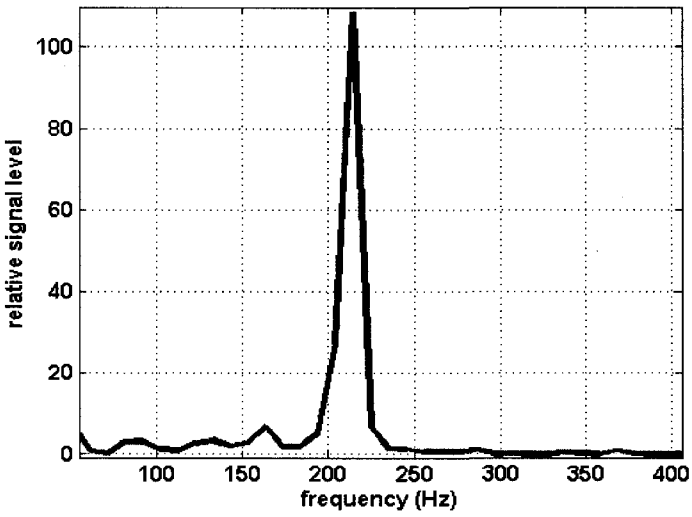

Fig. 4.4. The spectrum of the received signal of the heterodyne receiver for the FMCW radar and a line length of 8 m.

Spread spectrum signal measurement

As a second step, we make the same experiment using the SS radar. The PN code rate used in this experiment is selected to be 40 MHz with a code length of 32. The demodulated signal from the mixer for this experiment is shown in Fig. 4.5. We observe a delay between the demodulated PN codes and the reference PN codes, which can be evaluated with the help of autocorrelation as described in section 3.3.1. This correlated output is shown in Fig. 4.6 and yields a SS signal range error of 2.5 m. This result may be further improved by implementing a faster PN code, which, however, is limited by the speed of the digital circuit used in the software defined radar platform.

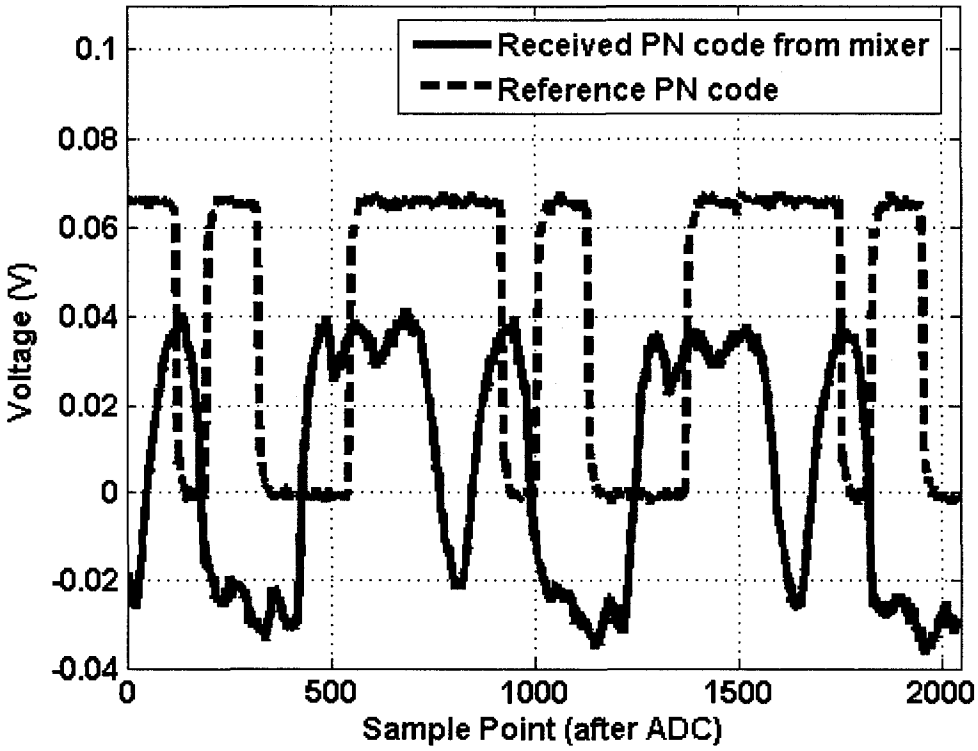

Fig. 4.5 The mixer output signal for the SS radar

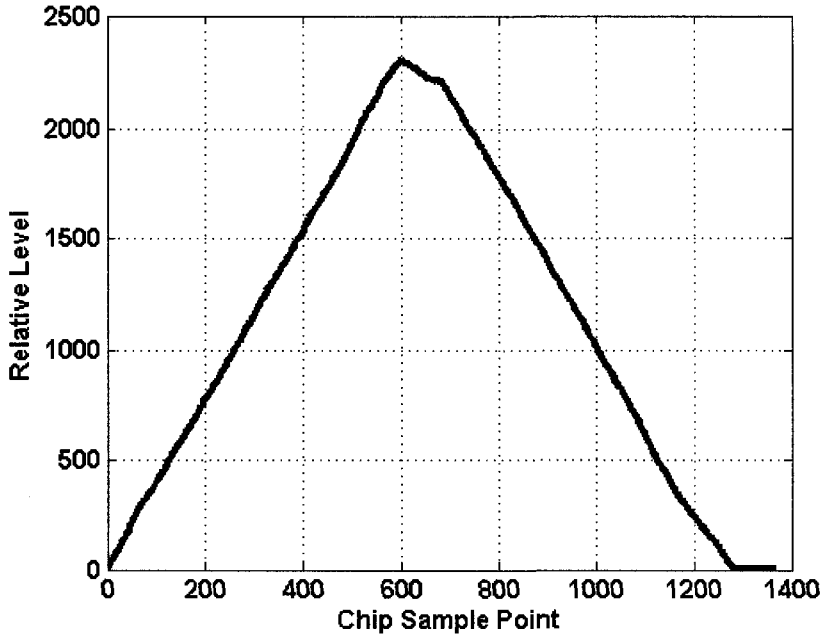

Fig. 4.6 The signal after autocorrelation for the SS radar

4.1.3 Summary

In this section, a 4 GHz software-configurable range radar has been proposed and described. Composite FMCW/SS measurements are suitable for multiple and adaptive applications. The FMCW radar can yield a good range resolution, while the SS range radar is able to provide the capacity of interference immunity. The economic viability of this type of multi-purpose ranging measurement system appears promising. Most of the currently proposed prototype systems are built with low-cost commercial components. The DDS can be used to adjust modulation schemes and frequency shifts, which make it possible to introduce software configurability into the transmitter, and moreover, the

DSP provides the corresponsive digital algorithm for certain signals in the receiver. This provides an effective method to design low-cost, compact, and synthesized microwave radars with a single RF front-end.

4.2 Design of a 24 GHz software defined radar system

This section illustrates a K-band (24 GHz) software-reconfigurable radar and communication architecture. The system has two time-divided operation modes: an FMCW range measurement and a PN code pulse radar [56] [57] mode. The FMCW radar is used for range and delay information, while the PN code pulse is also used for inter-vehicle communication. In this work, we propose a software defined radar and communication system that combines both FMCW and PN pulse radar functions which is different from SS radar. The two functions are switched in different time schedules.

4.2.1 Architecture of the 24 GHz software defined measurement system

The block diagram of the proposed system is shown in Fig. 4.7. The DDS serves as a generator for the modulated signals. The RF front-end consists of an up-converting chain and a down-converter assembly. The carrier frequency of the transmitted signal is 24 GHz. The received IF signal is processed in the DSP, and then the frequency and phase difference between the received signal and the reference signal can be evaluated.

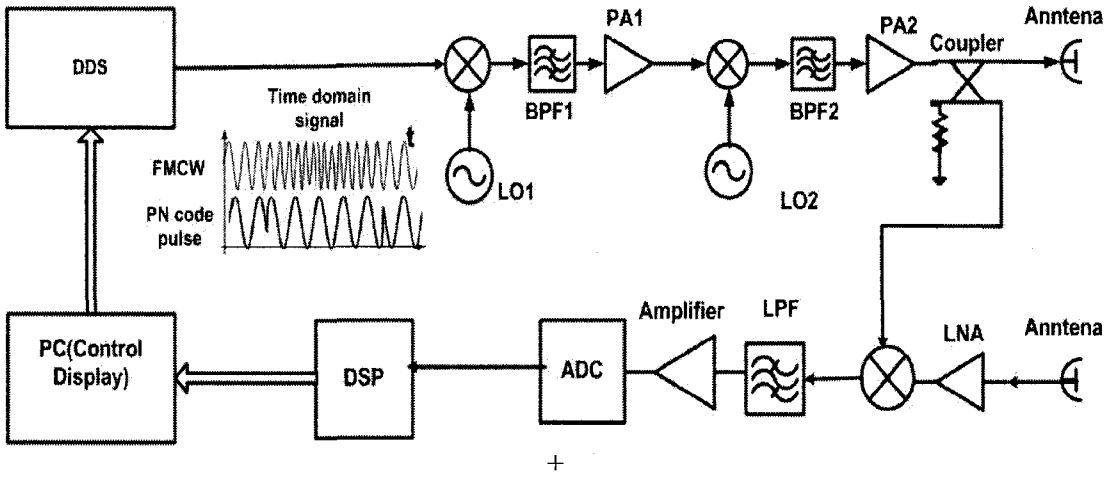

Fig 4.7 Block diagram of the 24 GHz software defined radar architecture.

The system shown in Fig. 4.7 provides two operating modes, namely, the FMCW and PN pulse radar modes which are separated by different time schedules. In this software-configurable radar system, we can generate and manipulate different waveforms in the base-band and use different algorithms to process the received signals, while the hardware of the system remains unchanged. The FMCW mode transmitted signal is a triangular frequency sweeping (chirp) signal with a repetition frequency of 12.5 kHz and a bandwidth of 300 MHz. The PN pulse radar uses a BPSK modulated signal with a modulation bandwidth of up to 40 MHz and a code length of 16. Beyond its use in radar, the SS signal can also be used for digital communications, which may allow the complete integration of radar and communication functions within the same block. The chirp bandwidth and sweep time for the FMCW signals are programmable in the DDS and so is the chip rate (the number of bits per second in the spreading signals) of the SS signals.

In the FMCW radar mode operation, the mixer output signal is processed in the DSP based on the FFT technique in order to precisely extract the beat frequency. A modified Hanning window reduces the side lobes to a tolerable level. The target distance is evaluated from the maximum peak in the spectral domain.

In the SS radar, the range of a target is calculated from the travelling time of the reflected wave using equation (3.6). Our system also adopts the SS technique for communication purposes. The data information is evaluated by a correlation of the received PN code and the reference PN code, which is shifted according to the travelling time. The sequence pattern of the PN code is coded by the front-seat information. The autocorrelation function for the PN code is given in equation (3.7). The correlator is designed on the basis of the autocorrelation characteristic of the PN code, and the DSP algorithms for processing these SS signals use an autocorrelation function such as given in equation (4.2). After correlation, a decision based on the maximum-likelihood (ML) criterion is taken. From this decision, vehicle information is obtained, and multiple inter-vehicle communications can be set up. In this system, every vehicle broadcasts its front-seat information by transmitting the assigned PN code, which includes its front-seat information. Thus, every vehicle is able to detect the signals of the other vehicles [58].

To obtain other vehicles' information in the proximity of one vehicle, a PN coded pulse radar system is developed. Different from ordinary pulse radar, the proposed system makes use of many different PN codes instead of a single pulse. As the duration of one pulse equals to one chip duration, the system uses long codes applying the same principle as used in code division multiple access (CDMA). Information received from

other vehicles is recovered by multiplying it with the reference PN code $c_{reference}(t_n)$, which yields the recovered PN code $c_{recover}(t)$ as follows:

$$c_{recover}(t) = c_t(t_k) * c_{receiver}(t_l) * c_{reference}(t_n) \quad 4.10)$$

The recovered PN code $c_{recover}(t)$ is then correlated with $c_{reference}(t_n)$ obtained from (4.2) and the correlator output is decided by the ML criterion. After the decision, the data information (PN code) is obtained. With this algorithm, each vehicle can select and obtain its own reflected pulses or those of other vehicles. From the obtained information, a vehicle within near range can easily retrieve other vehicles' information as different vehicles are identified by different reference PN codes. The obtained information consists of inter-vehicle information such as distance, range, and warnings. Here, this information is referred to as the radar information. Like PN codes for communication, the PN codes for radar systems include data information (velocity, direction, etc.) of each vehicle. In software defined radar and communication systems, the vehicle can detect the distance to each of its surrounding vehicles using FMCW radar and communicate with them using the PN pulse radar as shown in Fig 4.8.

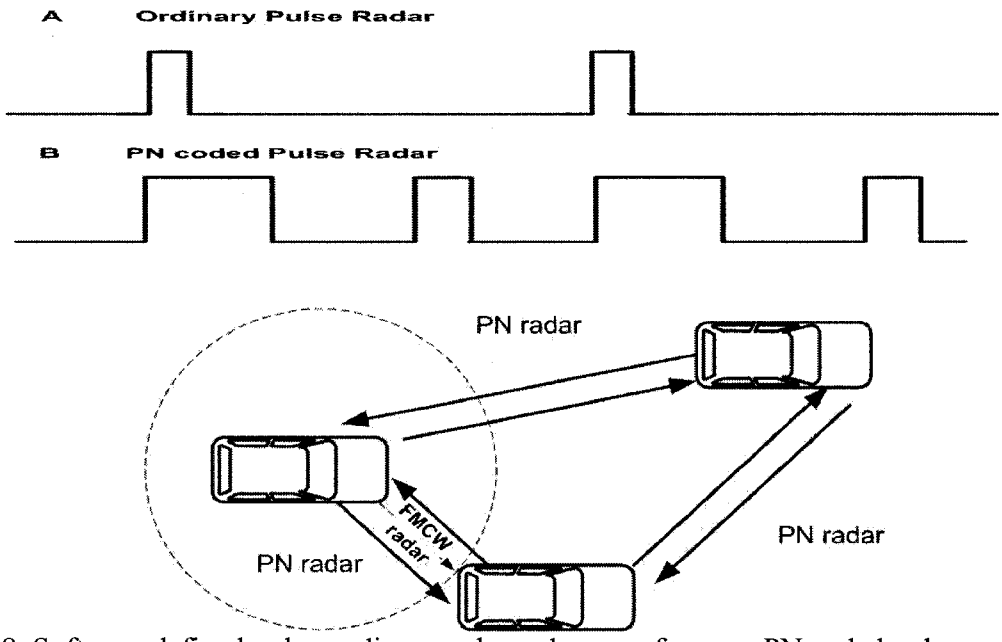

Fig. 4.8. Software defined radar: ordinary pulse radar waveform vs. PN coded pulse

radar signals; working principle detecting velocity and distance information by the FMCW radar, inter-vehicle communication by the PN code pulse radar.

The system signal processing algorithm used for this radar is shown in Fig. 4.9. At first, the time delay (range information) is obtained from the FMCW radar or the PN pulse radar. Subsequently, the recovered PN code is correlated with the reference PN code in order to gather vehicle information. The final decision is taken based on the maximum value of the correlator output. Each of these algorithms and calculations are processed in the system center computer.

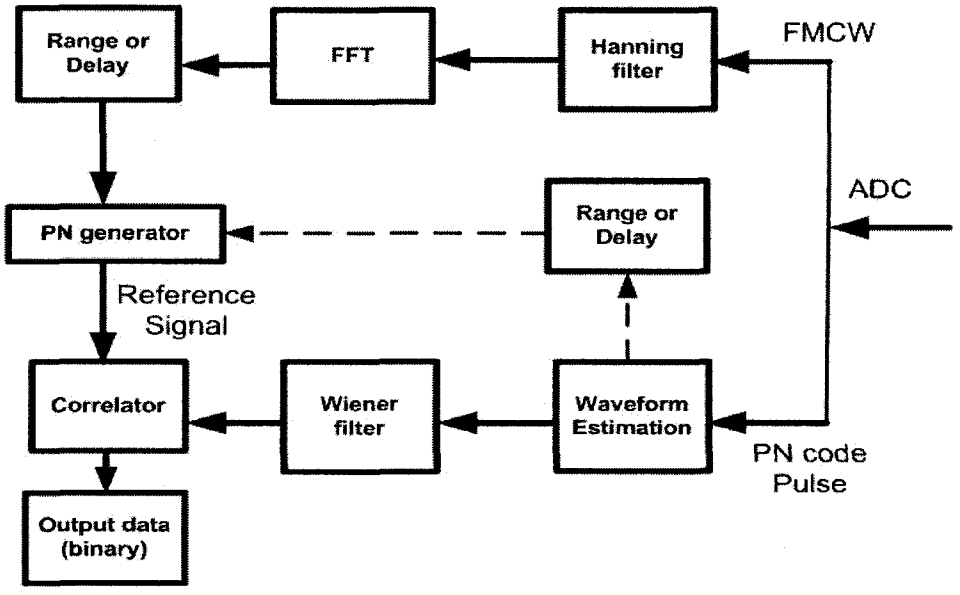

Fig. 4.9. DSP algorithms of software-defined radar and communication system.

4.2.2 Measurement setup

For this experiment, a test bed as shown in Fig. 4.10 is used. The frequency sweeping range of the transmitted FMCW signal is selected from 24 GHz to 24.30 GHz with a sweep period of 80ms and is generated by the DDS. Also the generation of the PN code is modulated by the DDS using BPSK. The control configuration computer represents the central unit of the entire system. Finally, the received IF signal after the mixer is processed by the DSP to evaluate measurement data.

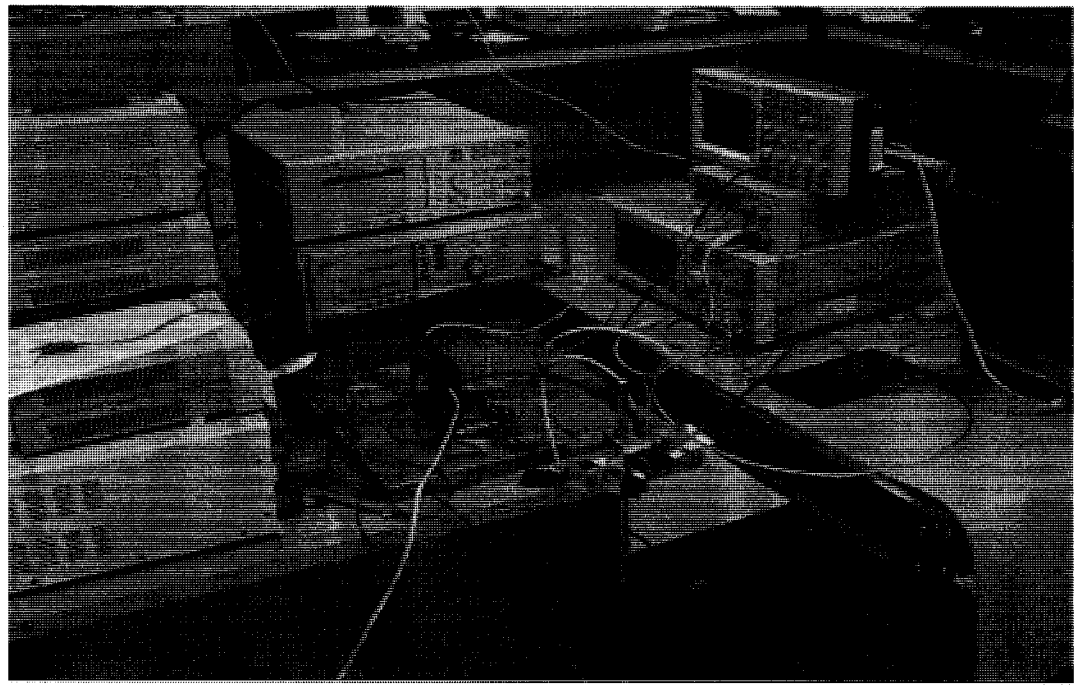

Fig 4.10. Test bed configuration of the 24 GHz software defined radar.

In the following experiment, the FMCW operation mode will be tested with two real targets at 3.5 and 4 m, respectively. The mixer output signal is the beat signal between the transmitted signal and the received (delayed) signal. In order to evaluate the distance, the acquired time domain data is processed in DSP with the help of an FFT. From its spectrum we can calculate the range of the two targets. From this experiment, the maximum range error of FMCW measurement is calculated to be 0.15 m. The range error is mainly determined by the sweeping bandwidth of the FMCW signal and can thus be reduced by increasing the sweeping bandwidth. The time domain output signal after the mixer for a single target at 3.5 m is shown in Fig. 4.11 with its corresponding spectrum shown in Fig. 4.12. The time-domain signal after the mixer for the experiment

with two targets at both 3.5 and 4 m is shown in Fig 4.13 with the corresponding spectrum in Fig. 4.14. Range resolution is the closest distance between two targets. In our experiment, if the two targets are less than 0.2 m apart, there is only one peak in the spectrum. From these results, we observe a range resolution of 0.2 m.

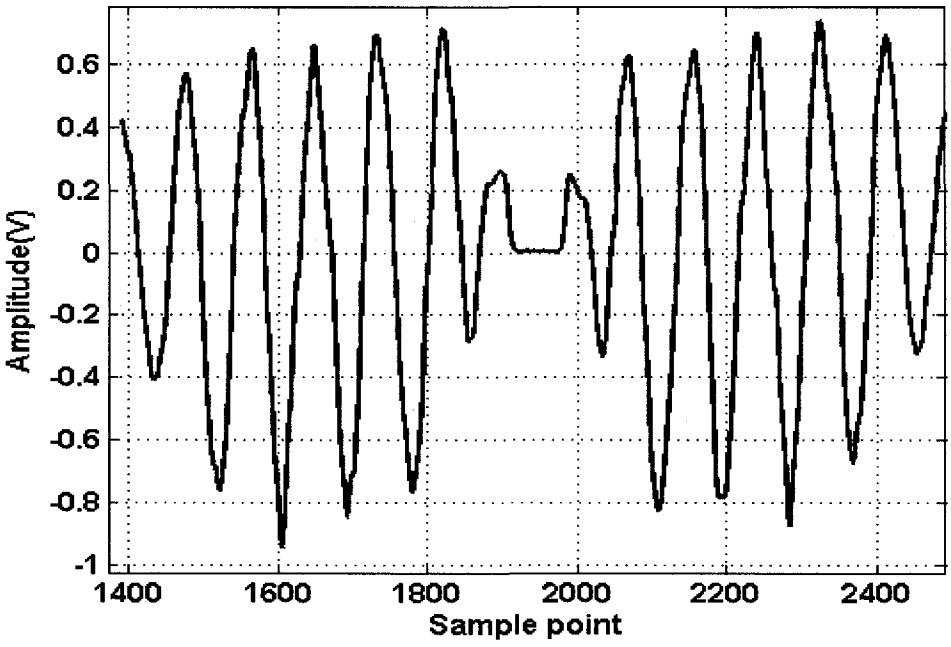

Fig 4.11 Time-domain signal results for a single target at 3.5 m

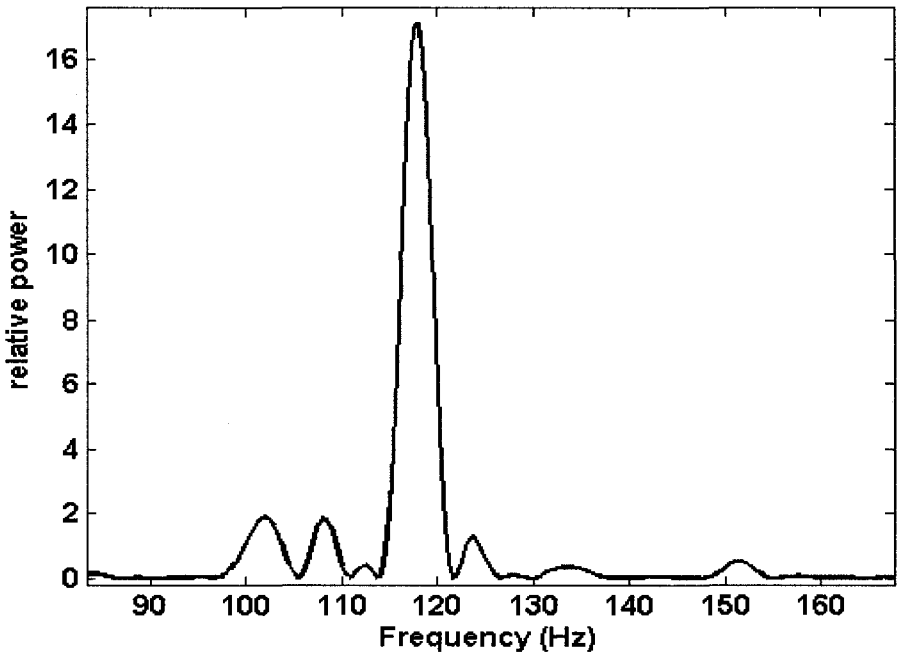

Fig 4.12 FFT results for a single target at a distance of 3.5 m

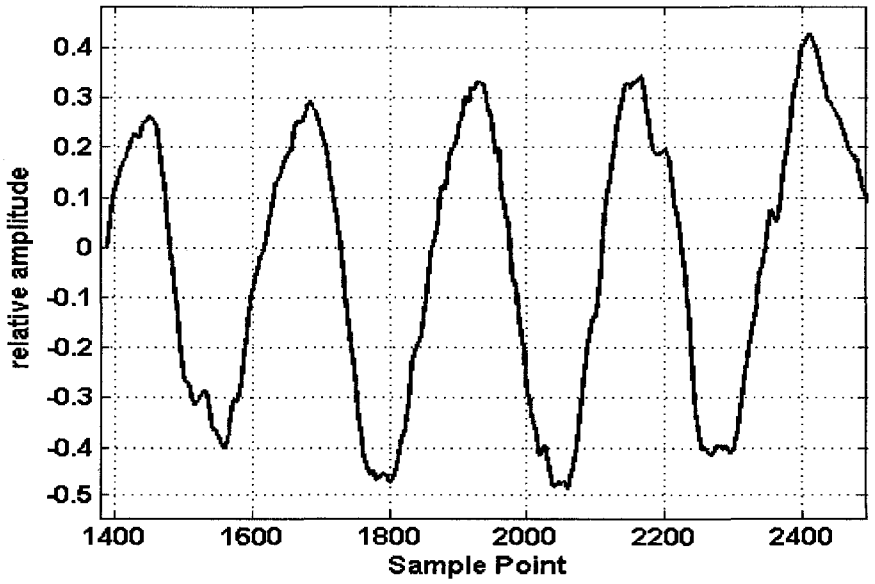

Fig 4.13 Measured results of two targets at 3.5 and 4 m

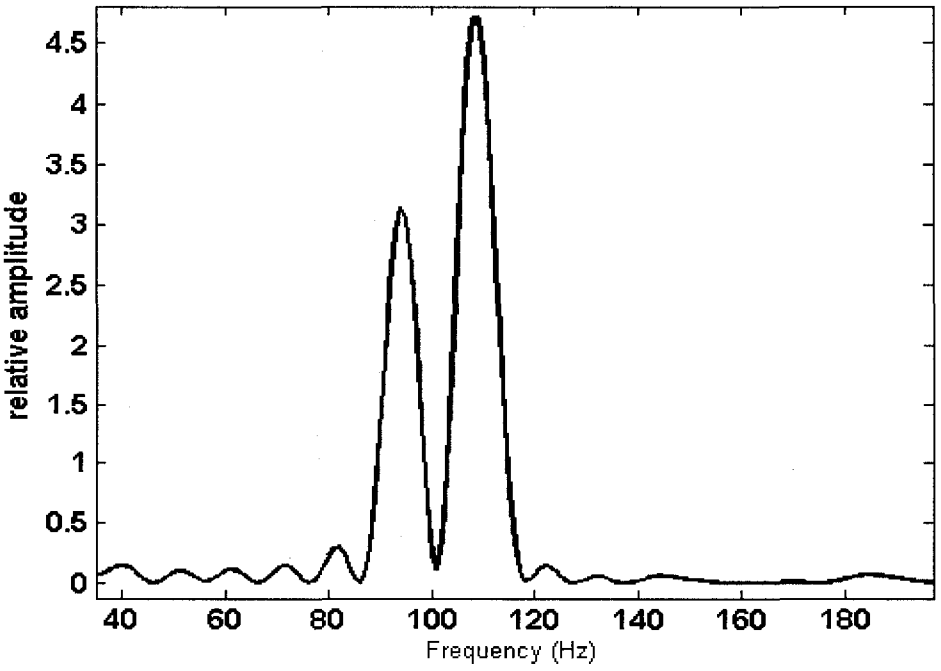

Fig 4.14 FFT results for two targets at distances of 3.5 and 4 m

As our second experiment, the SS operation mode of the realized K-band (24 GHz) radar has been tested. The test setup consists of the radar using a horn antenna and a flat metal plate serving as a reflecting target that is placed at distances from 1 to 6 m. The PN code is again modulated by the DDS with BPSK modulation offering pulses with a duration time of less than 12 ns. The transmitted frequency of the microwave front-end lies between 24 and 24.008 GHz. The transmitted and received signals are then mixed in a double balanced mixer, and the IF signal is filtered and amplified by a low noise amplifier. The very low pulse duration time of 12 ns corresponds to a range resolution of approximately 0.3 m with an ADC offering a sampling frequency of 500 MHz. Simulation results are shown in Fig. 4.15. The transmitted PN code is mixed with the

received PN code. Because the transmitted signal and the reflection are mixed in the receiver, the distance can be determined by the time duration of the peak value, and it is shown that different distances yield different peak-value time-delays. The measurement results for this experiment are shown in Fig. 4.16. Up to a distance of 6 m, the precision is better than 0.3 m. For larger distances, the SNR of the received signal is not sufficient in this experiment. The waveform estimation is done in the DSP. Subsequently, signal recovery is performed with the help of the reference PN code. The recovered signal is then correlated with the reference PN code based on the ML criterion. The transmitted PN code is recovered from the receiver as well and is shown in Fig. 4.17. This PN code includes the front-seat information. As a pre-examination of the proposed system, our experiments indicate that the system can successfully achieve the required performance in terms of distance measurement and digital communication. The data information is fully recovered and can be reused in inter-vehicle communication. It is to be mentioned that in all the presented experiments, the range is obtained from the FMCW radar mode, whereas the data information is acquired with the help of the PN code pulse radar. The presented experiment shows that the software defined radar gives complete and comprehensive information between the radar and surrounding targets in a self-consistent manner.

The software defined radar, however, provides a low cost and flexible way to build a combined radar and communication system for vehicle applications. It is thus necessary to establish an inter-vehicle communication system that is applicable to this environment. To solve these problems, this work proposes a software defined radar together with an

inter-vehicle communication system using SS techniques [59]–[61] within the same platform.

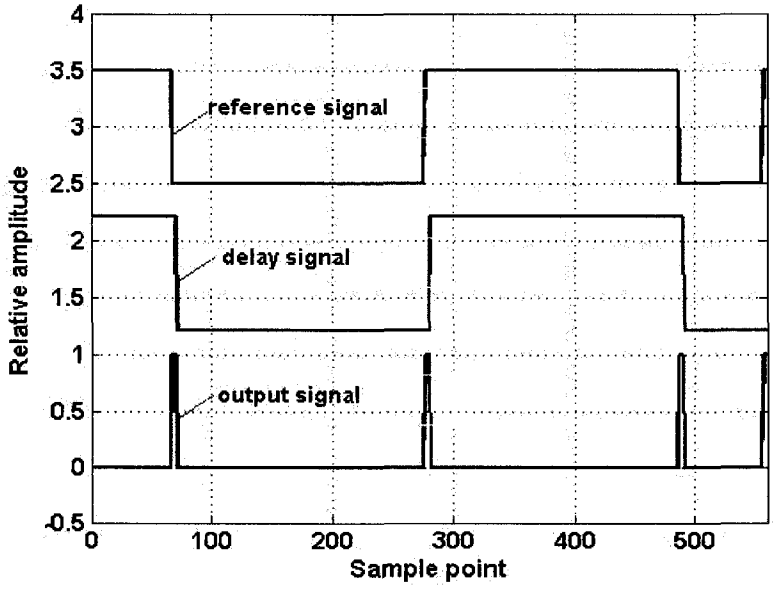

Fig. 4.15. IF signal of the PN code pulse radar (simulation).

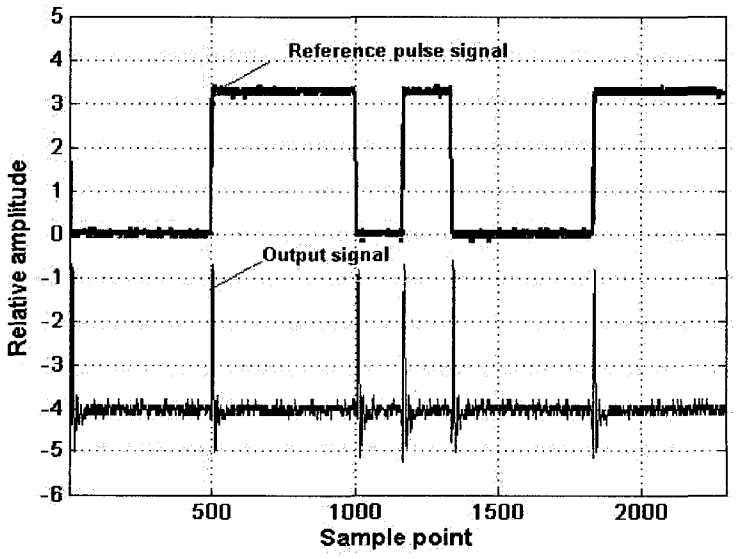

Fig. 4.16. IF signal of the PN code pulse radar (measurement).

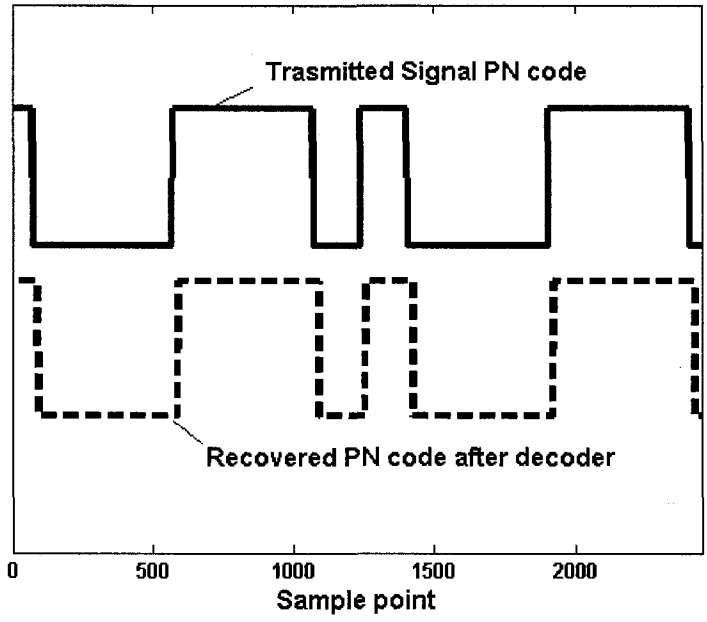

Fig 4.17 The binary recovered signal from the experiment

4.3. FFT and MUSIC algorithms-related experimental results

An experimental test setup in our laboratory was used to perform short-range measurements (up to 5 m). The adjustable DDS system parameters include μ denoting the sweeping rate, ΔF corresponding to the sweep bandwidth, and F_{step} as the frequency increment of the DDS. With a system setup of $\mu = 1.2e10Hz/s$, $F_{step} = 20Hz$, and $\Delta F = 300MHz$ we obtain a sweep cycle of 50 ms. Fig 4.18 shows the FMCW radar test arrangement. A series of measurements with a target placed at different distances from the receiver was performed. Averaging was not used in this work and every

distance measurement corresponds to data processing obtained over a signal acquisition window equal to 25 ms.

In addition, a calibration step is performed after obtaining range measurement result. The signal has also to travel through the whole circuit, so we have to consider the time delay it takes for circuit and cables within the calculations, especially when a long cable is used between the circuits. This happens because the reference plane for the distance is not the antenna plane, but the mixer plane, because the transmitted and received signal are mixed to produce the IF signal frequency which is proportional to the distance. This causes only a constant error and by measuring the distance to a reference target you can easily remove the constant error.

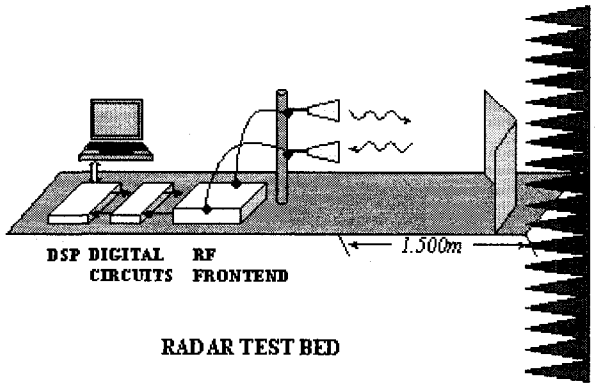

Fig. 4.18 FMCW radar test set up for short-range measurements

In our data processing, both for FFT and MUSIC algorithms, 8192 data points are used. This gives a frequency resolution of 8.79 Hz. As a reference, the range is measured with the help of a laser meter to 3 m with a precision of of 10^{-4} m, which we consider sufficiently accurate for our purposes.

4.3.1 Experimental Results

In our first measurement, the beat frequency yields 240 Hz. Fig. 4.19 shows the results of the MUSIC algorithm signal processing. From this result, we obtain a beat frequency of 232 Hz after calibration. Fig. 4.20 shows the results of the classical FFT algorithm. After calibration, the beat frequency calculated from this result is 223 Hz. These frequencies yield a range of 2.96 m from the MUSIC algorithm as well as 2.85 m for the FFT. From Fig. 4.19 and 4.20 it is obvious that the MUSIC scheme can eliminate noise and give a very sharp and distinctive peak, whereas it is substantially more difficult to determine the frequency peak with the FFT algorithm. However, the MUSIC algorithm requires considerably more computational effort, which could represent a critical point in terms of real-time signal processing and measurement.

For a range measurement of 2 m, Fig. 4.21 shows the results of MUSIC and FFT algorithms in comparison. The frequency is determined to 169 Hz in the MUSIC algorithm and 147 Hz in the FFT after calibration, compared to a theoretical beat frequency of 160 Hz. This yields ranges of 2.01 m and 1.86 m for MUSIC and FFT algorithms, respectively. From Fig. 4.21 we can see that the MUSIC algorithm peak results in the center of two peaks of the FFT algorithm. This result shows once more that the MUSIC algorithm offers a more distinctive identification of the desired frequency in order to calculate the correct range. This is not the case with the FFT technique.

In addition, we observe another, smaller, peak in Fig. 4.21 with the MUSIC algorithm, which corresponds to a doubled beat frequency. A possible explanation for this

phenomenon is multi-reflection of the transmitted signal. A comparison of the relative range errors determined by both MUSIC and FFT algorithms is shown in Fig. 4.22.

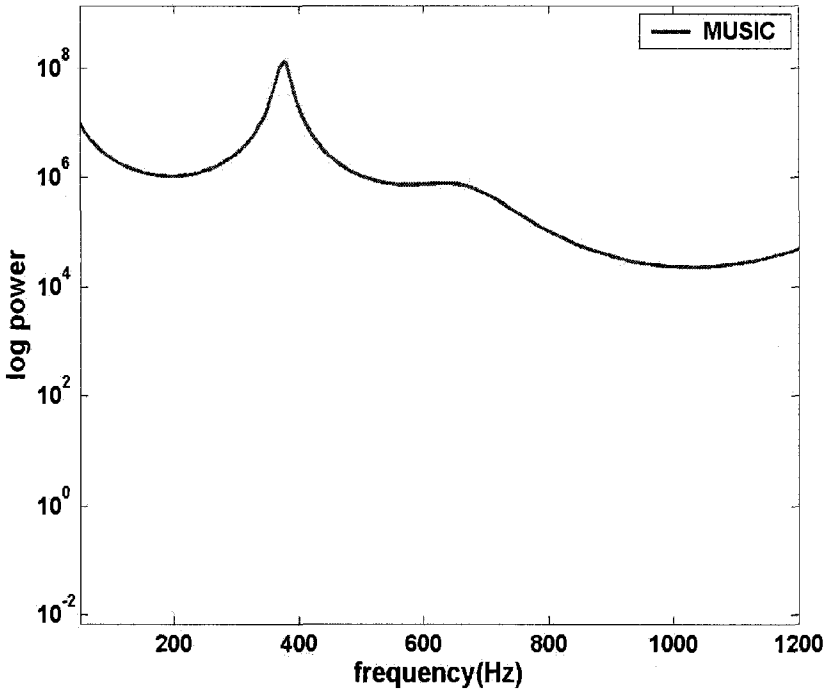

Fig. 4.19. Spectral response of the MUSIC algorithm

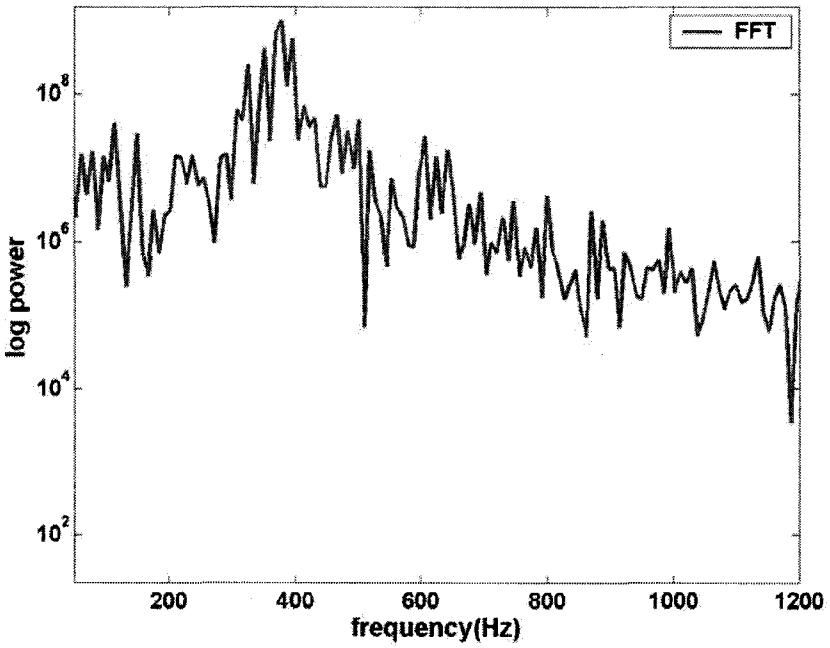

Fig. 4.20. Spectral response of the FFT algorithm

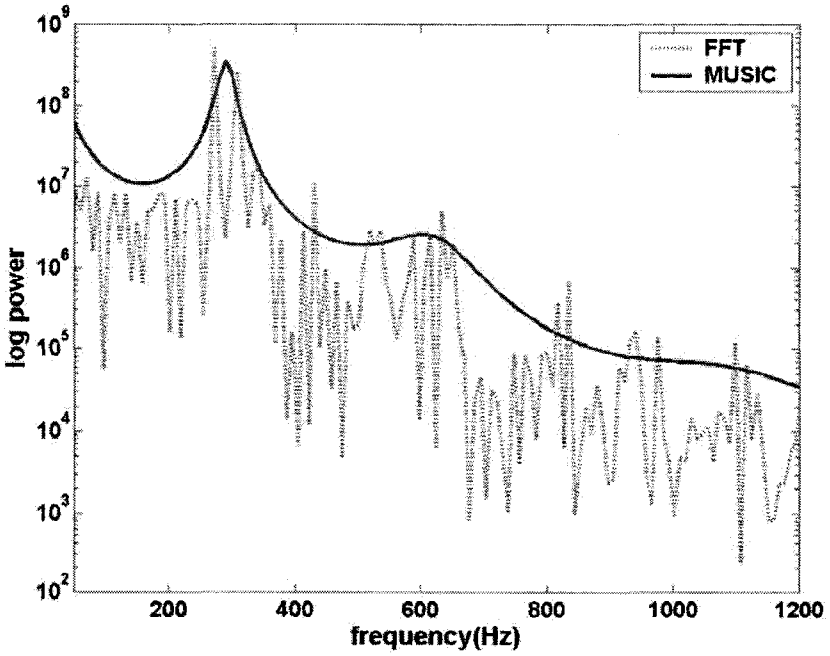

Fig. 4.21. Comparison of MUSIC and FFT spectral response algorithms

Finally, the average relative error (the absolute error divided by the reference range) of the ranging measurement from the MUSIC algorithm is calculated to 2.9% compared to a range error of 7.3% for the FFT. Thus, we conclude an improvement of the absolute range measurement error with the MUSIC algorithm.

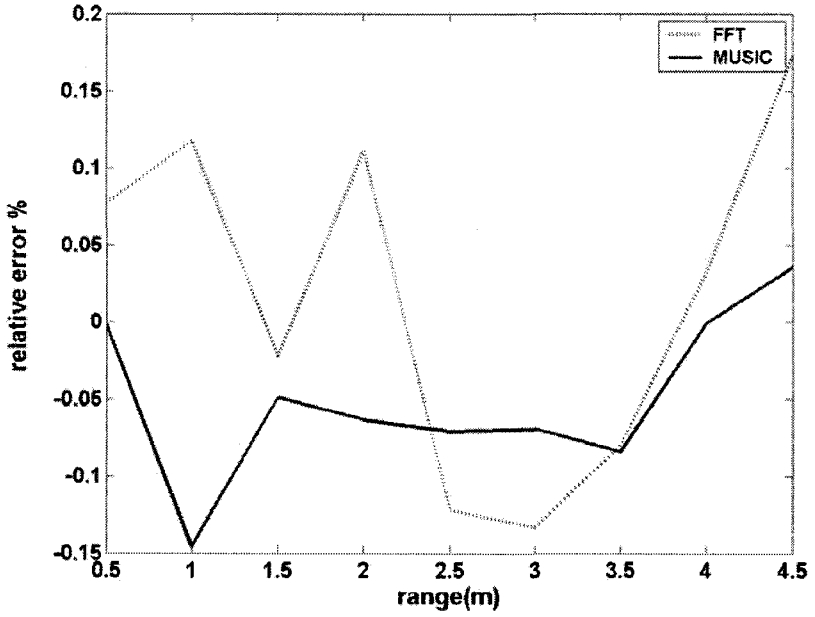

Fig.4. 22. A comparison of the relative error of the two algorithms

4.3.2 Conclusion

In this section, we have presented a range estimation algorithm for our software defined radar system. We have demonstrated that the signal estimation by means of the MUSIC algorithm can enhance the range resolution. By processing the experimental

data, it has been confirmed that the MUSIC algorithm is able to yield more accurate results, which is well applicable even in a high noise environment.

This frequency estimation technique has been verified by theory and measurements with our experimental 24 GHz software defined radar setup. Moreover, the presented method is applicable in a scenario involving multi-targets and velocity measurements.

4.4 Summary

A 24 GHz software-configurable radar and communication system based on a heterodyne receiver has been proposed and demonstrated both in simulation and measurement. The system provides two time-divided modes, namely, an FMCW and a PN code pulse mode. The advantage of this type of software-configurable radar is its combination of FMCW/PN code pulse radar, which retains the benefits of both methods and results in a capability of obtaining a high precision range measurement and communication function at the same time. The measurements of the developed system in K-band yield a maximum error of approximately 15 cm. The key feature of the proposed technique is the use of a DDS, which can adjust modulation schemes and frequency shifts in order to introduce software configurability into the transmitter. The second main component is the DSP providing the capacity for processing computationally complex digital algorithms for different radar modes. Altogether, this system provides an effective method to develop a low-cost, compact, and multi-function radar/wireless communication system with a single front-end design.

CHAPTER 5

SIX-PORT-BASED SYNTHETIC SOFTWARE DEFINED RADAR

This chapter proposes and presents a simple C-band software-reconfigurable range radar architecture using a six-port in the receiver. This concept is presented at microwave frequencies and promises a straightforward scaling of the circuit architecture into the millimeter-wave range. The proposed system provides three time-divided modes of operation, namely, a coarse FMCW range measurement mode in combination with a high precision CW mode and an SS mode for high interference situations. In the FMCW and CW modes, the six-port is used both as a phase detector and a mixer. In the SS scheme, the system uses a phase demodulator. In previous measurement systems, the signal waveforms are generated in a similar way but do not use three different schemes to combine performance advantages such as low LO power requirements, direct frequency conversion, and anti-interference capability. Software defined measurement is flexible and versatile and can be used to realize a combined system and is easily usable as a software defined radar system in combination with an appropriate antenna, such as a horn antenna. This chapter presents a brief introduction into the six-port concept, and its integration into a software defined radar system is outlined with simulations and the

fabrication and measurement of a C-band radar prototype at 4 GHz.

5.1 Calibration of the six-port

By using the six-port receiver for phase demodulation in a CW system, the phase difference between the transmitted and reflected signals related to the target can be calculated from the four power detectors [62], which in turn yield the target range. The maximum unambiguous range follows from the condition $\Delta\varphi = 2\pi$. A range of 15 m, for example, requires a frequency shift of 10 MHz. However, this maximum range restriction can be solved by using additional signals with different frequencies or other modulation methods such as the FMCW scheme.

In order to determine the values for the coefficients in (5.2), the six-port circuit needs to be calibrated before an accurate measurement is possible. Many six-port calibration techniques have been developed [63], from which the calibration method outlined by Woods-Somlo-Hunter is selected for the purposes of this work [36]. A relation between the complex reflect coefficient of the load at port 2 and the power levels at ports 3-6 in the six-port is described by an equation formulated by Woods [36] as follows:

$$\Gamma = r + jx = \sum_{i=1}^{4}(F_i + jG_i)P_i \Big/ \sum_{i=1}^{4} H_i P_i \,, \tag{5.1}$$

where Γ is the reflection coefficient vector at a certain frequency, P_i is the reading of the i^{th} power of the detector, and F_i, G_i, H_i, are real constants. Without loss of generality, these constants may be normalized by setting $H_4 = 1$, leaving eleven real constants to be determined from equation (5.1) by a suitable calibration procedure involving the successive connection of known terminations (standard reflections) to the measuring port. Five and a half terminations [36] are used in this calibration: four phased (offset) short terminations, a matched load, and an intermediate termination with a reflection coefficient $|\Gamma| \sim 0.3 - 0.5$. The phase of the intermediate reflection needs not be known a priori. The six-port calibration setup is shown in Fig. 5.1.

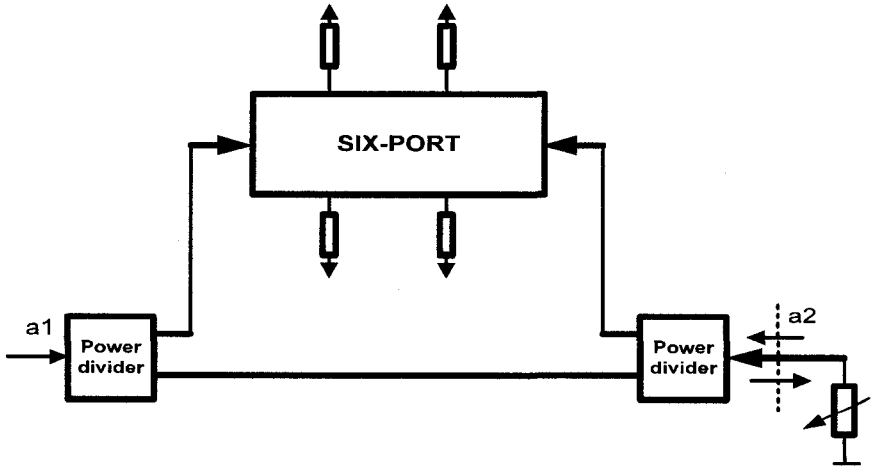

Fig. 5.1. Six-port calibration setup.

In general, Schottky diodes are used as power detectors in six-ports. To make sure that the output voltage of the power detector is proportional to the detected power, the diodes should be operated in the square-law region. The term "square law" comes from the output voltage being proportional to the input power (input voltage squared). Most microwave detectors inherently satisfy the square law for input power levels up to about –15 dBm. The measured characteristic curve of the Schottky diode used in the designed six-port is shown in Fig. 5.2. The non-ideal square law property of Schottky diodes may introduce errors into the measured phase results. Due to these non-ideal characteristics, we also adopt a calibration of the detector diodes in our work. The relation between the output voltage and the input power of the detector is calibrated on the basis of the measured results in Fig. 5.2. When the output voltage is obtained from a detector, the corresponding input power is calculated from the curve in Fig. 5.2. Thus, the power detectors can work beyond the square-law region without bringing errors into the system. Therefore, the calibration of the entire six-port circuit becomes a two-stage process combining the detector and six-port calibrations. Such a two-stage procedure can guarantee a more accurate measurement over a wider dynamic power range than the traditional six-port calibration. Once the detector calibration is finalized, the six-port circuit works not only within but also beyond the square-law region. In this way, higher detector input power levels can be used, which yields the advantage of improved

conversion loss when the six-port is used as a mixer in the FMCW mode.

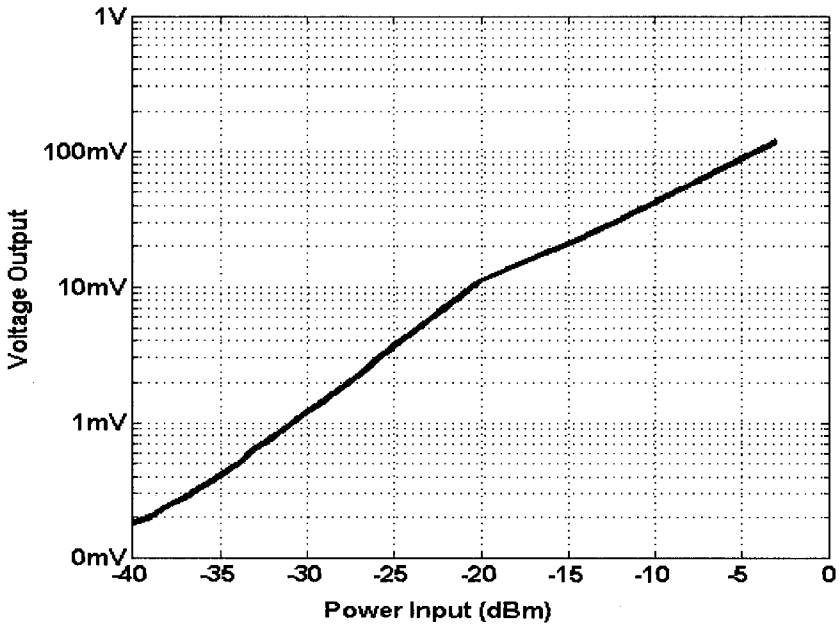

Fig. 5.2. Measured dynamic characteristics of the used Schottky detector.

In the proposed software-defined radar scheme, the same six-port circuit is also designed to discriminate frequency information or carry out a frequency translation in the FMCW radar. The basic principle of the FMCW radar is well known in the fact that the frequency of a transmitted signal changes with time in a prescribed manner. By comparing the frequency of the (time-delayed) received signal with the frequency of a sample of the non-delayed transmitted signal, a measurement of the transit time can be

completed from the beat frequency. Usually, the frequency information of the six-port is contained in the phase difference $\Delta\varphi$ between port1 and port2. In our proposed software-defined measurement system, the frequency shift between port 1 and port 2 can be extracted directly from the signals at ports 3-6 because the Schottky diode power detectors also provide a mixing function and can therefore give the beat frequency directly from the received FMCW signals.

It is well-known that a Schottky diode is a nonlinear component with a DC *I-V* characteristic that can be expressed by [64]

$$I(V) = I_0 + i = I_0 + vG_d + \frac{v^2}{2}G_d^{'} + \cdots, \tag{5.2}$$

where I_0 is the bias current, $G_d = \frac{1}{R_j}$ and R_j is the junction resistance of the diode. $G_d^{'} = \alpha G_d$, where $\alpha = q/nkT$ and q is the charge of an electron, k is Boltzmann's constant, T is the temperature, and n is the ideality factor. The three-term approximation for the diode current in equation (5.2) is called the small-signal approximation, which is adequate for low power applications.

In the six-port circuit shown in Fig. 5.1, an RF signal (the received signal with a frequency ω_r) and an LO signal (the reference signal with a frequency ω_0) are combined with directional couplers and fed to the power detectors. The square term v^2 in (5.2) is given by the following output current [40]:

$$
\begin{aligned}
i &= \frac{G_d'}{2}(v_1 \cos w_r t + v_2 \cos w_0 t)^2 \\
&= \frac{G_d'}{4}[v_1^2 + v_2^2 + v_1^2 \cos 2w_r t + v_2^2 \cos 2w_0 t \\
&\quad + 2v_1 v_2 \cos(w_r - w_0)t + 2v_1 v_2 \cos(w_r + w_0)t]
\end{aligned} \tag{5.2}
$$

In the Schottky diode power detector, a bypass capacitor is inserted to form an RF ground for the diode. This capacitor determines the minimum rise and fall times of the detector circuit and the minimum detectable RF pulse length. The current terms at high frequencies $\omega_r + \omega_0, 2w_r$ and $2\omega_0$ are filtered out in the phase detector. The IF current term at frequency $\omega_r - \omega_0$ represents the beat frequency of RF and LO signals for the FMCW mode. The frequency of this IF signal can be obtained through a FFT in the DSP. This shows that the six-port can be used as a mixer in the FMCW radar. The Schottky diode power detectors used in the present six-port circuit have a video bandwidth of 10 MHz. So the beat frequency is passed by diode power detectors.

5.2 Design of software defined measurement system based on six-port

The block diagram of the proposed system is shown in Fig. 5.3. The transmitting part consists of a DDS and a microwave up-converter chain; the receiving part consists of a six-port circuit, an ADC, a DSP and a PC working as a controlling/monitoring device. The up-converter chain translates or modulates a low-frequency (baseband) signal from the

DDS to a microwave carrier signal with a center frequency of 4 GHz in our work. A portion of the transmitted signal is connected to port 1 of the six-port circuit serving as the reference signal. The four power detector output signals pass through four operational amplifiers and are subsequently fed to four ADCs. The data acquired by the ADCs are processed by the DSP platform and the frequency as well as the phase difference between the received and reference signals are calculated. In order to test the performance of this C-band hybrid range measurement system, multiple lossy cables of variable lengths are used to estimate the measurement accuracy of the proposed software reconfigurable range radar in the range measurement. The cable lengths vary from 0.32 m to 16 m. Meanwhile, these cables are also measured by using a commercial network analyzer (ANRITSU 37397G) to obtain a reference length for comparison.

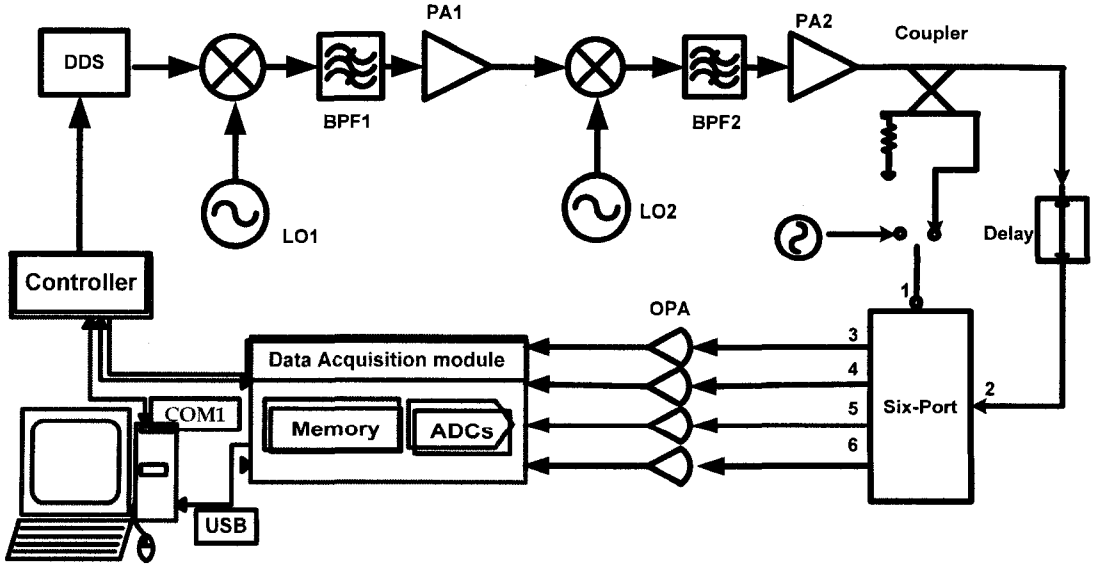

Fig. 5.3. System block diagram of the six-port range measurement system.

Usually, different analog radar configurations are used to fulfill different functions. However, in software defined radar, because DDS and DSP are programmable, we can generate different waveforms in the baseband and use different algorithms to process the received signals. Therefore, various radar functions can be realized within a single hardware configuration. In our work, the radar is realized with three functions: FMCW radar, CW radar, and SS radar. The three waveforms for these modulation schemes are generated by the DDS and shown in Fig. 5.4. The waveform for the FMCW radar is a triangular frequency sweeping (chirp) signal at a repetition frequency of 12.5 kHz with a bandwidth of 75 MHz. The CW radar waveform is a two-tone signal with a frequency difference of up to 10 MHz. The SS radar waveform is a BPSK modulated signal with a modulation bandwidth of up to 40 MHz. The SS signal can also be used for digital communication. The FMCW sweep parameters consisting of the chirp bandwidth and the sweep time are programmable in the DDS and so are the frequency difference between CW signals and the chip rate of the SS signal. Subsequently, the received signal is processed in the DSP with different processing algorithms. The DSP algorithm is shown in Fig. 5.5.

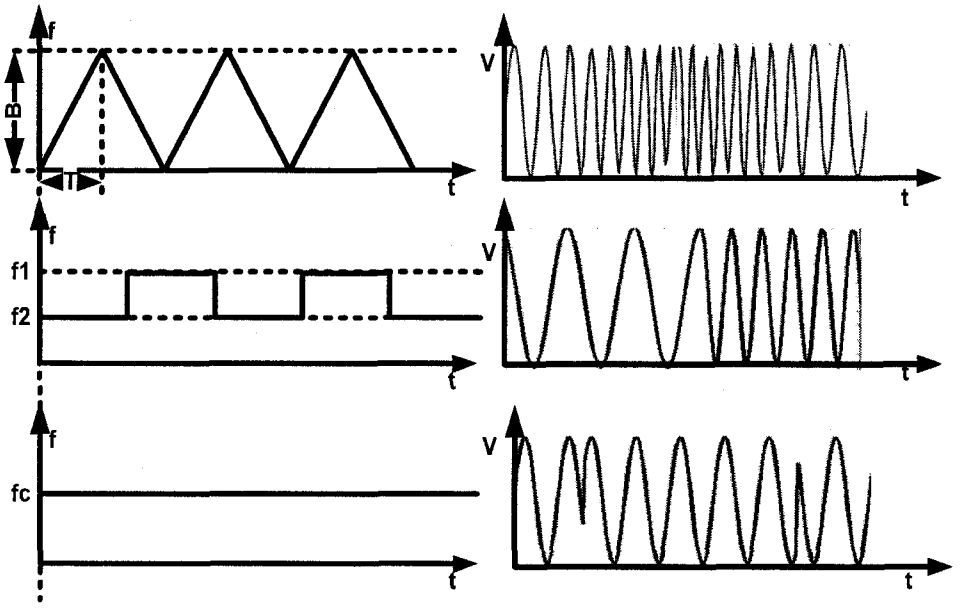

Fig. 5.4. The three signal waveforms used in the proposed software-defined system.

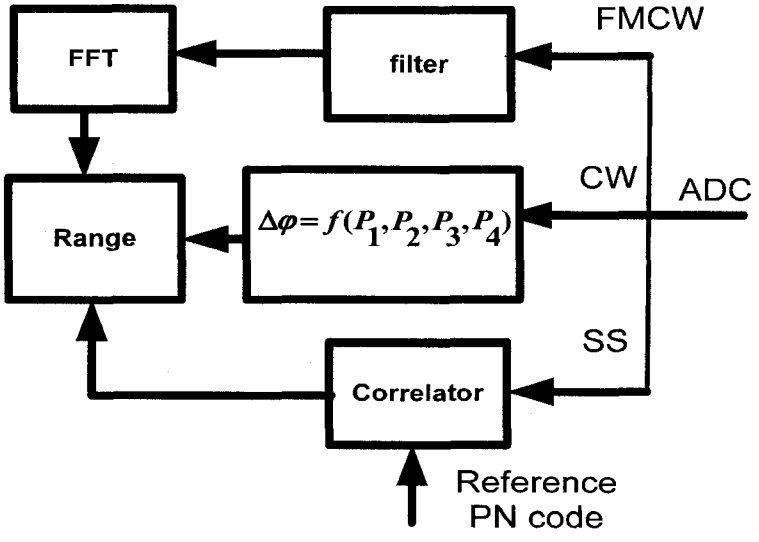

Fig. 5.5. DSP algorithm for the signal processing of different modulation schemes.

5.2.1 Measurement results and discussion

In order to test the performance of the presented S-band composite microwave ranging system, the lengths of different cables are measured to estimate the accuracy of the software defined radar system in distance measurements. The cable lengths vary from 0.32 m to 16 m. In addition, the cable lengths are measured with a commercial network analyzer to obtain reference lengths. The test bench setup for this experiment is shown in Fig. 5.6.

The frequency sweeping range of the transmitted FMCW signal is from 3.965 GHz to 4.040 GHz with a sweep period of 15 ms. For the six-port receiver, the LO power level is selected to –10 dBm. The time domain output signals of the four six-port power detectors for the case of a 16 m cable are shown in Fig. 5.7. The graph shows the beat signal between the transmitted signal and the received (delayed) signal. As expected, in Fig. 5.7 the four signals at the output of the power detector have the same frequency but different amplitude and phase.

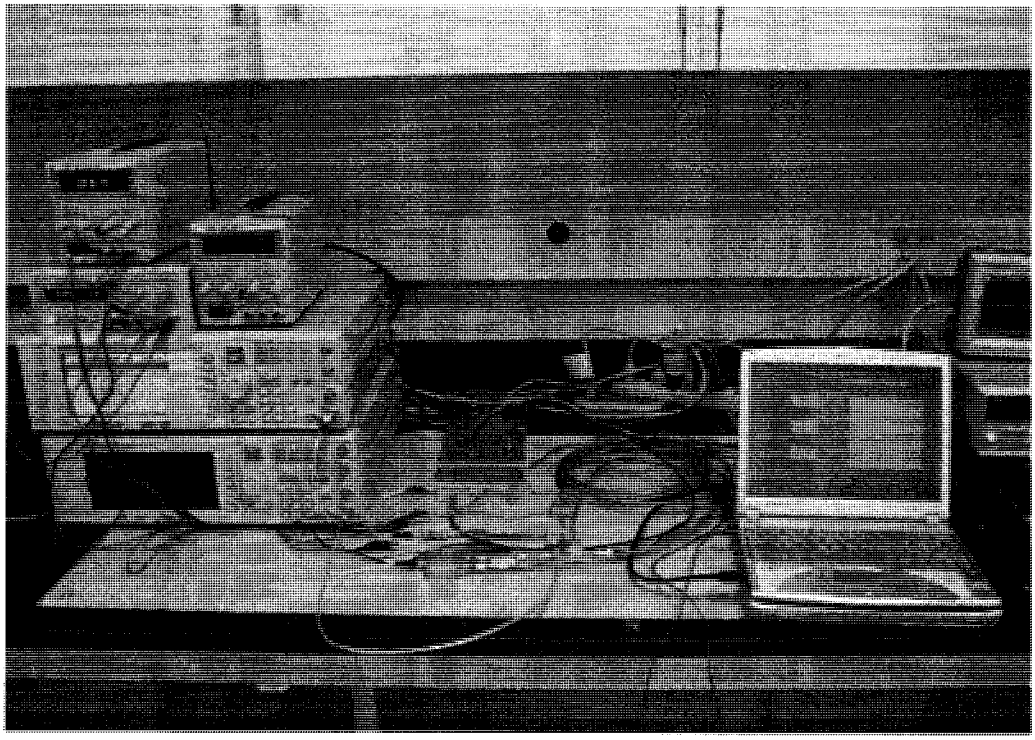

Fig. 5.6. Test bench setup for the measurement of the S-band software defined radar.

The four time-domain output signals plotted in Fig. 5.7 are evaluated with an FFT to convert them to the frequency domain, and their spectral components are shown in Fig. 5.8 . The peak frequency corresponds to the measured cable length according to equation (4.5). A complete list of measurement results for the FMCW radar are presented in Table 5.1 showing a maximum range error of 50 cm. This range error is mainly determined by the sweeping bandwidth of the FMCW signal and can be reduced by increasing the sweeping bandwidth as it has been described in chapter 2.

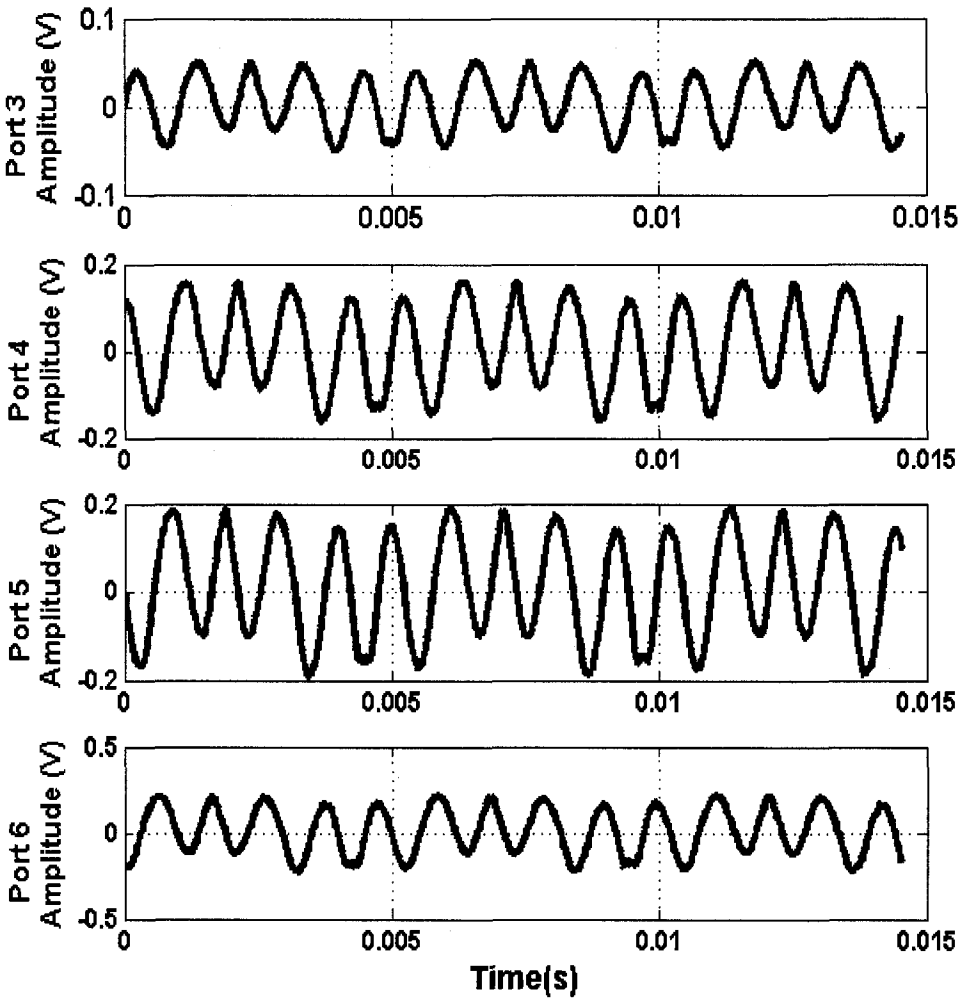

Fig. 5.7. Received signals in the time domain from FMCW measurements.

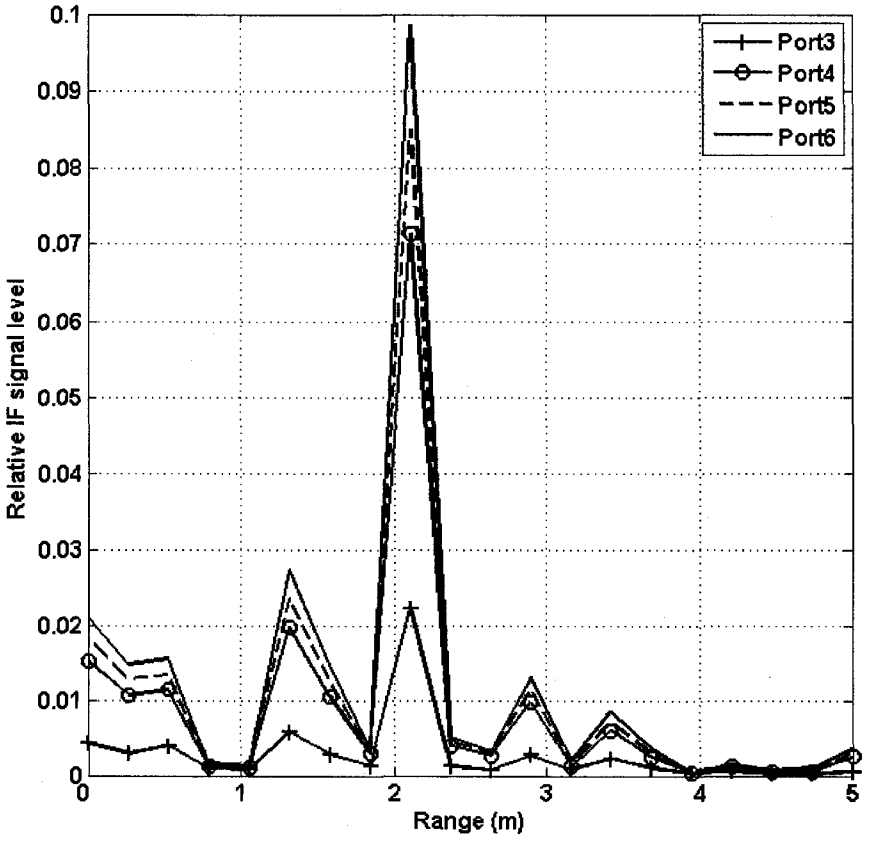

Fig. 5.8. Spectrum of the received signal after the FFT processing.

In the CW mode, two signals at frequencies of 4.0 GHz and 4.01 GHz, respectively, are used yielding a frequency shift of 10 MHz and therefore a maximum unambiguous range of 15 m, which is much larger than the range resolution of the FMCW radar. Thus, the problem of maximum range restriction can be solved by combining the CW radar with the FMCW radar. Another advantage of this combination is that the FMCW radar can discriminate multi-targets but the CW radar fails to do so. The time domain output signals of the four six-port power detectors are shown in Fig. 5.9. Our measured results suggest an

accuracy of 5 cm for range measurements due to a phase uncertainty of 1.2° for the six-port circuit. Because the phase errors of the six-port circuit can basically be improved by using different frequencies, a more accurate range measurement can be obtained by selecting additional signals with a larger frequency difference.

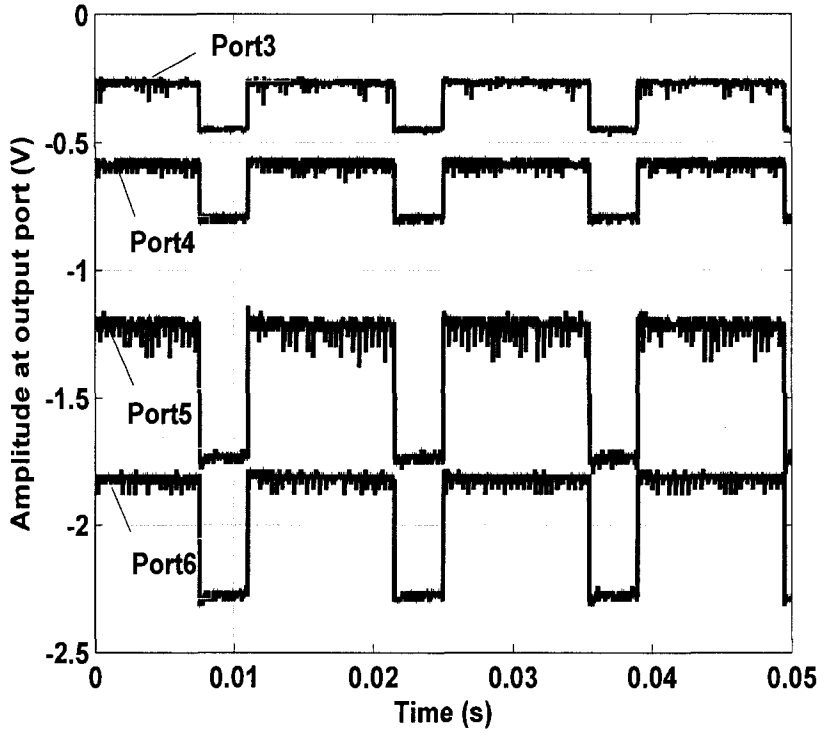

Fig. 5.9. Time-domain detector output signals for a 4 GHz CW measurement (Δf = 10 MHz).

By combining FMCW and CW functionalities in one system using different time slots, a multi-functional radar with a high-range resolution can be developed. Table 5.1 shows measurement results comparing a combined FMCW/CW system and a stand-alone

FMCW radar. The first column serves as a reference showing the results obtained from the network analyzer. The second column gives the FMCW measurement results. The maximum measurement uncertainty is about 50 cm, which depends mainly on the modulation frequency bandwidth of the sweeping signal, as mentioned earlier. The third column gives results obtained from the combined FMCW/CW system without performing a detector calibration. The range error without calibration is 17 cm as the output voltage of the detectors working beyond the square-law region cannot yield the true power level. The fourth column displays results including the detector calibration, showing that the largest range measurement error is less than 5 cm. Therefore, the calibration of the detectors in the six-port circuit can solve the nonlinear problem arising by operating the power detectors beyond their square-law region, which effectively increases the input dynamic range of the radar receiver. In addition to this improvement, the shortcoming of the CW radar in terms of inherent range ambiguity can be reliably resolved on the basis of non-ambiguous FMCW range measurements. Furthermore, the range measurement accuracy of the combined range radar can be easily improved by increasing the frequency difference between the two-tone signals with the same phase detection accuracy of the six-port circuit.

5.2.2 Summary

A software-reconfigurable range measurement system based on the six-port receiver technique has been proposed and demonstrated experimentally. The system has two time-divided modes, namely, the FMCW and the CW mode. The combination of FMCW/CW modes within a single hardware platform retains the merits of both methods and results in the unique ability to obtain a high-precision range measurement. The six-port is shown to work not only as a precision phase detector in the direct receiver in the FMCW mode but also as a mixer in the CW mode. The imposed power level of the six-port circuit can be elevated beyond the square-law region while the power detectors in the six-port circuit are calibrated to a precision power measurement. Therefore, the input dynamic range of the receiver in the proposed system is increased and the conversion loss is improved when it is used as a mixer.

Measurements of the developed system operating in C-band have shown a maximum error in the range of 5 cm. They have confirmed that a better accuracy can be achieved with the proposed platform as compared to a sole FMCW system and moreover the software-defined radar has solved the range ambiguity problem related to the CW radar. It has been shown that the DDS can be effectively deployed to adjust modulation schemes and frequency shifts in the proposed system, which makes it possible to introduce a very

TABLE 5.1
Cable lengths measured from the proposed
software defined system compared with results from network analyzer.

Length measured with network analyzer (m)	Length measured with FMCW radar (m)	Length measured with FMCW/CW without detector calibration (m)	Length measured with FMCW/CW with detector calibration (m)
0.32	0.53	0.44	0.35
0.58	0.57	0.65	0.61
0.77	0.55	0.74	0.75
1.01	0.51	1.16	1.05
1.29	1.04	1.30	1.33
1.46	1.06	1.63	1.49
1.60	1.52	1.50	1.57
10.01	10.50	10.18	10.06
11.89	12.04	11.99	11.92
12.50	12.56	12.35	12.45
13.21	13.07	13.34	13.21
14.44	14.56	14.53	14.49
15.32	15.57	15.26	15.31
16.01	16.49	16.07	16.03

The maximum range error of the FMCW radar is 0.5 m. The maximum range error of the FMCW/CW radar without the detector calibration is 0.17 m. The maximum range error of the FMCW/CW radar with the detector calibration is 0.05 m.

flexible software reconfigurability in the transmitter, while the DSP provides adaptive digital processing algorithms for different modes in the receiver. Such a software-defined design provides an effective method to build up low-cost, compact, multi-functional or versatile microwave and millimeter-wave radars with a single front-end design.

5.2.3 Comparison of Mixer and Six-port measurements

In this section, a performance comparison of software defined radars using the mixer and six-port techniques as downconverting elements in the receiver are presented. As a first step, the FMCW mode is investigated followed by an experiment employing the SS radar operation.

FMCW signal measurement

The frequency sweeping range of the transmitted FMCW signal is selected from 3.965 GHz to 4.040 GHz with a sweep period of 80 ms. The time domain output signals at the six-port power detectors for a line with a length of 8 m yield the beat signals between the transmitted and the received (delayed) signal. It is comparable to the output signal from the system using a mixer, because in this case the six-port is used as a downconverting element.

All the previous experiments have been carried out in the time domain and have been subsequently transformed into the frequency domain with the help of an FFT for signal processing purposes. Fig. 5.10 shows the spectral components of the time domain output signal from both mixer and six-port. For the heterodyne receiver, the LO power is selected to 10 dBm, whereas for the six-port receiver it is –10 dBm. This result highlights the

performance of the six-port system. It needs to be mentioned that in this experiment, the received signal level from the six port is less compared to the mixer because the LO power needs to be lower in order to remain in the linear operating region. The measured results for both of the two FMCW systems show a range error of 50 cm.

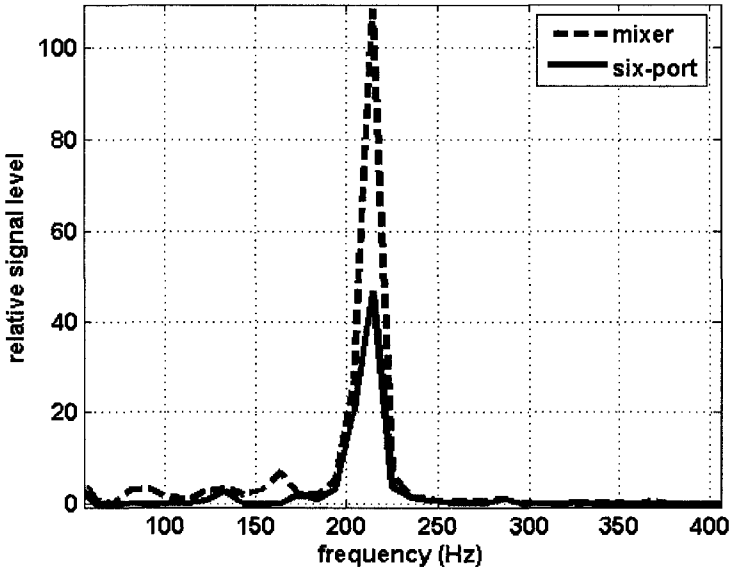

Fig. 5.10. Spectrum of the received signal of the heterodyne receiver and the six-port receiver

Spread Spectrum signal measurement

In our experiment for the SS radar, the heterodyne receiver [65] and the six-port receiver are both used as the BPSK demodulators for the SS signals. The DDS is used to generate PN code sequences for the BPSK modulation. The demodulated signal from the

mixer and the six-port using PN code rates of 40 MHz and 1 MHz, respectively, are shown in Fig. 5.11 and Fig. 5.12. In both cases, the code length is selected to 32. From the results, we observe a delay between the demodulated and the reference PN codes. It is also clearly visible that the demodulated PN code from the six-port shows a lower signal level and a much longer rise and fall times compared with the results for the mixer. The reason for this phenomenon is the use of Schottky detectors in the six-port. In a Schottky detector, a bypass capacitor forms an RF ground for the diode determining the minimum rise and fall times of the detector circuit and the minimum detectable RF pulse time. The Schottky detectors used in the presented system have a video bandwidth of 10 MHz.

Fig. 5.13 shows the output of the correlator of the received SS signal from the mixer for a PN code rate of 5 MHz. In Fig. 5.14, an experiment with a PN code rate increased to 40 MHz is shown. In this case the output of the correlator for the received SS signal is not detectable with the six-port detector because the code rate is beyond the video bandwidth of the Schottky detectors. Thus, the front end transceiver using a mixer provides a better result for the SS modulation scheme. The range error of the SS signal measurement is 2.5 m. This relatively poor performance is due to limitations in PN bandwidth and carrier frequency.

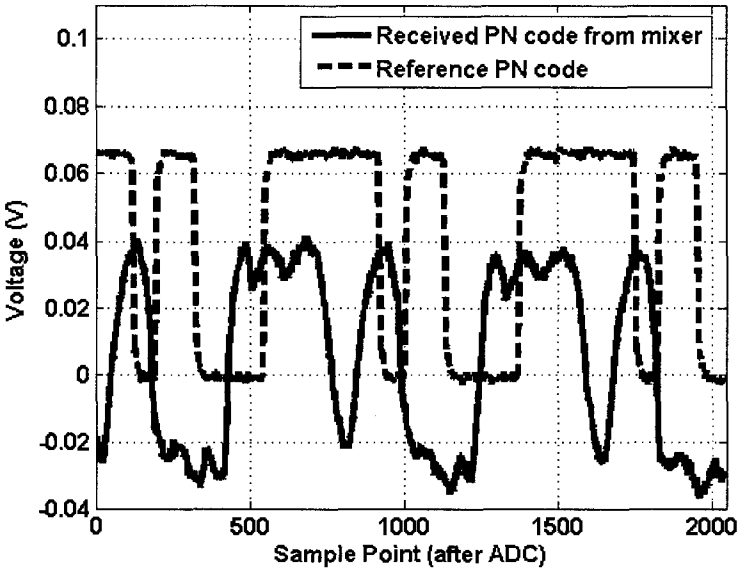

Fig. 5.11 The SS modulation received signal for the case of the mixer.

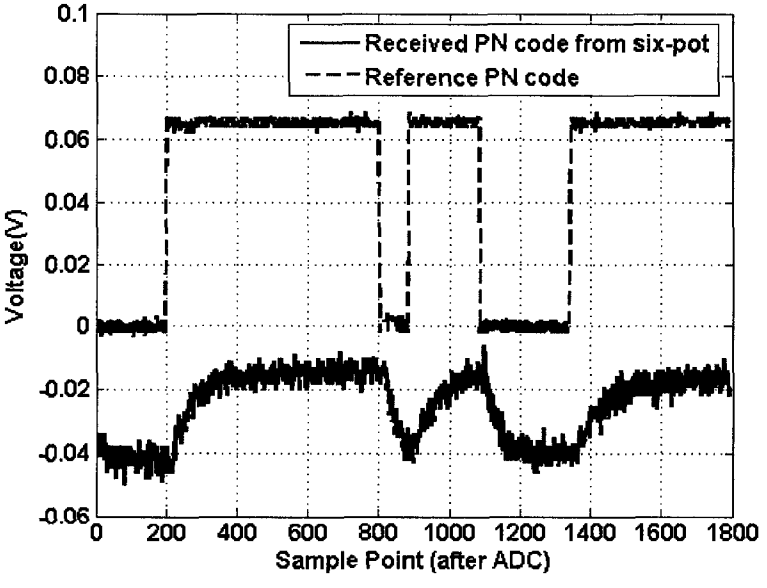

Fig. 5.12 The SS modulation received signal for the case of the six-port.

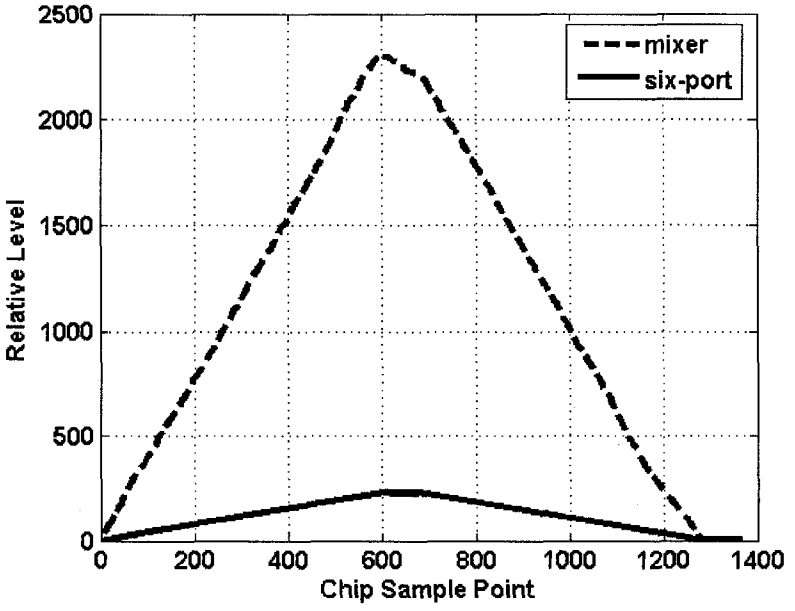

Fig. 5.13. Comparison of the two demodulation techniques of the SS modulation at a modulation rate of 5 MHz.

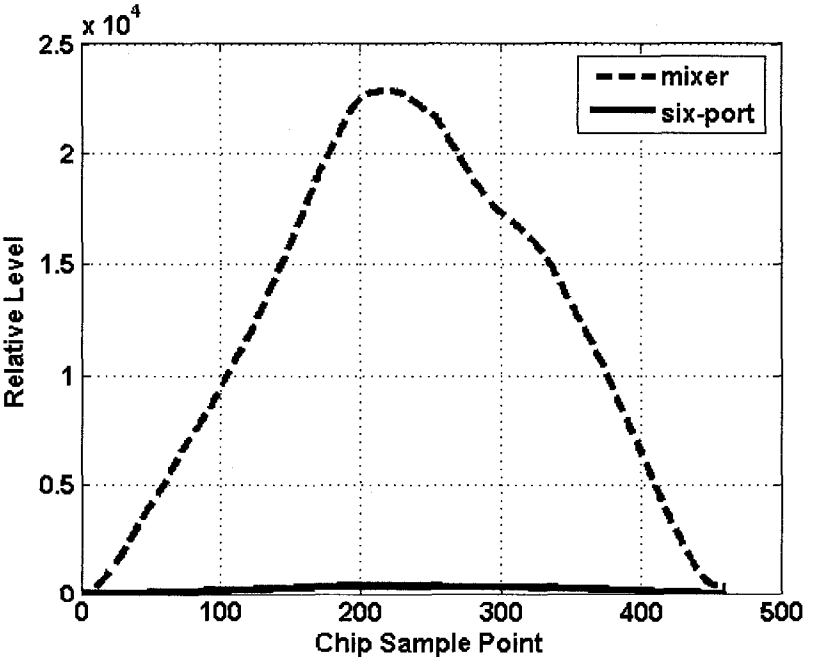

Fig. 5.14. Comparison of the two demodulation techniques of the SS modulation at a modulation rate of 40 MHz.

Finally, the measurement results for performance comparison between the mixer and six-port systems for various signal waveforms are summarized in Table 5.2. A major disadvantage in the use of a six-port demodulator is its four output ports, which require a higher number of operational amplifiers and ADCs. The second critical issue is its longer response time. However, the six-port system is well suited for accurately measuring the phase difference in systems such as the two-tone CW radar, which represents a very attractive principle for radar measurements. Moreover, six-ports are well established as telecommunication receivers and in quadrature phase shift keying (QPSK) modulation.

TABLE 5.2
MEASUREMENTS of SOFTWARE-DEFINED SYSTEM

	Mixer	Six-port	Note
FMCW	±0.5 (m)	±0.5 (m)	Range error
CW	N/A*	±0.06 (m)	Range error
SS	±2.5 (m) **	±10 (m) ***	Range error
LO power	+10*dBm*	−10*dBm*	Power Level
Received power	−10*dBm*	−30*dBm*	Power Level
Received frequency	*No limit*****	Below 10MHz***	Frequency

* No experimental measurement.
** The limitation of the PN code bandwidth and the carrier frequency
*** Depends on the video bandwidth of the Schottky detectors
**** Compared with six-port, depends on the specification of the mixer.

5.3 Multiple frequency CW radar signal processing results

High-speed or broadband RF electronics find wide-spread applications in numerous fields such as automotive industry, home-land security, sensor networks, and industrial automation. Collision avoidance cruise control (ACC) [66] has created, for example, a great market expectation for intelligent transport systems with some ACC prototypes being on the way to mass production. It requires accurate information of speed and range relative to the surrounding vehicles or obstacles, especially to the closest one in the same

lane. Most developments are based on the FMCW technique. This technique has been well accepted for its simplicity, even if it has a few drawbacks such as the difficulty of obtaining accurate distance measurements for short ranges. To give a general idea of the most important requirements for automotive radar systems, the maximum range for common commercial automotive radars is about 160 m with a range resolution of 1 m. The near range refers to distances below approximately 40 m.

Two experiments have been carried out. The first makes use of a modulation with two discrete frequencies, while the second deploys the proposed three-frequency technique. Tables 5.3 and 5.4 present the specific parameters used in these experiments.

Table 5.3 Two-frequency test conditions

Parameters	**Value**	**Units**
T	50	ms
Δf_1	48	MHz
$R_{max,1}$	3.125	m
$\sigma_{R,1}$	115.2	deg/m

Table 5.4 Three frequency test conditions

Parameters	**Value**	**Units**
T	50	ms
Δf_1	48	MHz
Δf_2	24	MHz
$R_{max,1}$	3.125	m
$R_{max,2}$	6.25	m
$\sigma_{R,1}$	115.2	deg/m
$\sigma_{R,2}$	57.6	deg/m

The most important challenge arising with this type of radar is to measure the range without a Doppler shift. The output from the mixer toggles between two or three constant voltages, which are related to their phase according to equation (3.11). Fig. 5.15 shows a time domain measurement of this signal. This signal is acquired and the voltage levels are averaged for noise reduction before calculating the phase values.

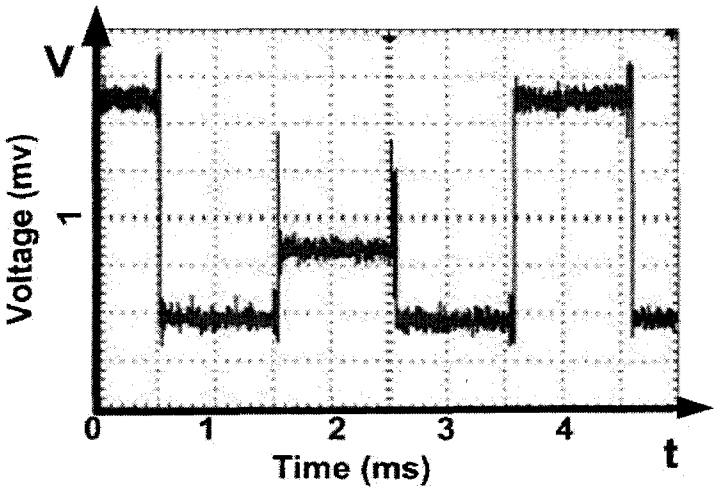

Figure 5.15 Measured time domain signal at the mixer output

The phase discriminator is limited to phase discrimination resolution. As discussed before, the maximum unambiguous range is calculated on the basis of phase discrimination over an interval of 2π. Thus, for static targets (without Doppler shift), the radar measurement capability is limited to half of the calculated unambiguous maximum range. Signal level fluctuations at the phase detector port (mixer RF port) also impair the phase measurement and limit the ranging measurement accuracy. It is only possible to measure range accurately over very short distances surrounding a calibrated range. Range calibration can be performed by associating measured phase values to a known target distance.

Fig. 5.16 shows the measured results obtained with the two-frequency and the three-frequency configurations. When $\Delta f_1 = 24\ MHz$, the measurement error standard deviation is 0.2%. When $\Delta f_2 = 48\ MHz$, the error standard deviation becomes 0.3%.

This shows the advantages of the proposed three-frequency radar. Within a range of $R_{\max 1}$ as mentioned before, we can obtain more accurate results. Beyond $R_{\max 2}$, we need to deal with a larger unambiguous range.

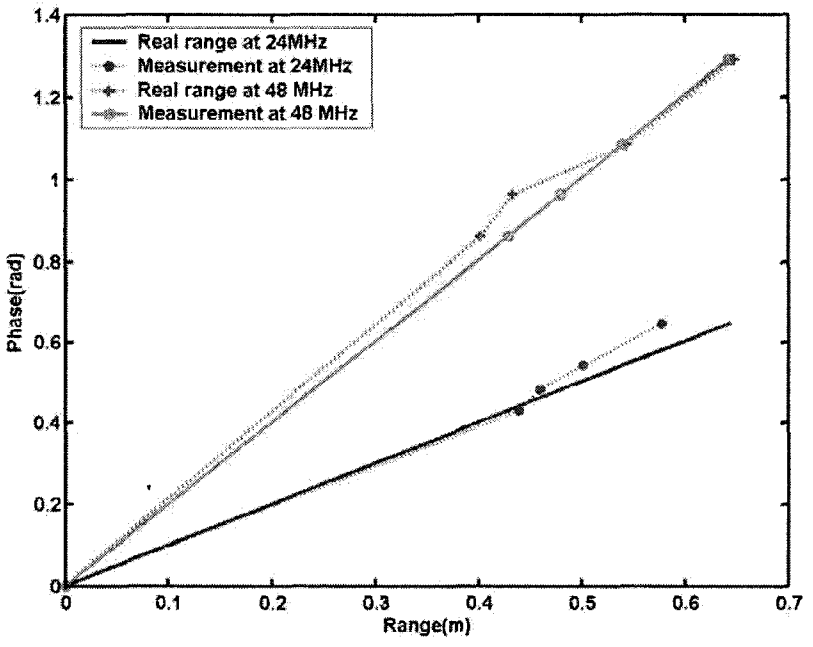

Fig. 5.16 Comparision of measured target distances versus phase

This section has presented a new scheme for radar measurements on the basis of a three-frequency technique. It has been shown that the proposed system provides a number of advantages compared to the conventional two-frequency FSK and FMCW radar sensors. Performance and characteristics of the proposed scheme have been evaluated in this work and have been compared with modeling results of our system design platform. Measured results suggest that the proposed three-frequency radar shows

an enormous potential as an alternative to the standard FMCW technique for low-cost and high-performance commercial radar systems.

5.4 Design of a 24 GHz six-port based software defined radar

In this section, we will present a six-port based software defined radar system for the 24 GHz ISM-band deploying the FMCW scheme. For simplicity, we only consider signals reflected from static targets. The radar signal is generated with a DDS and then translated and multiplied to transmit a signal at 24.125 GHz. Although the proposed architecture allows for more than one type of modulation signals, only the FMCW scheme has been implemented, tested, and discussed in this work in order to highlight the proposed super-resolution technique. A heterodyne receiver is used to translate radar echoes to baseband frequencies using the transmitter signal as a reference. This baseband signal is then digitized for signal processing.

Fig 5.17 shows the basic architecture of our proposed software defined radar. The first part includes the echo signal acquisition module and the intelligent radar signal generator, which can generate a number of signal formats under various modulation techniques. The second part is the so-called IF module that up-converts the radar signal from 300 MHz to 2.6 GHz. Finally, the front-end module includes the 24 GHz

RF-circuitry and the antennas.

Figure 5.17 explains the basic system diagram for the mixer scheme. In order to gain full benefit from such a software-configurable receiver architecture with respect to the use of such receivers in different application scenarios, it is necessary to provide flexible signal generation techniques for the clock or reference oscillators with respect to frequency and amplitude of the signal. The six-port direct conversion technique is another approach for software configurable receivers at millimeter-wave carrier frequencies as outlined in section 2.4.2.

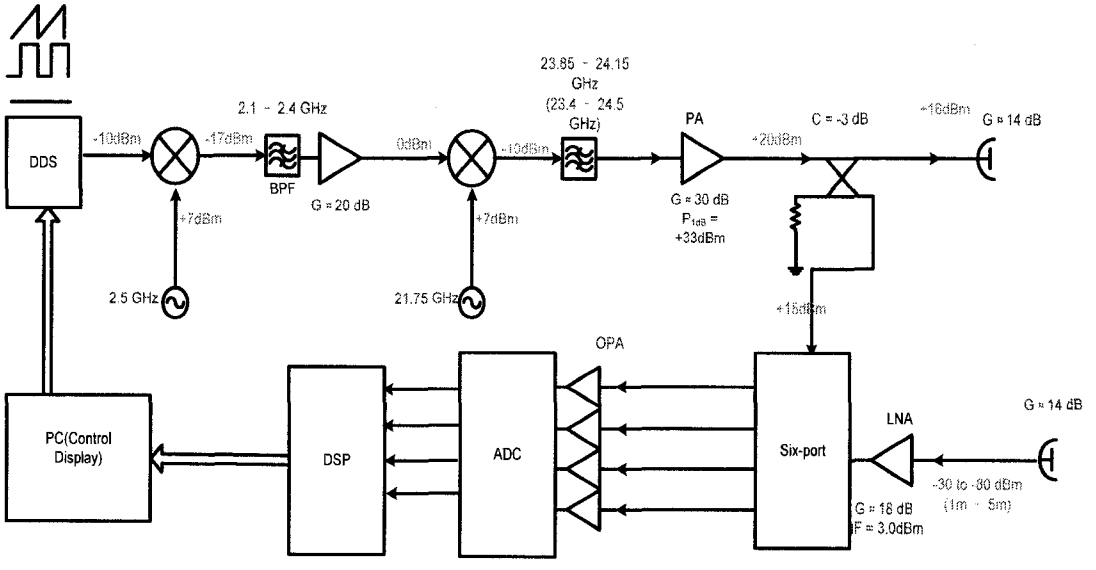

Fig 5.17 Block diagram of the six-port based software defined radar.

Six-port technology shows special properties compared to conventional heterodyne architectures that strongly depend on the application of interest. In the following, we will

show a number of advantages and disadvantages for this scheme.

The main advantage of the six-port technology is its possibility for software configuration and calibration. Furthermore, six-port technology becomes very attractive when extremely high carrier frequencies at millimeter wavelengths are used. Additionally, the same hardware can, in general, be used for different standards simply by using suitable baseband processing algorithms. Thus, in the future, extremely broadband six-port RF front-end might be the technology of choice for SDR platforms. This can help to support a certain service as different bands and standards can be probed and selected to transmit information in harsh environmental conditions. The six-port technique is very well suited for accurately measuring the phase difference of two waves, which makes the principle very attractive for determining the angle of an incident wave-front. In a simple approach, described in previous section, and can yield more accurate results in the case where a plane wave at a fixed frequency has to be detected.

The important topic is the development of software-defined radars based on six-ports up to several GHz and a subsequent up-conversion into millimeter-wave frequencies. In parallel, new technologies for tunable or switchable input filters can reduce the requirements for ADCs and therefore lead to multi-standard millimeter-wave radars. Six-port technology owns the inherent advantage of this architecture. Nevertheless, the suitability of the six-port technology for complex modulation schemes and the

competitiveness of dynamic properties are still to be shown. The combination of FPGAs, which contain the protocol software of a certain system, with a DDS to adjust modulation schemes and frequency shifts introduces software configurability also in the transmitter section of future microwave and millimeter-wave systems.

5.5 Conclusion

A software defined measurement system based on six-port technology has been described. Composite FMCW/CW/SS measurements have shown better accuracy than those obtained with a stand-alone FMCW system and appear suitable for high-precision applications. Software defined SS measurement systems provide interference eliminating capabilities. Moreover, an intensive study comparing receivers using mixers and six-ports has been done. The heterodyne receiver shows especially good performance in terms of circuit response time, but nevertheless the six-port is performant enough to be used as a demodulator for telecommunication systems. The economic viability of this type of ranging system appears very promising. Most of the current prototype systems have been built using low-cost commercial components. DDSs are used to adjust modulation schemes and frequency shifts, which makes it possible to introduce software configurability into the transmitter, and the use of a DSP provides the means for

processing the corresponding digital signal processing algorithms in the receiver. The major expense involved in a version suitable for industrial use would be in building a compact, synthesized microwave radar with single front end design.

The six-port-based software defined measurement system represents an alternative to the standard FMCW/CW system offering a distance accuracy better than 6 cm. The six-port performs coherent detection without the need for balanced mixers and precise phase shifters. Moreover, range measurements in the range of several cm are possible without additional difficulty. The suitability of the six-port technology for complex modulation schemes and the competitiveness of the dynamic properties have been shown.

CHAPTER 6

SYSTEM PERFORMANCE STUDY OF THE SYNTHETIC SOFTWARE DEFINED RADAR

Conventional radars for range measurement such as FMCW, CW, and SS radar are generally used as completely independent units. However, synthetic software defined radar systems can be designed by combining them to improve system performances and also provide multiple functionalities. It is known that different radars result in different accuracy, range ambiguity, and different overall performances. In this work, two architectures (mixer and six-port) are designed for the demonstration of synthetic software defined radar systems. Link budgets for both architectures will be compared in the following. Furthermore, we will develop a model and perform experiments to analyze the performance. An imperfect detection process, white noise, and phase noise are all taken into consideration in order to determine the range measurement performance. Finally, simulation and measurement results are compared with theoretical calculations and modeling results.

6. 1. Analysis of the receiver sensitivity

Generally a system is built up from building block components and signal processing is carried on with expected performance to verify the system characteristics [67]. Radar

systems in this case consist of transmitter and receiver, each of which with their specific parameters. Signal processing is performed on the base-band part of the receiver. In order to ensure the required signal processing performance [67], the receiver sensitivity has to be minimized.

6.1.1 Receiver performance parameters

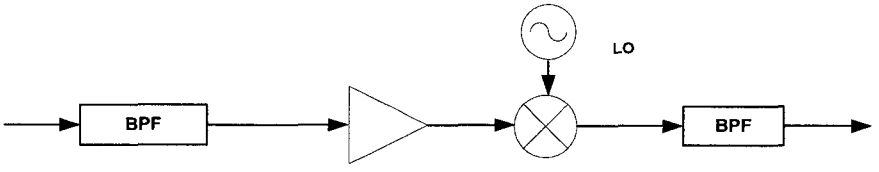

Fig. 6.1 Block diagram of a simple radar receiver

The receiver has a set of generic building blocks as shown in Fig.6.1. First the received signal from the antenna or the previous stage is filtered by a bandpass filter (BPF). The functions of BPF are to attenuate spurious responses and select the desired frequency components within the pre-selected bandwidth. Then a low-noise or automatic-gain controlled amplifier enhances the signal energy to an expected level before mixing it with the LO signal. A well designed system makes use of multiple stages of the same building blocks for enhancing system performance. Obviously, different requirements on amplifiers, mixers and oscillators have to be met at different stages. In general, the three main aspects that describe receiver performance are noise, spurious responses, and nonlinear intermodulation distortion which will be outlined in the following:

a. Noise is introduced by certain components (amplifiers and oscillators, for example). SNR is changed by noise figure.

b. Spurious responses are related to undesired signals, which are generally found at different frequency bands

c. Intermodulation products come from nonlinearity properties of amplifier, mixer and inter-products of mixers. These effects can become too adverse to cover the desired responses. The intermodulation distortion is the most important parameter to describe system dynamic range.

These three aspects are also related to the other parameters. Receiver sensitivity depends on the system noise figure, and calculating noise figure requires the characteristic parameters of each component. These three performance criteria are related to circuit parameters as well, which will be described in detail in the following paragraphs.

1) Noise figure

Receiver sensitivity is related to the system noise figure, whose calculation requires cascading the noise figure of every single component in the receiver circuit.

The receiver sensitivity can be described by the minimum detectable signal S_{min} as follows [67]:

$$S_{min} = F_T kTB\left(\frac{S}{N}\right)_o \tag{6.1}$$

Generally, communication receiver sensitivity is measured in volts, which is given by the following:

$$e = \sqrt{F_T kTB\left(\frac{S}{N}\right)_o R_G} \tag{6.2}$$

with F_T the total equivalent input noise factor (linear).

k Boltzmann's constant, 1.3×10^{23} (J/K)

T the temperature (K).

B the equivalent noise bandwidth of the system (Hz).

$\left(\frac{S}{N}\right)_o$ the required SNR at the detector output (linear).

R_G the system characteristic impedance (Ω).

To calculate the receiver sensitivity, the following equation is usually the most convenient to use:

$$\mathrm{S_{min}(dBm)} = -174\mathrm{dBm} + 10\log_{10}\mathrm{BW(Hz)} + \mathrm{F_T(dB)} \tag{6.3}$$

where BW is bandwidth of the system.

In (6.3), two parameters are to be investigated in order to solve the sensitivity equation. The first is the total equivalent input noise factor emerging from active components and resistive parts of the circuit which is to be computed separately. The second important parameter is the equivalent noise bandwidth of the system.

The equivalent input noise factor is derived from the noise figures and gains of each single component [67],

$$F_{in} = F_1 + \frac{F_2 - 1}{G_1} + \frac{F_3 - 1}{G_1 G_2} + \cdots \tag{6.4}$$

where the noise figure components F_i and gain factors G are linear. At room temperature, the noise figure of a passive device is given by the loss factor, which is the reciprocal of the gain.

The equivalent noise bandwidth of the system is important as it limits the absolute noise power and therefore determines the minimum detectable signal.

2) Intermodulation distortion and third-order intercept point

Intermodulation distortion can be characterized by the third-order intercept point (IP3), which can be defined from single or double sinusoid inputs.

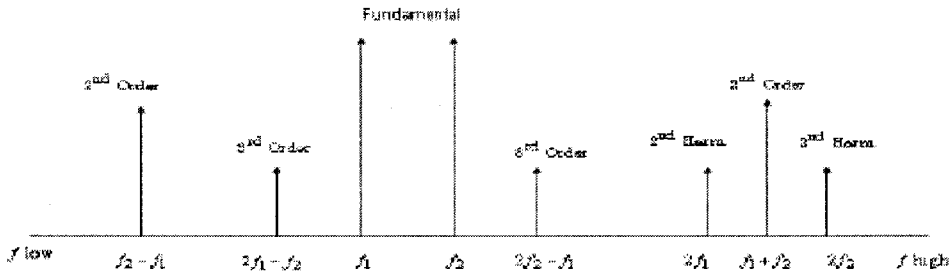

Fig. 6.2 Intermodulation distortion frequency spectrum

Fig. 6.2 shows a general picture of nonlinear frequency products for a test-setup with two fundamental frequencies (two tones). It is important to compare the fundamental signal and higher order products and as can be observed in Fig. 6.2, higher order products (especially third order terms) can occur at a very close vicinity of fundamental signal components. Thus, receiver intermodulation distortion is commonly characterized by means of the IP3 outlined in the following.

If we expand the amplifier gain using Taylor series we obtain:

$$G(s) = \alpha_1 + \alpha_2 \cdot s + \alpha_3 \cdot s^2 + \cdots \tag{6.5}$$

where s is the input power level and α is the coefficient. More precisely, this expansion also depends on the DC operation point. However, for simplicity of analysis we do not consider this in (6.3). The third order intermodulation components that we are interested in are the two fundamental input frequencies and their harmonic products.

The concept of the third order intercept point represents the input power for which the amplitudes of the third order products become equal to the fundamental frequency components. This gives the input third order intercept point (IIP3) [68] as

$$IIP_3 = \sqrt{\frac{4\alpha_1}{3|\alpha_3|}} \tag{6.6}$$

The above formulas are used to obtain the IP3 from different component characteristics. The IP3 of a component can be measured using a spectral analyzer. In addition, the IP3 of the entire system can be calculated from the IP3 of each system component. As for the cascaded components we can use (6.7) to calculate the overall IP3: (G_i is the gain of the component) :

$$IP3_{INPUT} = \frac{1}{\frac{1}{IP3_1} + \frac{G_1}{IP3_2} + \frac{G_1 G_2}{IP3_3}} \tag{6.7}$$

The gain G_i and $IP3_i$ are linear terms. Thus, the total input IP3 is also linear. A more concise logarithmic expression calculated for the total IP3 is:

$$IP3_{INPUT} = 10\log\left(\frac{1}{\frac{1}{IP_1}+\frac{1}{IP_2}+\frac{1}{IP_3}}\right) \tag{6.8}$$

where $IP3_{input}$ is the equivalent system input intercept point (dBm) with the IP_1 (mW) of the first stage and the IP_3 (mW) of the last stage transferred to the input. A simple straight-forward calculation resulting from equation (6.8) and (6.9) shows that the total equivalent IP3 is smaller than the IP3 of any of the components in the system. The IP3 is the most important parameter to specify system dynamic range.

6.1.2 Analysis of the receiver sensitivity for software defined radar

From the above discussion, the receiver sensitivities for our proposed software defined radars can be calculated. The link budgets for both proposed systems are shown in Fig. 6.3 and Fig. 6.4. From these figures, the maximum detectable range can be predicted. In general, the minimum detectable signal for radar and communication systems is the signal power for an SNR of 0 dB. The maximum detectable range (cable length) of the 4 GHz software defined radar is 25 m and the maximum detectable range of 24 GHz software defined radar is 100 m.

The software defined radar system design is based on the selection of different receiver circuit components. For our software defined radar system three radar forms are used that are generated by the same hardware architecture, which yields the same performance for the microwave front-end in all operation modes. The differences in the

proposed software defined radar result solely from the employed waveforms and signal processing algorithms. Therefore, in order to be able to compare the performance for different operation modes of the software defined radar, the main issue to investigate is the selected type of waveform, the range error related to different radar types, and the probability of detection which will be addressed in the following.

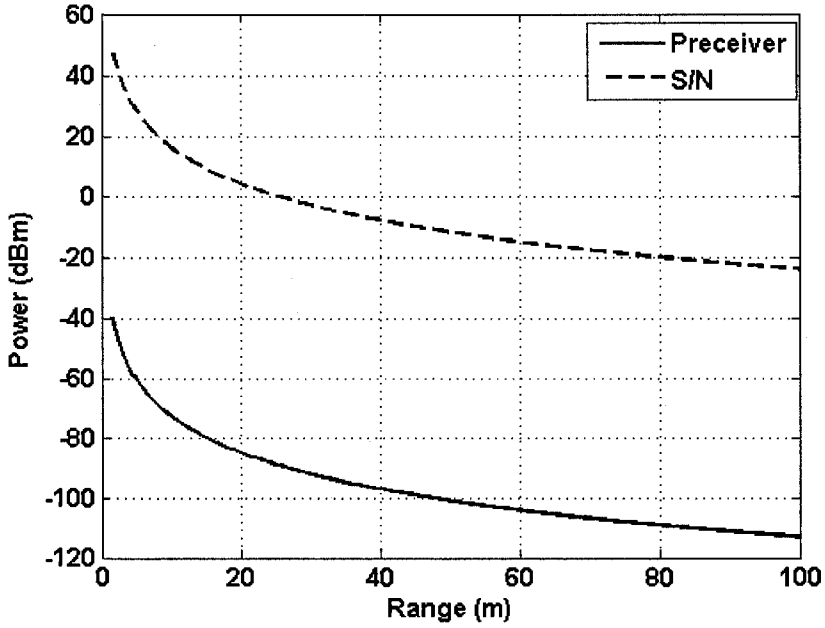

Fig. 6.3 The receiver sensitivity for the 4 GHz software defined radar prototype

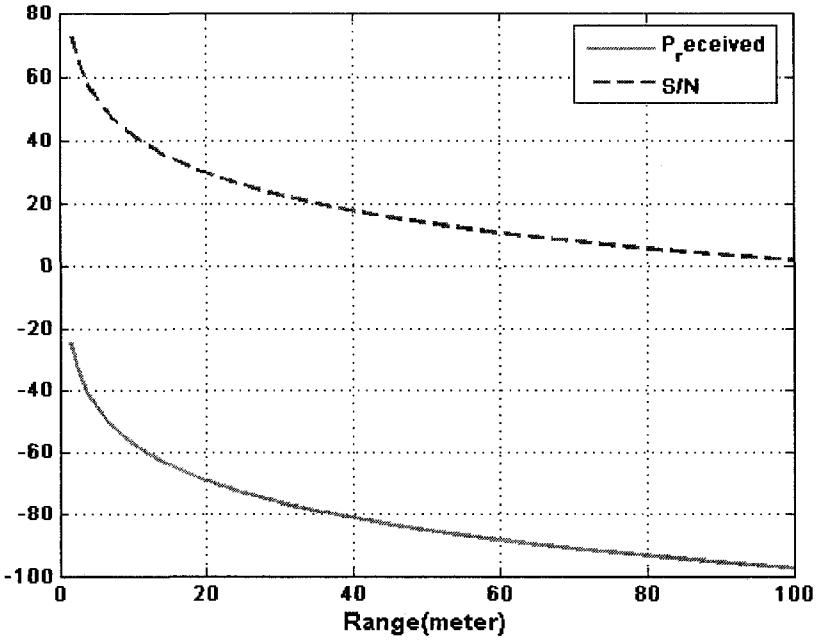

Fig. 6.4 The receiver sensitivity for the 24 GHz software defined radar prototype

6.2 Range estimation for a single target

In a radar system a signal is transmitted and the round trip delay τ_0 corresponds to the traveling time for the signal from the transmitter to the target and back. The range of estimation is therefore equivalent to an estimation of the time delay. The transmitted signal $r(t)$ is

$$r(t) = s_r(t) + n_a(t) \tag{6.9}$$

$$\begin{aligned} \varepsilon^2 &= \int_0^T \left| s(t-\tau) - r(t) \right|^2 dt \\ &= K - 2Re\left[R_{s_r s}(\tau) + R_{n_a s}(\tau) \right] \end{aligned} \tag{6.10}$$

ε^2 is the integrated squared difference between the total received signal and the shifted transmitted waveform, K is the energy in $r(t)$ and $s(t)$. $R_{s_r s}(\tau)$ is the autocorrelation function and $R_{n_a s}(\tau)$ the is cross- correlation function.

At a certain delay time or position τ_1 close to t_0, the sum of the envelope functions shows a maximum. To find this position, the above relation is differentiated and set equal to zero [69]-[74].

$$Re\left[R'_{\mu_r \mu}(\tau)+\eta'(\tau_1)\right]=0 \tag{6.11}$$

The estimation error $\tau_1 - t_0$ takes different values depending on the exact noise waveform in the interval [0,T]. As the noise voltage is a random function, it seems logical to calculate the root mean square (rms) value of the estimation deviation from the true position considering all possible noise waveforms.

$$\sigma_t = (\tau_1 - t_0)_{rms} = \frac{\left\{Re\left[(\eta'(\tau_1)\right]\right\}_{rms}}{R''_{\mu_r \mu}(t_0)} \tag{6.12}$$

where $\left\{Re\left[(\eta'(\tau_1)\right]\right\}_{rms} = \left[N_0(2\pi)^2 \int_{-\infty}^{+\infty} f^2 |M(f)|^2 \, df\right]^{1/2}$

and $R''_{\mu_r \mu}(t_0) = A(2\pi)^2 \int_{-\infty}^{+\infty} f^2 |M(f)|^2 \, df$ so

$$\sigma_\tau = \frac{\sqrt{N_0}}{\beta_0 \left[A^2 \int_{-\infty}^{+\infty} |M(f)|^2 \, df\right]^{1/2}} \tag{6.13}$$

where $\beta_0^2 = \dfrac{(2\pi)^2 \int_{-\infty}^{+\infty} f^2 |M(f)|^2 \, df}{\int_{-\infty}^{+\infty} |M(f)|^2 \, df}$, A is the average power, and $M(f)$ is the Fourier transform of the signal.

When the effect of the Doppler shift on the range correlation function is included, we obtain:

$$\sigma_\tau = \sqrt{\frac{N_0 \tau_0^2}{2S(\beta_0^2 \tau_0^2 - \rho^2)}} \tag{6.14}$$

where τ_0^2 and β_0^2 are the rms duration and bandwidth of the complex envelope of the received signal, S is the power of the received signal, and $N_0/2$ corresponds to the white noise average power. ρ is given by [71]:

$$\rho = 2\pi \frac{\int_{-\infty}^{+\infty} t\dot{\phi}(t) A^2(t) dt}{\int_{-\infty}^{+\infty} A^2(t) dt} \tag{6.15}$$

where $A(t) = cos((\omega_c + \omega_D)t + \phi(t))$ is the received signal and $\phi(t)$ is the frequency modulation term of the signal receiver. Equation 6.14 is called the Cramer-Rao Lower Bound (CRLB) [71]. For the cases of pulse and CW radar $\phi(t) = 0$, which yields, the two variances become:

$$\sigma_\tau = \sqrt{\frac{N_0}{2S\beta_0^2}} \tag{6.16}$$

Furthermore, in the pulse radar $\beta_0 = \beta_{rms}$, and the variance becomes $\sigma_\tau = \sqrt{\frac{N_0}{2S\beta_{rms}^2}}$

In the CW radar $\beta_0 = \Delta\omega$ [70], and the variance is $\sigma_\tau = \sqrt{\frac{N_0}{2S(\Delta\omega)^2}}$.

In the FMCW case, $\phi(t) = \mu t^2 / 2$ and $\dot{\phi}(t) = \mu t$. Thus, the best measurements are those yielding large $\beta_0^2\tau_0^2$ products with low ρ . Therefore, the linear frequency sweeping range must be carefully judged and chosen. All the variances are reduced by increasing the SNR. The FMCW radar requires a greater receiver dynamic range, a greater improvement factor, and a wider bandwidth. The CW radar sees more clutter than the pulse radar.

In the SS case, $\phi(t) = \pm 1$ and the signal waveform is a BPSK modulation. After the demodulation, the PN code is fed into the correlator. Thus, in order to determine the CRLB for the SS radar we need to consider the demodulation and acquisition of the correlation sequence. From basic CRLB mathematics, we know that the range estimation accuracy for the SS radar is related to the equivalent spreading bandwidth. From [75]-[78], the PN code length N is related to the noise performance and therefore also affects the range estimation. From Fig. 6.5, we observe that the SS radar shows the best performance in high white noise situations and is followed by the FMCW and the CW radars.

On the other hand, the SS radar shows the worst range accuracy for a high SNR because the range accuracy depends on the spreading bandwidth. This explains the need for a number of signal-processing algorithms as will be addressed in Section 6.4 in order

to improve accuracy for the SS radar. Based on these observations, the software defined radar is a combination of three radar types. This allows for the development of a highly noise resistant radar that shows a high range accuracy at the same time, which is shown theoretically in Fig 6.6. Furthermore, the phase noise performance of FMCW, CW, SS radars and SDR are shown in Fig. 6.7.

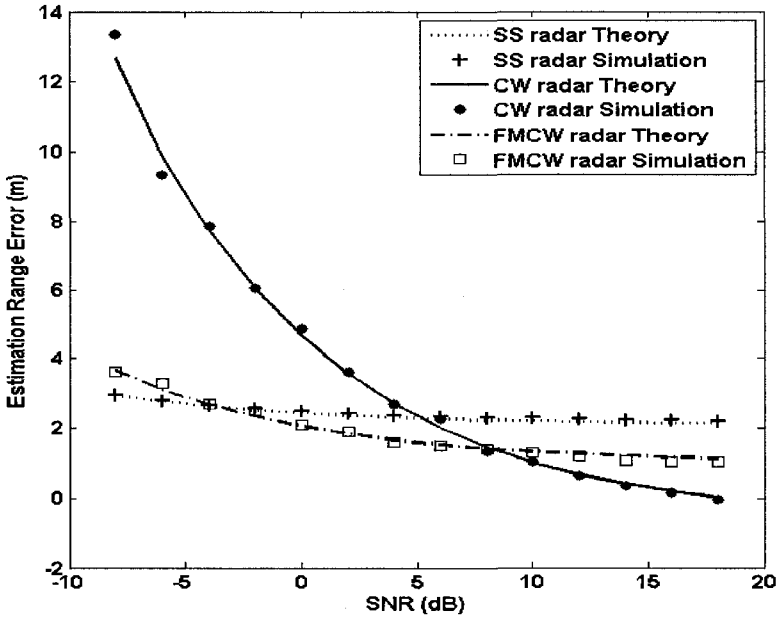

Fig. 6.5 The detection performance for FMCW, CW and SS radars vs. SNR

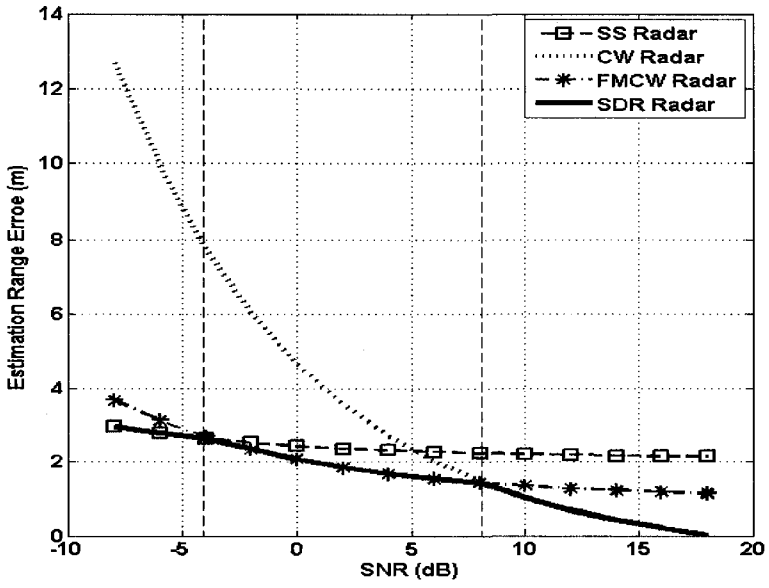

Fig. 6.6 The detection performance for the software defined radar vs. SNR.

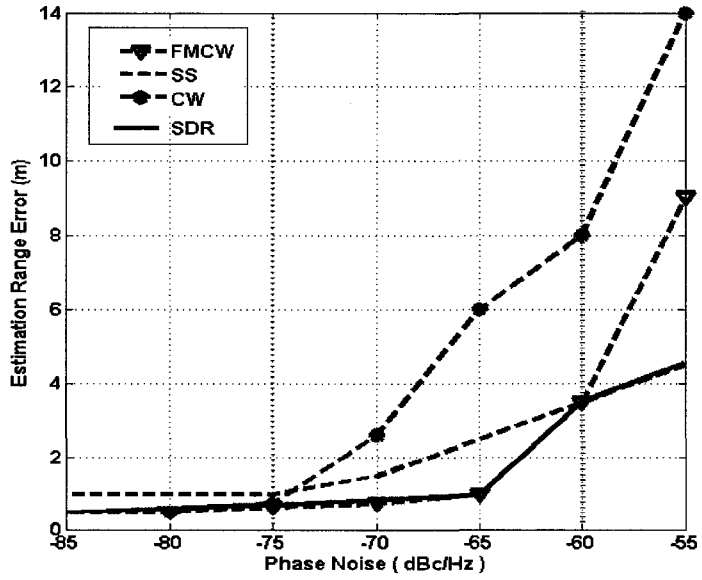

Fig. 6.7 The detection performance the software defined radar for vs. phase noise.

6.3 Mixer and six-port architectures compared as the phase detector

In Section 5.3.2 the performance of the mixer and the six-port as a demodulating element has been discussed. In this section, their performance as a phase detector is evaluated. It is well known that a single mixer is not adequate for phase detecting, while an in-phase-quadrature (IQ) mixer is generally used as phase detector. The principle for IQ detection is shown in Fig. 6.8.

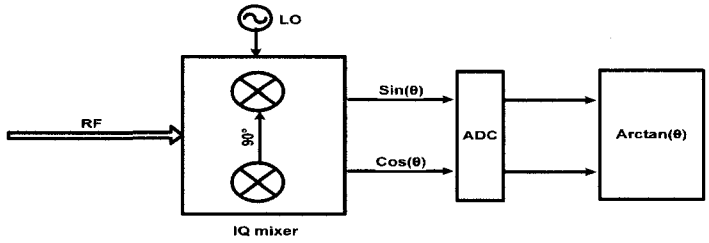

Fig. 6.8 Block diagram for IQ phase detector

For this analysis, we make use of the Matlab/Simulink models presented in Chapter 4 and 5. The IQ phase detector is modeled as shown in the Fig. 6.8. The six-port phase detector principle is described in Chapter 5. The simulations assume the same hardware transmitter and microwave front-end for each of the radar operation modes.

As a first experiment, the SNR is varied from –15 dB to 15 dB with a phase noise of –90 dBc at 100 kHz offset. These values suggest considering only the white noise effect and neglecting the phase noise. Simulation results for both mixer and six-port platforms are shown in Fig. 6.9. On the contrary, in Fig. 6.10 a simulation with the phase noise varying from –85 dBc to –55 dBc at 100 kHz offset with an SNR of 20 dB is conducted, where the white noise is neglected. From Fig. 6.9 and Fig. 6.10 we observe that the IQ

phase detector exhibits a better performance at low SNR. This result sounds reasonable, as the IQ phase detector employs a coherent detection scheme, whereas the six-port is a non-coherent detector [4], [79].

The capability of phase detection of a six-port is in the range of $(0, 2\pi)$. In $(0, 2\pi)$, the six-port has the same accuracy. The capability of phase detection of IQ phase detection lies usually in $(-\frac{\pi}{2}, \frac{\pi}{2})$. This means that six-port phase detection provides a maximum ambiguity range twice as large as the IQ phase detection. From a hardware point of view, six-port phase detection is easier to realize. However, its accuracy depends on the calibration, which can pose additional problems due to its complicated procedure. Therefore, a selection between the six-port and IQ phase detectors depends on different application scenarios.

A comparison of mixer and six-port architectures used as demodulators for BPSK signals is studied. The Matlab/Simulink models, which have been developed in chapters 4 and 5, are used. The probability of error (P_e) for coherent detection is [79]-[83]: $P_e = Q\left(\sqrt{\frac{2S}{N_0}}\right)$. Furthermore, the probability of error for incoherent detection is [75]-[79]: $P_e = \frac{1}{2} exp(-\frac{S}{2N_0})$.

In Fig 6.11, the performance of both mixer and six-port architectures is compared. The simulation result is in agreement with the theoretical considerations of coherent and incoherent detections in Fig 6.9 and Fig6.10. From Fig 6.11 we can see that the six-port performance is degrading once the SNR exceeds a certain limit, which results from the

power detector square law region limits as discussed in chapter 5. This problem can be avoided using detector calibration. Summarizing all the above considerations, the theoretical analyses and simulations show that coherent detection is preferred over its incoherent envelope counterpart.

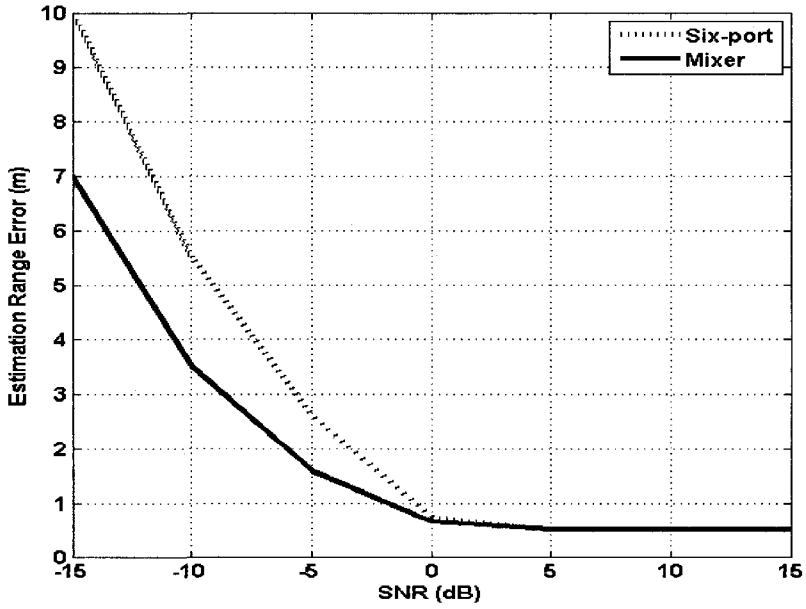

Fig. 6.9 The detection performance for the IQ mixer and six-port vs. SNR

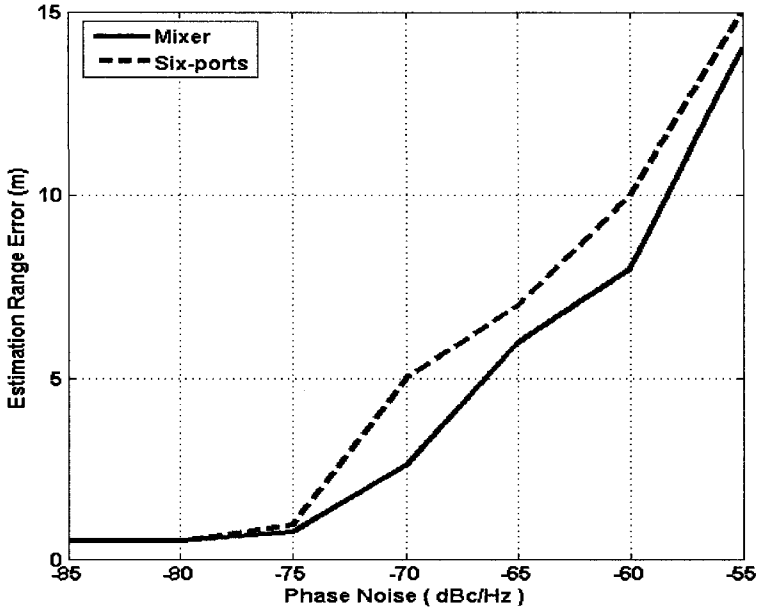

Fig. 6.10 The detection performance for the IQ mixer and six-port vs. phase noise

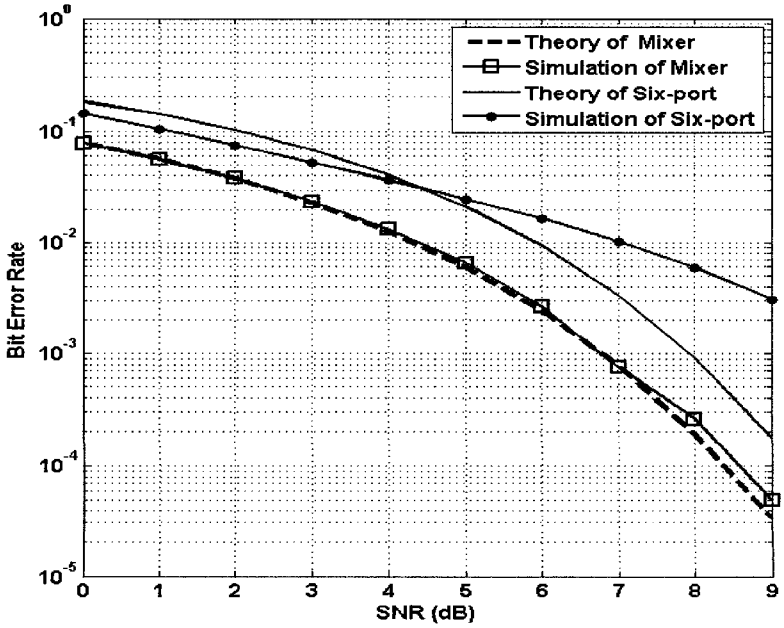

Fig. 6.11 The BPSK performance for the IQ mixer and six-port vs. white noise

6.4 Bit error rate in the PN code pulse radar mode

The SS radar mode is a conventional architecture included in the 4 GHz software defined radar. The received signal is demodulated with the LO signal, which is synchronized with the transmitter. After demodulation, the correlator gives the chip delay according to equation (2.9).

This concept is also used for communication systems, which proves the desired dual-functionality in combining communication and radar features in one device for the proposed software defined radio architecture. Furthermore, the PN code pulse radar [84] [85] mode is applied in the 24 GHz software defined radar and was described in Sec. 4.4.1. Its functionality as a communication system is proposed in [86] but not entirely proved and therefore, this section addresses this problem.

A simulation on the basis of the mixer model developed in Chapter 4 is performed. The result is shown in Fig. 6.12. The Bit Error Rate (BER) performance in one single channel is evaluated by the simulation. Considering these results we claim that in the future also the 24 GHz software defined radar architecture can alsobe used to develop a dual-functionality software defined radio combining communication and radar features in one device.

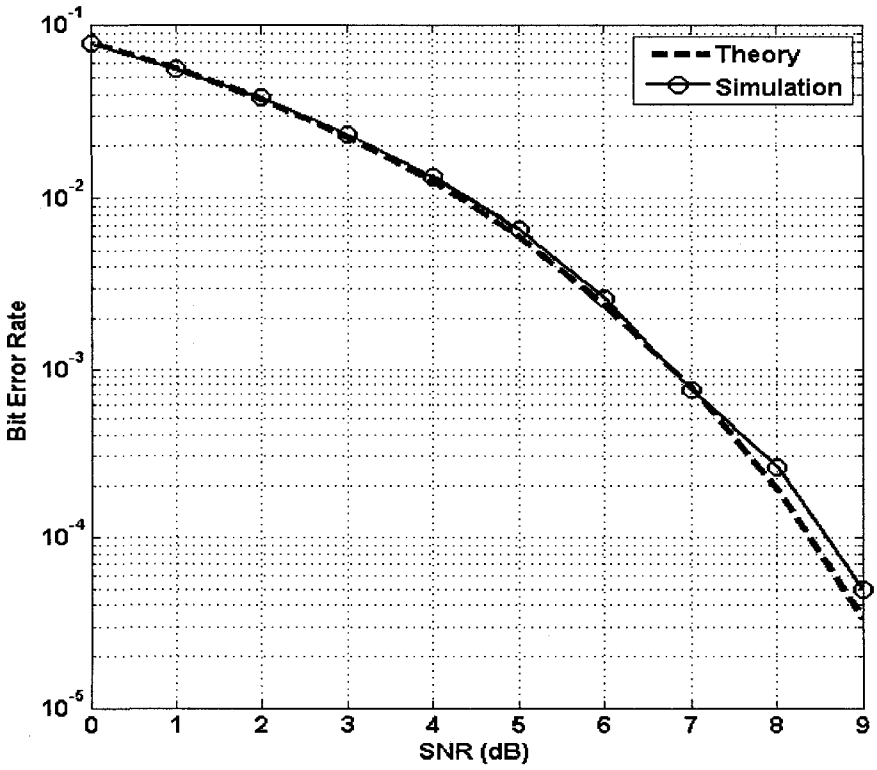

Fig. 6.12 Simulated BER for a data rate of 20MHz

6.5 Detection Probability and False-alarm

As outlined earlier, the software defined radar offers multi-mode operation (FMCW, CW, SS, etc). Different thresholds for detection are chosen for each mode. Whenever the measured receiver output exceeds the threshold, target detection must have occurred. The probability of a false alarm is the probability that noise will cross the threshold. For a better understanding, the threshold, the probability of detection, and the probability of false-alarm are shown in Fig. 6.13 [87].

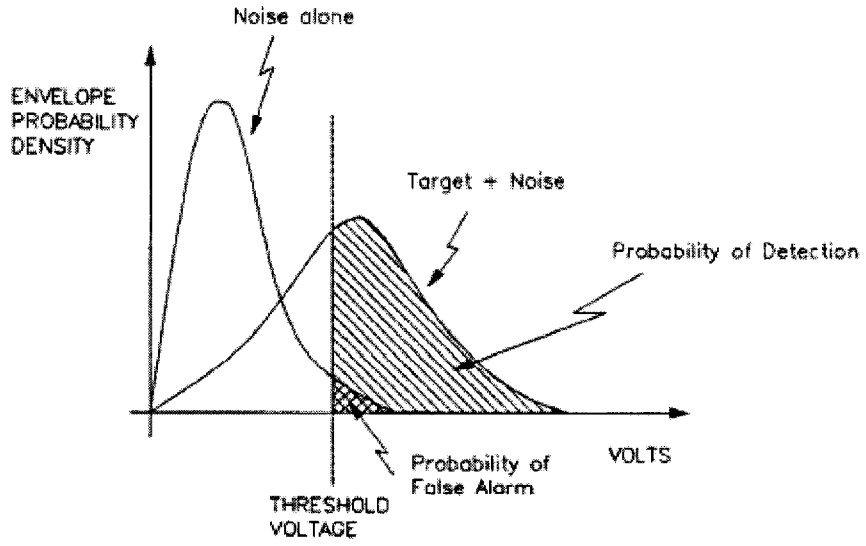

Fig. 6.13 The threshold voltage and the detection probability

The probability density function for stand-alone noise is plotted along with its counterpart for a measured target with additive noise. The crosshatched area to the right of the threshold voltage V_T under the curve for the SNR represents the probability of detection, while the double-crosshatched area under the curve for noise alone represents the probability of a false alarm. It is important to notice that if V_T is increased to reduce the probability of a false alarm, the probability of detection is reduced as well.

The specifications for false-alarm probability of practical radars usually follow from customer requirements and depend on the nature of the radar application. In this work, targets are measured in an indoor laboratory. In the future, experiments will be conducted in outdoor environments, which require a reconsideration of the false-alarm probability thresholds.

6.6 System limitations of Software defined radar

In this section we consider the degradation in the performance of software defined radar caused by (1) antenna gain, (2) low-noise front-ends, (3) dynamic range, (4) system stability, (5) A/D converters, (6) other aspects of digital processing.

Antenna gain

Software defined radars use directive antennas with relatively narrow beam widths that direct the energy in a particular direction. The antenna gain is an important factor in the whole system, as shown in the radar equation in Section 6.1.2. It is used to transmit energy to the target and to receive the echo energy. The side lobe levels are used for calculating clutter levels and the maximum ranges in the presence of interference or jamming. The first elevation side lobe below the main beam is responsible for most of the ground clutter. For this reason the side lobe limits are often given in the radar specifications. At a certain receiver sensitivity, a larger antenna gain results in a longer maximum range.

***Low*-noise front-end**

The receiver noise figure is related to the receiver sensitivity, which determines the maximum detectable range as shown in Section 6.1. A LNA is used in the receiver to reduce noise. The mixer is a key element in the heterodyne receiver converting the RF signal to the desired IF band signal. The mixer should have a low conversion loss, little additive noise, minimum spurious responses, and it should be insusceptible to burnout. The third-order intermodulation product [88] generally affects the dynamic range of the

receiver which was also mentioned in Sec. 6.1.2. The Noise that accompanies the LO signal in a single-end mixer can appear at the IF frequency because of the nonlinear action of the mixer. This noise can be reduced with the help of a filter between the LO and the mixer. Another way to eliminate LO noise is by choosing a balanced mixer. In addition, a balanced mixer can remove many products resulting from mixer intermodulation.

Dynamic range

Dynamic range is described as the ratio of the maximum to minimum input signal power the receiver can handle within the limits of acceptable amount of gain compression. The minimum signal corresponds to the receiver rms noise level which depends on the receiver bandwidth. The maximum signal is the signal that corresponds to the receiver saturation.

The mixer is often the limiting factor for receiver dynamic range [89]. The wider the bandwidth of the receiver is, the smaller the dynamic range will be because of the higher number of mixer intermodulation products (spurious responses) which occur within the frequency band. A wide bandwidth, as mentioned in Sec 6.2, also increases the noise level, which reduces dynamic range. Large dynamic range may be obtained in some radar applications by inserting variable attenuation into the receiver to make the receiver avoid overload, but this solution is limited to situations where rapid changes in the input signal are not expected.

System stability

Changes in amplitude, frequency, or phase of the oscillators as well as in the transmitted signal in the timing can result in uncanceled clutter echoes and cause degradation in performance. The phase noise affects the performance of the software defined radar, which was shown in Section 6.1.2. LO phase noise can be a serious problem to the performance of the radar. Thus, the development and use of stable oscillators are important issues. Because there are three modes in the proposed software defined radar, a DDS is used. DDS produces one or more frequencies a over wide spectrum by translating the stable frequency of a precision frequency source such as a crystal-controlled oscillator [90]. It offers the advantage of extremely fast frequency switching, small size step in frequency, excellent phase noise, reasonably good spurious performance, transient-free (phase continuous) changes in frequency, and flexibility in applying modulation.

A/D converter

The A/D converter, which converts analog to digital signals, is an important component of digital processing [91]. Its performance for radar is determined by the number of bits, into which it can quantize a signal, and the sampling rate at which it can operate. The number of bits decreases as the sampling rate or bandwidth increases. Thus the larger the bandwidth of the signals, the more difficult it is to maintain good performance. The A/D converter can sometimes be a limitation in wideband radar or when large clutter attenuation is required. Moreover, it exhibits a limited dynamic range determining the maximum signal that can be fed into the A/D converter without

saturation. Sometimes an automatic gain control (AGC) circuit is inserted before the A/D converter in order to avoid saturation.

Other aspects of digital processing

In the FMCW radar mode the method of FFT processing plays an important role. The range information is contained in the frequency content of the mixer output signal. To extract this range information, an FFT is used. Measurements at larger range require higher intermediate frequencies to be sampled. To satisfy sampling criteria according to the Nyquist theorem, the signal must be sampled at high rates and FFTs of large amounts of data are necessary. FFT becomes computationally slower with increasing data size, even with custom signal processing systems. For real-time applications it is therefore advantageous to limit the maximum processed bandwidth. The standard FFT procedure utilizes rectangular windows for the measured data. However, windowing as a preprocessing method for FFT leads to an improvement of the measured data. In addition, MUSIC and other spectrum estimation methods can be used to improve frequency estimation.

For the CW radar mode, the IQ phase detectors performance depend on the look-up table for $\arctan(\theta)$. The finer this look-up table is generated in the DSP, the better is the accuracy obtained in the range measurement. For the SS radar mode, a correlator is usually used. Moreover, SPM, TK operator, and wavelet algorithms are implemented to optimize the time delay estimation to less than one chip duration.

All these optimizing algorithms are based on the availability of a high speed sampling frequency in the ADC and a fast signal processing speed in the DSP. Currently, for our

system the Texas Instruments DSP Kit is used and it is scheduled to integrate these programs into an FPGA in order to accelerate the software defined radar response ability. From these key facts it is noticeable that the implementation of the real time applications for software defined radar represents a challenge for current hardware and software state of the art design.

CHAPTER 7

CONCLUSION AND FUTURE WORK

In this work, a flexible and reconfigurable software defined radar has been developed for use at 4 GHz and 24 GHz. The reconfigurability in this radar consists of the following features: the radar employs a dual-frequency CW mode using a phase detector, an FMCW mode with a mixer, and an SS radar mode with a phase demodulator. For each of these operation modes, a DDS generates the required signal waveforms, which brings versatility and flexibility combined with high-speed mode switching into the proposed radar system.

Furthermore, a number of different signal processing algorithms, namely, FFT, MUSIC, TK and Wavelet have been applied to the different modulation schemes in order to enhance resolution.

Both six-port and mixer architectures are studied in detail and outlined. The merits of the six port receiver architecture are its ability to combine three functions into one single device, as well as its low LO power requirements. One of its drawbacks, however, is the limited output frequency observed with six-port devices. As a counterpart, traditional mixers offer two circuit functions at the same time, while offering a less limited range in terms of output frequency. However, with mixers high LO powers are required and only IQ mixer are able to detect accurate phase.

Furthermore, the range resolution and maximum range performance for these

different types of radars has been discussed. The FMCW radar is suitable for long range measurements, and its resolution depends on the sweep speed of the DDS. A higher bandwidth gives more sweep speed and therefore a more accurate range measurement. On the contrary, dual frequency CW radar is accurate for short range measurements, while its resolution depends on phase accuracy that is determined by the sophisticated calibration procedure in the six-port. SS offers an anti-interference measurement for long ranges, and its resolution depends on the rate of the PN code.

Combining all these aspects, composite FMCW/CW/SS measurements have shown better accuracy than what could be obtained with a stand-alone FMCW system and appears highly suitable for high-precision applications. In addition, software defined SS measurement systems provide good interference eliminating capabilities. In terms of down-converting architecture, the heterodyne receiver shows excellent performance, but the six-port also is good enough and applicable as a demodulator for telecommunication systems. The economic viability of this type of ranging system appears to be very promising. Most of the current prototype systems have been built using low-cost commercial components. A DDS can adjust modulation schemes and frequency shifts, which makes it possible to introduce software configurability into the transmitter. Furthermore, a DSP provides the corresponsive digital algorithm for certain signals in the receiver. The major expense involved in a version suitable for industrial use would be in building a compact, synthesized microwave radar with a single front-end design.

The six-port-based software defined measurement system represents a low-cost alternative to the standard FMCW/CW system. Measured distance accuracy is better

than 5 cm. The six-port performs coherent detection without the need for balanced mixers and precise phase shifters. A major part of the work required in the six-port system is the calibration procedure. Also, range measurements as short as decimeters are possible without additional difficulty. The suitability of the six-port technology for complex modulation schemes and the competitiveness of the dynamic properties have been shown.

Major contributions are summarized as follows:

- Software defined radar has been developed
- Design of a six-port and IQ mixer based software defined radar
- Composite FMCW/CW/SS measurements gave an accuracy up to 5 c m
- Design of a three-tone CW SDR
- Design of a 24 GHz PN code pulse radar
- Comparison of FMCW/CW/SS range performance using CMLB
- Comparison of two system architectures for SDR

Proposals for future work on SDR include:

- Finalizing the measurement of the 24 GHz. software defined radar system based on IQ mixer.
- Calibrating the 24 GHz six-port and measuring the 24 GHz six-port based software defined radar system.
- Measuring the 24 GHz radar and radio system based on two different receiver architectures.
- Processing the acquired data from all of these systems and optimize the result.

REFERENCE

[1] H. Meikle, Modern *radar systems*, Boston : Artech House, 2001.

[2] Delphi Safety Warning Systems [Online]. Available: http:// www.delphi.com.

[3] F. L. Chevalier, *Principles of radar and sonar signal processing*, Artech House, 2000.

[4] M. I. Skolnik, *Introduction to radar systems*, McGraw Hill, 2001.

[5] D. K. Barton , *CW and Doppler radar*, Dedham, Mass : Artech House, 1978.

[6] R. L. Peterson, R. E. Ziemer, and D. E. Borth, *Introduction to spread-spectrum communications*, Englewood Cliffs, NJ : Prentice Hall, 1995.

[7] W. Wiesbeck, "SDRS: software-defined radar sensors," *Geoscience and Remote Sensing Symposium, IEEE 2001 International,* pp. 3259-3261 vol.7, 2001.

[8] J. Gagne and H. Zhang, "Software-defined Radar System: Concept and Application," *APMC,* pp. 1929-1931 vol.3, 2003.

[9] E. Adler, J. Clark., M. Conn, P. Phuong , and B. Scheiner, Low-cost technology for multimode radar *Aerospace and Electronic Systems Magazine, IEEE*, vol. 14, no. 6, pp. 23-27, 1999.

[10] H. Rohling. and M. Meinecke, "Waveform design principles for automotive radar systems," *Radar, 2001 CIE International Conference on, Proceedings,* pp. 1-4, 2001.

[11] Z Song, S. Tatu., M. R. Soleymani, K. Wu, and R. G. Bosisio, "RF coding in MMIC six port receiver," *Electrical and Computer Engineering, 2003. IEEE CCECE 2003. Canadian Conference on,* pp. 1929-1931 vol.3, 2003.

[12] J. Li, R.G. Bosisio, and K. Wu, A six-port direct digital receiver *Communications Magazine, IEEE*, vol. 38, pp. 140-147, 2000.

[13] R. Schmidt, Multiple emitter location and signal parameter estimation *IEEE*

Transactions on Antennas and Propagation, vol. 34, no. 3, pp. 276-280, 1986.

[14] H. Yamada, M. Ohmiya., Y. Ogawa., and K. Itoh, Superresolution techniques for time-domain measurements *IEEE Transactions on Antennas and Propagation,* , vol. 39, no. 2, pp. 177-183, 1991.

[15] J. F. Kaiser, "On a simple algorithm to calculate the `energy of a signal," *International Conference on Acoustics, Speech, and Signal Processing, 1990. ICASSP-90,* pp. 381-384 vol.1, 1990.

[16] X. X. Niu., P. C. Ching., and Y. T. Chan, "A wavelet-based algorithm for time delay and Doppler measurements," *1995 URSI International Symposium on Signals, Systems, and Electronics,* pp. 485-488, 1995.

[17] R. D. Ku¨hne, "From vision to reality Mobile communication application for traffic control and traffic management," *ITST*, pp. 443-447 vol.1, 2002.

[18] L. H. Eriksson and S. Brodén, High performance automotive radar *Microwave Jour*, vol. 34 , no. 3, pp. 276-280, 1996.

[19] G. A. Stove , "Automotive radar at 80-90 GHz," *Microwave Symposium Digest, , IEEE MTT-S International,* pp. 613-616 vol.2, 1992.

[20] D. A. Williams, "Millimetre wave radars for automotive applications," *Microwave Symposium Digest, 1992., IEEE MTT-S International,* pp. 721-724 vol.2, 1992.

[21] G. A. Ybarra ., S. M. Wu , L. G. Bilbro , S. H. Ardalan , C. P. Hearn., and R. T. Neece, Optimal signal processing of frequency-stepped CW radar data *IEEE Transactions on Microwave Theory and Techniques,* , vol. 43, no. 1, pp. 94-105, 1995.

[22] J. Mitola, The software radio architecture *Communications Magazine, IEEE,* vol. 33, no. 5, pp. 26-38, 1995.

[23] J. F. Luy, T. Mueller., T. Mack., and A. Terzis., Configurable RF receiver architectures *Microwave Magazine, IEEE,* vol. 5, no. 1, pp. 75-82, 2004.

[24] M. Watanabe., K. Okazaki., T. Fukae., A. Kato., K. Sato., and M. Fujise, "A 60.5 GHz millimeter wave spread spectrum radar and the test data in several situations," *Intelligent Vehicle Symposium, 2002. IEEE,* pp. 87-91 vol.1, 2002.

[25] WIGWAN-Wireless Gigabit with Advanced Multimedia Support [Online]. Available: http:// www.wigwam-project.com.

[26] V. Kroupa, *Direct Digital Frequency Synthesizers*, Piscataway : IEEE Press, 1998.

[27] J. Wang, Fundamentals of erbium-doped fiber amplifiers arrays [Online], Available: http://ww.qdot.com/current-developments-DSP.htm.

[28] I.Janiszewski, B. Hoppe, and H. Meuth, "VHDL-based design and design methodology for reusable high performance direct digital frequency synthesizers," *Proc. DAC 2001,* pp. 613-616 vol.2, 2001.

[29] M. I. Skolnik, *Radar handbook,* New York : McGraw-Hill, 1970.

[30] S. Srikanteswara, H. J. Reed., P. Athanas., and R. Boyle, A soft radio architecture for reconfigurable platforms *Communications Magazine, IEEE*, vol. 38, no. 2, pp. 140-147, 2000.

[31] K. Mizui. and M. Nakagawa, "Vehicle-to-vehicle multi-target communication and ranging system," *Electrical and Computer Engineering, 1998. IEEE Canadian Conference on,* pp. 425-428 vol.1, 1998.

[32] B. Huyart, E. Bergeault, Y. Delisle, and R.G. Bosisio, "A MMIC six-port eflectometer," *Proc. 35th Midwest Symp. on Circuits and Systems,* pp. 300-304 vol.1, 1992.

[33] J. Li, Millimeter-wave digital receiver 1996.

[34] J. Li, R. G. Bosisio ., and K. Wu, "A collision avoidance radar using six-port phase/frequency," *Microwave Symposium Digest, 1994., IEEE MTT-S International,* pp. 1553-1556 vol.3, 1994.

[35] G. F. Engen , The Six-Port Reflectometer: An Alternative Network Analyzer

Microwave Theory and Techniques, IEEE Transactions on, vol. 25, no. 12, pp. 1075-1080, 1977.

[36] G. F. Engen , A Six-Port Reflectometer and its Complete Characterization by Convenient Calibration Procedures *IEEE Transactions on Microwave Theory and Techniques,* vol. 82, no. 2, pp. 186-192, 1982.

[37] C. A. Hoer , A Network Analyzer Incorporating Two Six-Port Reflectometers *IEEE Transactions on Microwave Theory and Technique* , vol. 25, no. 12, pp. 1070-1074, 1977.

[38] G. S. Woods., D. L. Maskell , and M. V. Mahoney, A high accuracy microwave ranging system for industrial *IEEE Transactions on Instrumentation and Measurement,* vol. 42, no. 4, pp. 812-816, 1993.

[39] Y. Aoyagi., T. Fukuchi., H. Endo., M. Kusunoki., Y. Iso., K. Inoue., H. Ishizu., and R. Kohno, "76 GHz spread spectrum radar for autonomous intelligent cruise," *Intelligent Transportation System, ITSC 97 IEEE Conference on,* pp. 677-682, 1997.

[40] M. Burgos-Garcia., J. Sanmartin-Jara., F. Perez-Martinez., and J. A. Retamosa, Radar sensor using low probability of interception SS-FH signals *Aerospace and Electronic Systems Magazine, IEEE*, vol. 15, no. 4, pp. 23-28, 2000.

[41] P. Binns, "FMCW radar: a low cost sensor for automotive applications," *IEE Colloquium on Automotive Sensors* , pp. 6-1-6/6, 1992.

[42] S. Noda, K. Inomata, M. Watanabe , T. Fukae., and M. Tobioka, "A millimeter-wave radar for train application," *Vehicle Electronics Conference, Proceedings of the IEEE International,* pp. 153-158 vol.1, 1999.

[43] P. Stoica and R. L. Moses, *Introduction to spectral analysis*, N.J. : Prentice Hall, 1997.

[44] G. Wheeler, *Radar fundamentals*, Englewood Cliffs, N.J. : Prentice-Hall, 1967.

[45] T. Manabe and H. Takai, Superresolution of multipath delay profiles measured by PN *IEEE Transactions on Antennas and Propagation*, vol. 40, no. 5, pp. 500-509,

1992.

[46] E. S. Lohan , R. Hamila ., and M. Renfors, "Superresolution algorithms for detecting overlapped paths in DS-CDMA systems with long codes," *IEEE International Symposium on Personal, Indoor and Mobile Radio Communications,* pp. 1919-1923 vol.4, 2002.

[47] F. Bouchereau , D. Brady , and C. Lanzl, Multipath delay estimation using a superresolution PN-correlation *IEEE Transactions on Signal Processing,* vol. 49, no. 5, pp. 938-949, 2001.

[48] R. Hamila , E. S. Lohan., and M. Renfors, Subchip multipath delay estimation for downlink WCDMA system based on Teager-Kaiser operator *Communications Letters, IEEE*, vol. 7, no. 1, pp. 1-3, 2003.

[49] R. Hamila and M. Renfors, "Nonlinear operator for multipath channel estimation in GPS," *Electronics, Circuits and Systems, ICECS 2000,* pp. 352-356 vol.1, 2000.

[50] R. Hamila , J. Astola , F. Alaya Cheikh , M. Gabbouj , and M. Renfors, Teager energy and the ambiguity function *IEEE Transactions on Signal Processing,* vol. 47, no. 1, pp. 260-262, 1999.

[51] S. Q. Wu , H. C. So , and P. C. Ching, "Improvement of TDOA measurement using wavelet denoising with a," *Acoustics, Speech, and Signal Processing, ICASSP-.,* pp. 539-542 vol.1, 1997.

[52] X. X. Niu , P. C. Ching , and Y. T. Chan, Wavelet based approach for joint time delay and Doppler stretch *IEEE Transactions on Aerospace and Electronic Systems*, vol. 35, no. 3, pp. 1111-1119, 1999.

[53] P.C. Ching , H. C. So , and S. Q. Wu, On wavelet denoising and its applications to time delay estimation *IEEE Transactions on Signal Processing,* vol. 47, no. 10, pp. 2879-2882, 1999.

[54] S. Yan , S. Wu , Z. Yang , and Z. Shi , "A waveform generate unit suitable for software

defined HFSWR," *Wireless Communications, Networking and Mobile Computing, 2005 International Conference on,* pp. 495-498, 2005.

[55] J. G. Proakis. *Digital communications*, McGraw-Hill, 2001.

[56] I. Okazaki and T. Hasegawa, "Spread spectrum pulse position modulation-a simple approach for," *Singapore ICCS/ISITA '92. 'Communications on the Move',* pp. 300-304 vol.1, 1992.

[57] I. Okazaki and T. Hasegawa, "Spread Spectrum Pulse Position Modulation and its Asynchronous Cdma Performance - A Simple Approach for Shannon's Limit," *Spread Spectrum Techniques and Applications, IEEE Second International Symposium on,* pp. 325-328, 1992.

[58] T. Yashiro , T. Kondo , K. Ariyasu , and Y. Matsushita, "An inter-vehicle networking method using laser media," *Vehicular Technology Conference, 1994 IEEE 44th,* pp. 443-447 vol.1, 1994.

[59] M. Takeda, T. Terada, and R. Kohno, "Spread spectrum joint communication and ranging system using," *Vehicular Technology Conference,* pp. 1935-1939 vol.3, 1998.

[60] T. Yashiro, T. Kondo , H. Yagome , M. Higuchi , and Y. Matsushita, "A Network Based On Inter-vehicle Communication," *Intelligent Vehicles '93 Symposium,* pp. 345-350, 1993.

[61] T. Kondo , T. Yashiro , K. Ariyasu , and Y. Matsushita, "Inter-vehicle communication method for dynamic vehicle network," *Intelligent Vehicles '94 Symposium, Proceedings of the,* pp. 590-595, 1994.

[62] G. F. Engen, An Improved Circuit for Implementing the Six-Port Technique of Microwave Measurements *IEEE Transactions on Microwave Theory and Techniques,* vol. 25, no. 12 , pp. 1080-1083, 1977.

[63] G. F. Engen, Calibrating the Six-Port Reflectometer by Means of Sliding Terminations *IEEE Transactions on Microwave Theory and Techniques,* vol. 26, no. 12, pp.

951-957, 1978.

[64] D. Pozar. *Microwave engineering*, NJ : John Wiley, 2005.

[65] E .E. Funk and M. Bashkansky , Microwave photonic direct-sequence transmitter and heterodyne correlation receiver *Lightwave Technolog Journal*, vol. 21, no. 12, pp. 2962-2967, 2003.

[66] C. Gutierrez Miguelez , B. Huyart , E. Bergeault , and L. P. Jallet, A new automobile radar based on the six-port phase/frequency *IEEE Transactions on Vehicular Technology,* vol. 49, no. 4, pp. 1416-1423, 2000.

[67] P. Vizmuller. *RF design guide : systems, circuits, and equations*, Boston : Artech House, 1995.

[68] P. Combes, J. Graffeuil , and J. Sautereau. *Microwave components, devices, and active circuits* , New York : Wiley, 1987.

[69] L. Blake. *Radar range-performance analysis*, Mass: LexingtonBooks, 1980.

[70] A. Rihaczek . *Principles of high-resolution radar, Ne* w York : McGraw, 1969.

[71] S. Kay. *Fundamentals of statistical signal processing*, Englewood Cliffs, N.J. : PTR Prentice-Hall, 1993-1998.

[72] W. Burdic. *Radar signal analysis*, Englewood Cliffs, N.J. : Prentice-Hall, 1968.

[73] S. Hovanessian. *Radar system design and analysis* , Dedham, MA : Artech House, 1984.

[74] J. J. Bussgang , P. Nesbeda, and H.Safran, A Unified Analysis of Range Performance of CW, Pulse, and Pulse Doppler Radar *Proceedings of the IRE*, vol. 47, no. 10, pp. 1753-1762, 1959.

[75] D. Dardari, C. Chong, and M. Win, "Improved Lower Bounds on Time-of-Arrival Estimation Error in Realistic UWB Channels," *Ultra-Wideband, IEEE 2006*

International Conference on, pp. 531-537, 2006.

[76] W. G. Cowley, Phase and frequency estimation for PSK packets *IEEE Transactions on Communications*, vol. 44, no. 1, pp. 26-28, 1996.

[77] F. Rice, F. , B. Cowley, B. Moran , and M. Rice, Cramer-Rao lower bounds for QAM phase and frequency estimation *IEEE Transactions on Communications*, vol. 49, no. 9, pp. 1582-1591, 2001.

[78] T. Pany, B. Eissfeller and G. Hein, "A Two Dimensional (delay/Doppler) Multi Correlator in a Multi-frequency PC-based Software Receiver," *Proc. ION-GNSS 2006Conference on,* pp. 431-437, 2006.

[79] W. D. Gregg, Analog and digital communication : concepts, systems, applications, and services in electrical dissemination of aural, visual and data information, New York : Wiley, 1977.

[80] L. W. Couch . *Digital and analog communication systems*, N.J. : Pearson Prentice Hall, 2007.

[81] N. S. Tzannes. *Communication and radar systems*, Englewood Cliffs, N.J. : Prentice-Hall, 1985.

[82] M. Roden. *Analog and digital communication systems* , N.J. : Prentice Hall, 1996.

[83] K. Shanmugan. *Digital and analog communication systems*, New York : Wiley, 1979.

[84] F. Ono and H. Habuchi, New pulse spacing modulation based on spread-spectrum communication schemes *Communications, IEE Proceedings-*, vol. 151, no. 2, pp. 157-162, 2004.

[85] F. B. Gross and K. Chen, Comparison of detectability of traditional pulsed and spread spectrum radar waveforms in classic passive receivers *IEEE Transactions on Aerospace and Electronic Systems,* vol. 41, no. 2, pp. 746-751, 2005.

[86] L. H. Eriksson and B. As, A high performance automotive radar for automatic AICC *Aerospace and Electronic Systems Magazine, IEEE* , vol. 10, no. 12, pp. 13 1995.

[87] D. Kazakos and P. Papantoni-Kazakos, *Detection and estimation*, New York : Computer Science Press, 1990.

[88] S. Maas, Microwave *mixers*, Boston, MA : Artech House, 1993.

[89] R. Pettai, *Noise in receiving systems*, New York : Wiley, 1984.

[90] J. Scheer and J. L. Kurtz, Coherent *radar performance estimation*, Boston : Artech House, 1993.

[91] D. Hoeschele, *Analog-to-digital and digital-to-analog conversion techniques*, New York : J. Wiley, 1994.